EFFECT OF DIFFERENT DESIGN PARAMETERS ON THE SEISMIC PERFORMANCE OF REINFORCED CONCRETE BUILDINGS WITH FILLER-JOIST TYPE FLOORS

A Thesis

By

Berk Berker

Submitted to the

Graduate School of Science and Engineering

In Partial Fulfillment of the Requirements for

The Degree of

Master of Science

in the

Department of Civil Engineering

Özyeğin University

August 2022

EFFECT OF DIFFERENT DESIGN PARAMETERS ON THE SEISMIC PERFORMANCE OF REINFORCED CONCRETE BUILDINGS WITH FILLER-JOIST TYPE FLOORS

Approved by:

Asst. Prof. Taner Yılmaz, Advisor,
Department of Civil Engineering
Özyeğin University

Asst. Prof. Derya Deniz,
Department of Civil Engineering
Özyeğin University

Date Approved: 11 November 2022

Asst. Prof. Eren Vuran,
Department of Civil Engineering
Yeditepe University

Dedicated,

To my family

ABSTRACT

Filler-joist floor systems have been widely used in recent years for the typical reinforced concrete residential buildings in Turkey. Compared to traditional beam-slab flooring systems, ribbed flooring systems may be insufficient in transferring shear forces to the shear walls and columns due to insufficient floor thicknesses, and as a result, they can cause severe damage under earthquake loads. For this reason, the current seismic design code of Turkey only allows for the use of this system with limited restrictions. The aim of this study is to evaluate the seismic performance of this type of structural systems under different design parameters including reinforced concrete slab thickness, filler block depth, number of stories and existence of shear walls. In this respect, a generic study building is investigated for different combinations of considered design parameters and three-dimensional analytical models of each study building are subjected to linear and nonlinear static analyses. The outcomes of this research proved that RC buildings with this floor system is more susceptible to seismic damage with thinner slabs and without shear walls.

ÖZETÇE

Dişli döşeme sistemleri son yıllarda Türkiye'deki tipik betonarme konut binalarında yaygın olarak kullanılmaktadır. Geleneksel kiriş-döşeme tipi döşeme sistemleri ile karşılaştırıldığında, dişli döşeme sistemleri döşeme kalınlıklarının yetersizliği nedeniyle perdelere ve kolonlara kesme kuvvetlerinin aktarılmasında yetersiz kalabilir ve sonuç olarak deprem yükleri altında ağır hasarlara neden olabilmektedir. Bu nedenle, Türkiye'nin mevcut sismik tasarım yönetmeliği bu sistemin kullanımına sadece bazı kısıtlamalarla izin vermektedir. Bu çalışmanın amacı, betonarme döşeme kalınlığı, dolgu blok derinliği, kat sayısı ve perde duvar varlığı gibi farklı tasarım parametreleri altında bu tip taşıyıcı sistemlerin sismik performansını değerlendirmektir. Bu bağlamda, genel bir çalışma binası, dikkate alınan tasarım parametrelerinin farklı kombinasyonları için incelenmiş ve her bir çalışma binasının üç boyutlu analitik modelleri doğrusal ve doğrusal olmayan statik analizlere tabi tutulmuştur. Bu araştırmanın sonuçları, dişli döşeme sistemine sahip betonarme binaların, yeterli kalınlıkta döşemeler ve perde duvarlar olmadan sismik hasara karşı daha hassas olduğunu kanıtlamıştır.

ACKNOWLEDGEMENTS

First of all, I would like to thank my advisor, Asst. Prof. Taner Yılmaz, for supporting me on this challenging path without getting bored or tired until the last moment.

I would also like to acknowledge thesis committee members Asst. Prof. Eren Vuran and Assoc. Prof. Derya Deniz for their feedbacks and supports. I also wish to thank Gizem Bakır and Gizem Tekin Akbaş for her kind guidance during and after the pandemic.

Finally, I would like to express my deepest respect and gratitude to my lifelong teachers Fikret Berker and Afet Berker, and to my wife Deniz Berker for her understanding and support during this process.

TABLE OF CONTENTS

LIST OF TABLES

LIST OF FIGURES

LIST OF ABBREVIATIONS

Abbreviation	Definition
F-5-s7-b25	Frame-5 story-slab thickness 7cm-beam depth 25cm
F-5-s10-b30	Frame-5 story-slab thickness 10cm-beam depth 30cm
F-5-s12-b36	Frame-5 story-slab thickness 12cm-beam depth 36cm
F-8-s7-b25	Frame-8 story-slab thickness 7cm-beam depth 25cm
F-8-s10-b30	Frame-8 story-slab thickness 10cm-beam depth 30cm
F-8-s12-b36	Frame-8 story-slab thickness 12cm-beam depth 36cm
F-12-s7-b25	Frame-12 story-slab thickness 7cm-beam depth 25cm
F-12-s10-b30	Frame-12 story-slab thickness 10cm-beam depth 30cm
F-12-s12-b36	Frame-12 story-slab thickness 12cm-beam depth 36cm
SW-5-s7-b25	Shear Wall and Frame-5 story-slab thickness 7cm-beam depth 25cm
SW-5-s10-b30	Shear Wall and Frame-5 story-slab thickness 10cm-beam depth 30cm
SW-5-s12-b36	Shear Wall and Frame-5 story-slab thickness 12cm-beam depth 36cm
SW-8-s7-b25	Shear Wall and Frame-8 story-slab thickness 7cm-beam depth 25cm
SW-8-s10-b30	Shear Wall and Frame-8 story-slab thickness 10cm-beam depth 30cm
SW-8-s12-b36	Shear Wall and Frame-8 story-slab thickness 12cm-beam depth 36cm
SW-12-s7-b25	Shear Wall and Frame-12 story-slab thickness 7cm-beam depth 25cm
SW-12-s10-b30	Shear Wall and Frame-12 story-slab thickness 10cm-beam depth 30cm
SW-12-s12-b36	Shear Wall and Frame-12 story-slab thickness 12cm-beam depth 36cm

CHAPTER I

INTRODUCTION

1.1 Background and Motivation

The continuous need for housing in recent years and rapidly growing population have resulted in increasing number of residential building projects in Turkey. Filler-joist floor (FJF) systems have been prevalently used in reinforced concrete (RC) buildings that have been constructed in the last 2-3 decades. This floor system can be regarded as a special type of waffle slabs, where the spacing between joists are filled with various types of filler blocks. In typical designs of the structures with such floor systems, shallow beams are used to match the total depth of filler blocks and RC slab on top, so that formworks for slabs are more efficiently and economically set up. Also, the seamless design without any interruption due to beams or waffle slabs makes it an architecturally favorable floor system by contractors and clients. However, relatively low stiffness of floor slabs owing to the use of shallow beams and thin slabs can cause extreme lateral drifts under earthquake excitations, which may yield to an unexpected reduction in seismic performance. Figure 1.1 shows the schematic drawing of FJF and the application of it in a typical RC residential building in Turkey.

This design practice (i.e. RC buildings with FJF) in Turkey has been also extensively encountered in the buildings that have been reconstructed after the passing of a new law called "Urban Renewal Law" in the year 2012, which encourages the renewal of older buildings for the ultimate aim of mitigating the seismic risks of aging and structurally deficient building stocks. However, during the renewal process, total plan areas of buildings usually remain the same, while the renewed structures are built with more number of stories in order to cover the financial cost of demolition of the old building and the construction of the new one. However, occurrence of extreme lateral drifts under seismic loads can endanger the expected seismic performance of these renewed buildings as well, although they are built with improved design applications, better design and construction controls, enhanced material strengths.

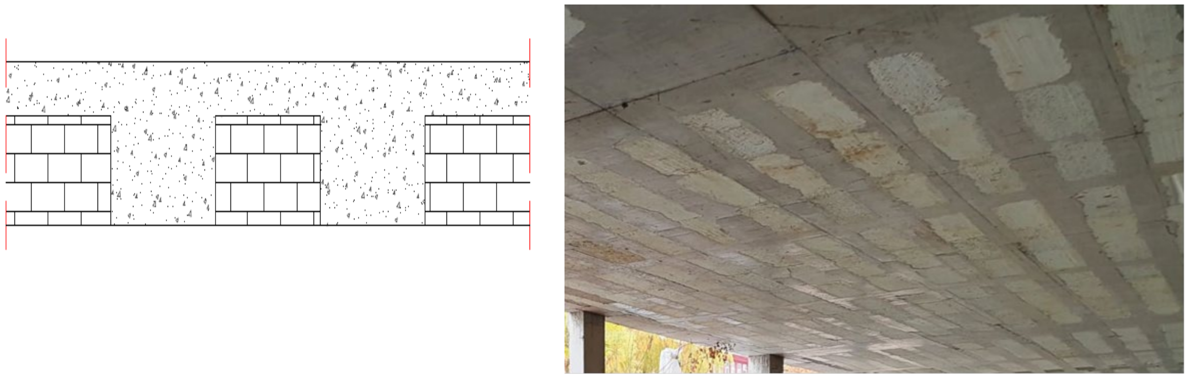

(a) (b)

Figure 1.1 (a) Schematic drawing of FJF, (b) application of FJF in a residential building in Istanbul Turkey.

The seismic hazard intensity in most parts of Turkey is significantly high, as can be observed from the seismic hazard map presented in Figure 1.2 that shows the expected peak ground accelerations (PGA) for an earthquake event with a return period of 475 years. This makes the structural design of buildings against earthquake loads extremely critical to prevent economic and life losses that can be caused by devastating earthquake events in Turkey. Although there is a significant experience regarding the seismic behaviour and performance of RC buildings with regular beam-slab type of slabs, the real-life performance of RC buildings with FJF systems have only been tested in a few earthquake events that happened in the last two decades. For this reason, an analytical assessment of the performance of this type of buildings under varying levels of seismic intensities and considering different design parameters is needed to verify the limits of the use of FJF systems for future design and construction of RC buildings.

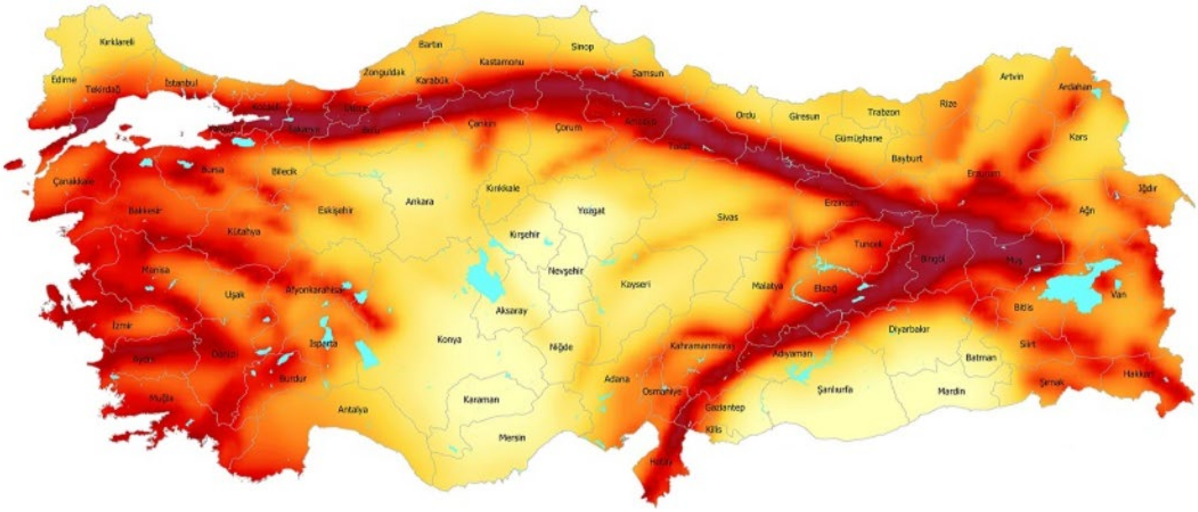

Figure 1.2 Seismic hazard map of Turkey [1].

There are a number of prominent factors that can negatively affect the structural behaviour and seismic performance of RC building with FJF systems. As mentioned above, one of the major factors is that the relatively low stiffness of floor slabs can produce excessive lateral drifts under earthquake loads. Therefore, it is commonly recommended to not use such threaded slab systems without shear walls in earthquake zones. The provisions regarding the design of threaded slabs in the seismic design codes of Turkey showed some differences in years. For instance, it was mandatory to have shear walls if such slabs are used according to the 1975 specification [2]; while this type of slabs were allowed without shear walls in the 1997 specification for only the frames with high ductility level. In the current building seismic design code that came into effect in 2018 [3], the use of floor joist floor systems is allowed for only a limited range of building height and level of seismic hazard. The provisions in this code required that such floor systems can only be used for buildings with a certain maximum height and under low level seismic SDC. Nevertheless, a detailed seismic performance assessment may be needed to verify the extent of these limitations and quantify how seismic performances of such buildings are changed under different design parameters.

Filler-joist slabs cannot fully return to their starting position after they have completed their linear displacement capacity. Plastic joints and permanent displacements begin in the building and its elements [4]. In addition, when the earthquake forces are perpendicular to the direction of the secondary beams (i.e. joists), the related in-plane forces will only be carried by slabs. Thus, lateral displacement capacities of the buildings with filler-joist slabs may be lower than estimated from linear analyses. Also, high displacement demands caused by inherent flexibility of these structures should be limited to achieve the required performance levels, while existing force-based design methodology may not be satisfactory to identify this problem, as advanced analysis methods should be employed for including more accurate estimates of displacement demand into design procedures [2]. One of the objectives of this thesis is to use nonlinear analysis such as pushover and time-history analyses to address this problem.

In this thesis, an analytical study is carried out to investigate the effect of various design parameters such as RC slab thickness, filler block height, number of stories and existence of shear walls on the seismic behaviour and performance of RC buildings with filler-joist floor systems. For this purpose, a generic RC building which is representative of typical residential buildings in Turkey is constituted and 3-dimensional finite element models of the building are generated for all combinations of considered design parameters. As the first step of the study, response spectrum analyses are performed to get the elastic seismic demands of the buildings under the design earthquake event, and analysis results are used to design column sizes and longitudinal reinforcement of the buildings with different number of stories. Secondly, nonlinear static analyses are conducted in two orthogonal directions of the building to obtain the pushover curves, and the effect of different design parameters on the structural capacities are evaluated based on the resulting pushover curves. Thirdly, nonlinear time-history analyses are performed under a set of 11 ground motion records that are matched with the design acceleration response spectrum for the design earthquake event. The resulting inelastic displacement demands are compared with the previously obtained elastic displacement demands. As the final part of the study, pushover curves and building modal properties are employed to generate equivalent single-degree-of-freedom (SDOF) systems of each building model, and these SDOF systems are subjected to nonlinear time-history analyses to estimate the inelastic top displacement demands of the buildings. A multi-stripe analysis approach is utilized to compute the exceedance probability of structural drift ratios associated with different performance limits for a wide range of seismic intensities, and finally seismic fragility curves of each study building (with different combinations of design parameters) are generated for the immediate occupancy, life safety, and collapse prevention performance limits.

1.2 Aims and Objectives

The main aim of this thesis is to evaluate the effect of various design parameters including slab thickness, number of stories and use of shear walls in the structural system on the seismic behavior and performance of reinforced concrete buildings with filler-joist floors. To achieve this aim, the following specific objectives are specified:

1. To obtain the modal properties of the RC buildings with FJF systems so that dynamic behavior of these buildings can be evaluated under different set of design parameters,
2. To produce pushover (capacity) curves of the RC buildings with FJF systems so that the global lateral capacity of the buildings can be evaluated under different set of design parameters,
3. To compute elastic and inelastic displacement and base shear force demands resulting from response spectrum and nonlinear time-history analyses, respectively, so that a comparison can be made between elastic and inelastic demands for each building with a different set of design parameters,
4. To generate seismic fragility curves of the RC buildings with FJF systems under different design parameters to assess the seismic performance of these buildings for a range of seismic intensities,
5. To evaluate the validity of the design provisions regarding the use of FJF systems by using the outputs obtained from this thesis.

1.3 Organization of the Thesis

This thesis consists of a total of six chapters with the content that is briefly explained below:

In Chapter 2; a review of the literature on seismic performance assessment of RC buildings with floor-joist floor systems, and the provisions and recommendations given in the current Turkish Building Earthquake Code (TBEC) [3] is presented.

In Chapter 3, firstly the general features of the study building and generation of the 3-D finite element models are introduced. Then, the overall methodology and results of the modal, response spectrum and nonlinear static analyses of the study buildings are presented in this chapter.

In Chapter 4, the methodology and results of the nonlinear time-history analyses performed on the 3-D models of the study buildings are presented. Then the comparison made between elastic and inelastic displacement demands are discussed in this chapter.

In Chapter 5, the methodology employed for generation of seismic fragility curves is explained. Then, the computed seismic fragility curves for each study building under three performance limits are presented and the obtained results are discussed.

In Chapter 6, overall summary and major outcomes obtained at the end of the study is presented. The chapter is concluded with the recommendations for future studies on the thesis topic.

CHAPTER II

LITERATURE REVIEW

2.1 Previous Studies on Performance Assessment of Reinforced Concrete Buildings with Filler-Joist Floor System

Filler-joist floor systems have been widely used in recent years for typical reinforced concrete residential buildings in Turkey. Thus, evaluation of the seismic performance of this type of buildings is extremely important for taking the necessary precautions to prevent life and economic losses after destructive earthquakes. The damages and collapses of the RC buildings in the past earthquake events in Turkey have been generally attributed to some commonly encountered design and construction errors such as existence of structural irregularities including torsional irregularity and soft/weak story, inadequacy in lateral reinforcement and detailing, low material strengths and poor quality of workmanship. On the other hand, the low lateral stiffness of the structural systems as a consequence of the use of shallow beams can cause extreme lateral drifts and it can arguably be the major factor on the collapse of these buildings when floor-joist floor systems are employed.

Dönmez [2] presented a comprehensive review on the history of the performances of RC buildings with FJF systems in the past earthquakes in Turkey. According to this review, the seismic damage of this type of buildings were firstly observed in 1967 Adapazarı Earthquake, which caused the collapses of eight such buildings. In the 1992 Erzincan Earthquake, damaging of this type of buildings were reported, and it was realized after this earthquake event that the relatively new blocks of a state hospital building which was constructed with FJF system totally collapsed, while the older blocks with regular beam-slab floor systems withstanding earthquake loads. It was also observed that the buildings having less than four stories and shear walls were less damaged compared to the buildings with more than four stories [5].

Later in the 1998 Adana-Ceyhan Earthquake, twelve RC buildings with FJF systems were reported to be collapsed along with many other buildings sustaining damage. The deficiencies in material quality, workmanship and detailing were noted to be the main factors in these collapses. The 1999 Kocaeli Earthquake resulted in the occurrence of many damaged RC buildings with FJF systems, and the common deficiencies of RC buildings such as insufficient transverse reinforcement, torsional and vertical irregularities primarily affected the performance of these buildings as well. The last time when RC buildings with FJF systems were prominently damaged was after the 2011 Van-Erciş Earthquake, where the strong-column weak beam type mode of failure was encountered although the design seismic demands were smaller than the design level [6]. This outcome demonstrates that the existence of highly flexible filler-joist floor systems and insufficient use of shear walls in this type of structural systems may have caused the lateral sway failure mechanism.

There are also other significant design issues that can be effective on insufficient seismic performance of this type of structural systems. One of the most important issues is the design decision of placing the direction of secondary beams (i.e., joists), since it can significantly alter the modal characteristics and seismic displacement demands of the structure. Floor slabs having joists placed in the direction of earthquake loading behave rigidly and earthquake loads can be transferred from slabs to vertical members. However, when earthquake loads act perpendicular to the direction of joists, these elements would not make any contribution to the transfer of loads and only thin slab on top of the joists would serve for this purpose [7]. Nudo et al. [8] found out that when secondary beams are placed in parallel with the main beams, 40% of bending moment demands are met, while this ratio reduces to 11% if these beams were perpendicular to the main beams.

Another issue regarding the use of filler-joist floor systems arises when shear walls are added in the structural systems to increase the overall stiffness of building and to limit lateral drifts. It is known that the use of flat plate floor systems can generally prompt large lateral displacements and transfer of shear forces from floors to vertical elements can be problematic compared to regular beam-slab type of floor systems. In a similar manner, the same problem may exist for filler-joist floor systems as well. Thus, it is crucial to select the right beam depth for ribbed slabs and analyze the structure under seismic loads whether loads are safely transferred to core walls [9]. In case slabs cannot transfer loads to shear walls, the loads will be redistributed to other elements, and it can cause a loss of rigidity in the structure while floor slabs will be overloaded by the redistributed forces [10]. In this regard, Turkish Building Earthquake Code [3] has brought new measures to address this problem, where additional reinforcement (named transfer reinforcement) is required as shown in Figure 2.1 to enable the transfer of slab forces to shear walls. This issue is one of the most important aspects of the design of filler-joist or ribbed floor systems, as it shows the necessity of having wide beams that continue along the long side of shear walls.

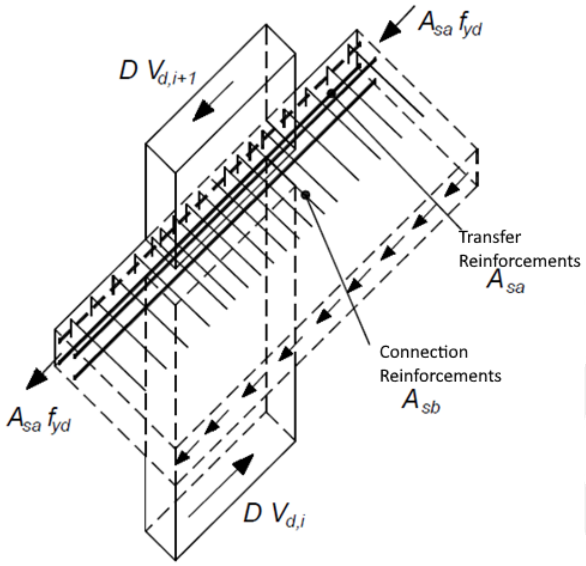

Figure 2.1 Additional transfer reinforcement requirement per TBEC [3].

Although strong-column weak-beam principle can be satisfied relatively easily in RC buildings with FJF systems because of the shallow depth of beams, there are still a couple of issues related with the beam-column joints, which may bring some uncertainty in the structural performance of this type of buildings. These issues that need to be addressed in design of wide-beams were listed by Dönmez. [6] as (i) geometry of the members, (ii) existence of longitudinal bars outside the column core area, (iii) slip of the reinforcing bars.

Several design codes dictate some restrictions for the width of wide-beams because of the uncertainties in the load transfer mechanisms at the wide-beam column joints. For example, ACI 318-11 [11] require that the width of a wide-beam should be smaller than the sum of 1.5 times the column width perpendicular to the beam w_c, plus the beam depth d_b. Also, it is required that longitudinal bars in the wide-beam outside the column core should be confined with transverse reinforcement. Similar provisions about the geometry of wide-beams in TBEC [3] are presented in Chapter 2.2 of this thesis. Kulkarni and Li [12] carried out a study that involves experimental and numerical investigation on wide-beam column joints to assess their seismic behavior under the effect of several critical design parameters. Their primary outcome was that although having good shear force and deformation capacities, the stiffnesses of these joints are relatively lower than normal beam-column connections.

In a study by Lopez-Almansa et al. [13], it was recommended that torsional reinforcement shall be designed carefully if the beam width is greater than the column width at a beam-column joint. They also demonstrated the importance of the effective width for beams and mentioned that the reinforcement at beam-column connections is crucial for the serviceability of a building. During an earthquake action, transverse beams at a connection of a wide-beam and column are cracked, and the severe pinching causes a reduction of torsional stiffness leading a lower performance than expected [4].

In addition to the aforementioned issues that are specific to the design of filler-joist floor systems, it is worth to mention structural irregularities that can cause a significant reduction in the performance of RC buildings under seismic effects. Structural behavior of buildings can be significantly influenced by plan and vertical irregularities, and they should be accounted for during design stages. General approach for the seismic design of a structure should be to select the most appropriate structural system and have an orthogonal plan as much as possible. Nevertheless, more caution has to be taken when complex or faulty structural systems are selected, as elastic analysis may be not yield accurate results for the and nonlinear analyses may be needed to validate whether such structural systems can achieve the seismic performance required by the design codes.

TBEC [3] classifies plan irregularities into three main types, which are torsional irregularity, discontinuity of floor slabs and heavy overhangs. Torsional irregularity originates from uneven arrangement of vertical load-resisting members in plan, thus the eccentricity between the center of rigidity and center of mass of a floor slab creates additional torsional moment leading to a variation of shear forces taken by vertical elements. Discontinuity of floor slabs is referred to the case of having large voids within slabs that can make seismic loads to be transferred to vertical load-resisting members difficult or having abrupt changes of strength and stiffness within floor slabs. When seismic forces are not being able to transferred, the efficiency of structural elements would be reduced, which makes the structural design become more challenging [14].

Although the effect of vertical irregularities on structural performance can change according to the number of stories of a building, it can be said that they can significantly increase the story drifts under earthquake excitations. In addition, vertical irregularities may cause bending moments and shear forces at the lower stories of buildings which may not have been taken into consideration during design stage [15]. TBEC [3] classifies vertical irregularities into three main types, namely weak story, soft story and discontinuity of vertical structural system. Weak story is caused by the irregularity of the strength of adjacent stories, while soft story is due to the irregularity of the stiffness of adjacent stories. Discontinuity of vertical structural system can be caused by columns or shear walls sitting on a beam of a lower story, or columns sitting onto overhanging or hunched beams of lower story, or shear walls sitting on the columns of a lower story.

Chintanapakdee and Chopra [16] stated that the effects of strength irregularity, stiffness irregularity and combined stiffness and strength irregularity have similar effect on the height-wise variation of story drifts vertical irregularities. Damage observations in past destructive earthquakes in Turkey showed that existence of soft-story is one of the main causes of damage in RC buildings, and this effect can be increased significantly if filler-joist floor systems are used due to the low lateral stiffness of such buildings [17]. Including shear walls in the structural systems can significantly minimize the risk of occurrence of soft-story mechanism by reducing lateral drifts. In a numerical study conducted by Turker and Gungor [18] on low-rise and medium-rice RC buildings with wide-beam and ribbed-slab, it was found out that the target performance of a 4-story building with high ductility were achieved, while the performance of the medium-rise building was not sufficient without shear walls.

Seismic behavior and performance of RC buildings with filler-joist floor slabs have been investigated in a number of thesis studies in Turkey in the last 20 years. In the majority of these studies, seismic performance of this type of structural systems were only evaluated with respect to the results of nonlinear static analyses (i.e. pushover analysis). A summary of some of the notable thesis works are listed below:

Özdaş [19] conducted nonlinear static analyses of a reinforced concrete building for different number of stories ranging from one-story to ten-stories. In this study, pushover curves were computed for the two cases of floor slabs with and without filler blocks, and it was found that the use of filler blocks resulted in lateral drifts about 50% more compared to the case without filler blocks. This outcome is interpreted to be attributed to the added masses to floor slabs due to the weight of filler blocks. Also, all analyses in this study were carried out in three different structural analysis programs, namely Sta4, IdeSTATİK and SAP2000, and some discrepancies were observed between the obtained analysis results.

İnce [17] investigated the effect of soft story irregularity on the seismic performance of RC buildings with filler-joist floor slabs. In this study, linear elastic and nonlinear static analyses were performed on buildings for different number of stories and results were compared between filler-joist slabs and conventional slab-and-beam systems. The results of this study revealed that the use of filler-joist floor slabs resulted in increased interstory drifts compared to the conventional slab-and-beam systems. Also, the increase in the ground story height was found to have negative effect on building performance.

Özden [20] investigated the seismic performance of six real-life RC buildings with filler-joist floor slabs in Antalya. In this study firstly, linear elastic seismic analyses were conducted in four different structural analysis software, namely Sta4CAD, IdeCAD, ProtaStructure and ETABS. Then, nonlinear static analyses were performed in ETABS and performance of these buildings were assessed according to TBEC [3].

Anıs [21] analyzed the lateral behaviour and capacity of RC buildings for three different slab systems (i.e. flat slab, solid slab and waffle slab) and for three number of stories (i.e. 6-story, 12-story, and 18-story building) by performing nonlinear static (i.e. pushover) analyses. It is concluded in this study that use of waffle and solid slabs can lead to a decrease in the interstory drift ratios between floors compared to flat plate system.

Other than these thesis studies, seismic performance of RC buildings with FJF systems were also evaluated in the studies of Dönmez et al. [22] and Karaaslan [23] through seismic fragility curves. In these studies, a nonlinear rotational spring representing the hysteretic behaviour of wide-beam column connections is selected and calibrated with respect to experimental research available in literature. Then, this spring element is incorporated into the structural model of a generic planar frame which is representative of this type of buildings. Pushover analyses were conducted to determine the drift limits for different performance levels, and nonlinear time-history analyses were performed under a series of ground motion records to generate the seismic fragility curves.

The focus of this thesis is to investigate the influence of total depth of floor slabs and existence on shear walls on the seismic fragilities of RC buildings with FJF systems. Hence, as will be explained in the methodology presented in Chapters 3, 4, and 5, the generic building analyzed in this study has a symmetric floor plan and no soft/weak story features in order to neglect the effect of planar and vertical irregularities on the seismic behavior. In addition, the issues pertinent to wide-beam column connections as explained above are not modeled within the finite element models of the study building, because of the lack of available research on modeling such connections and its difficulties in inclusion of such effects into the analytical models.

2.2 Current Code Requirements on RC Buildings with Filler-Joist Floor Systems

In this subchapter, the code requirements on the design of RC buildings with filler-joist floor systems in Turkey are presented. The last update of Turkish seismic design code for buildings [3] has come into effect in the year 2018. Before this version, the provisions regarding the use of filler-joist floor systems showed some variations as mentioned in İnce [17] and Dönmez [22]. After the occurrence of substantial damage of this type of buildings after the 1967-Adapazarı Earthquake, the use of filler-joist floor systems was firstly prohibited for the buildings that are located in seismic zones 1 and 2 (i.e., high level of seismic hazard) by the seismic design code issued in 1968. Later, the seismic design code issued in 1975 allowed for the application of filler-joist floor systems at seismic zones, but brought the requirement of using RC shear walls if building height exceed a certain limit.

The two updates of the seismic design code issued in the years 1998 and 2007 also permitted the use of filler-joist floor systems in the buildings located in seismic zones, only if the requirement of high-ductility structural systems is satisfied. On the other hand, if high-ductility structural system requirements were not met, these codes regarded the structural systems as average-ductility systems. Also, if shear walls were not included in this type of structural systems, such buildings could only be allowed for a maximum height of 13-m and at seismic zones of 3 and 4 (i.e., relatively low seismic hazard level).

TBEC [3] introduces four levels of seismic design classes (DTS) based on the seismic hazard level of the building of interest and the building service class (BKS) as shown in Table 2.1. The short period design spectral acceleration (S_{DS}) under DD-2 earthquake ground motion level (i.e., earthquake event having a return period of 475 years) can be obtained from the seismic hazard map of Turkey [1] according to the building's geographical coordinates and its local site class. BKS in this table indicates the importance of the building. For example, buildings that are required to be operational after an earthquake (e.g., hospitals) or buildings where large number of people are present for long periods (e.g., schools), museums or critical facilities that are used to store hazardous materials are designated with BKS = 1. In addition, TBEC [3] defines eight building height classes (BKS) with respect to the height of buildings and seismic design classes. Table 2.2 presents only a portion of this classification, which shows the range of building heights for building height classes of BKS = 6, 7, and 8. In this table, H_N refers to the building height in meters, and it shall be taken as the height above the top level of basement if building has a basement surrounded with rigid walls.

According to TBEC [3], the required target performance level for newly constructed buildings (except tall buildings with BYS ≥ 1) is "Damage Control" under the DD-2 design earthquake ground motion level. This performance level corresponds to a limited nonlinear behavior, where damage in elements of the structural system is limited.

Table 2.1 Definition of seismic design classes (DTS) per TBEC [3].

Short period design spectral acceleration (S_{DS}) under DD-2 earthquake ground motion level	Building service class	
	BKS = 1	BKS = 2, 3
$S_{DS} < 0.33$	DTS = 4a	DTS = 4
$0.33 \leq S_{DS} < 0.50$	DTS = 3a	DTS = 3
$0.50 \leq S_{DS} < 0.75$	DTS = 2a	DTS = 2
$0.75 \leq S_{DS}$	DTS = 1a	DTS = 1

Table 2.2 Definition of building height classes (BYS) per TBEC [3].

Building Height Class	Seismic Design Classes		
	DTS = 1, 1a, 2, 2a	DTS = 3, 3a	DTS = 4, 4a
BYS = 6	$10.5 < H_N \leq 17.5$	$17.5 < H_N \leq 28$	
BYS = 7	$7 < H_N \leq 10.5$	$10.5 < H_N \leq 17.5$	
BYS = 8	$H_N \leq 7$	$H_N \leq 10.5$	

TBEC [3] classifies the ductility levels of structural systems into three types, namely high-ductility, limited-ductility, and mixed-ductility structural systems. The relevant provisions on the allowable ductility levels of the structural systems for buildings with filler-joist floor systems are presented below.

- **Section 4.3.4.1 of TBEC [3]** states that limited-ductility structural systems cannot be used for the buildings with seismic design classes of DTS=1a, 2a, 3a, and 4a.
- **Section 4.3.4.3 of TBEC [3]** states that reinforced concrete structural systems consisting of frames with single direction threaded slabs with or without infill (hollow core) shall be classified as “limited-ductility structural systems” if they do not include shear walls, and they shall only be used in the buildings having the seismic design category of DTS=3 and DTS=4. Such structural systems may be constructed with high-ductility RC shear walls with tie-beams and/or shear walls without gaps; or they can be arranged as a combination of high-ductility steel eccentric and/or centrally-braced frames, and regarded as “mixed-ductility structural systems.

- **Section 4.3.4.6 of TBEC [3]** states in RC and steel mixed-ductility structural systems, the sum of the overturning moments resulting from earthquake loads at the base of RC shear walls with high-ductility tie-beams or solid walls (i.e. RC walls with or without gaps) and central, eccentric or buckling-restraint steel braced frames shall not be less than 75% of the total overturning moment resulting from earthquake loads at the base for the whole building.

The response modification and overstrength factors (i.e., R and D factors, respectively) for whole range of structural systems and their applicable building height classes are presented in TBEC [3]. The relevant R and D factors for RC buildings with filler joist floor systems are displayed in Table 2.3.

Table 2.3 Response modification and overstrength factors for Definition of building height classes (BYS) per TBEC [3].

2. Mixed-Ductility Structural Systems (referring the clauses of 4.3.4.1, 4.3.4.6 in TBEC [3]			
	R	D	BYS
A23. Buildings that resist earthquake effects by limited-ductility moment-resisting RC frames having threaded slabs with or without filler blocks and high-ductility RC walls with tie-beams (walls with gaps)	6	2.5	BYS ≥ 6
A24. Buildings that resist earthquake effects by limited-ductility moment-resisting RC frames with or without filler blocks and high-ductility solid RC walls (without gaps)	5	2.5	BYS ≥ 6

Based on Table 2.3 and abovementioned provisions, the rules of TBEC [3] on this type of structural systems can be summarized as follows:

- This structural system is only allowed for building height classes of BYS ≥ 6, which corresponds to a building height of less than 17.5m in seismic design classes of DTS= 1, 1a, 2, 2a, and less than 28m for other seismic design classes.
- If seismic design class of the building of interest is DTS= 1 or 2, this type of structural system is not allowed without any shear walls. However, if shear walls are incorporated into the

earthquake load-resistant system, then they will be allowed by regarding them as mixed-ductility structural systems.

- For the remaining seismic design classes (DTS= 3 or 4), these buildings can be constructed without shear walls, but in this case, they will be regarded as limited-ductility structural systems. However, if shear walls are incorporated into the earthquake load-resistant systems, then they be regarded as mixed-ductility structural systems.
- Shear walls used within the structural system of a buildings are required to take more than 75% of the total overturning moment of the entire structure.

Another specific provision on the design of filler-joist floor systems in RC buildings is about the stiffness and strength of slabs. **Section 7.11.2 of TBEC [3]** states that for the structural systems subject to earthquake effects, slab thickness for cast-in-place threaded slab system (with or without fillers) shall not be less than 70 mm. However, in order to ensure that the shear forces due to vertical loads and the in-plane earthquake forces can be transferred safely, shear force connections shall be made between the joists and slab, and these connections shall be shown to be sufficient by calculation. For the thicknesses of other slabs, the thicknesses given in TS 500 2000 conditions will be valid.

As the last word of this chapter, according to the force-based design approach in TBEC [3], capacity-protection design principles are taken into consideration, where inelastic behaviour is required to be restricted to some certain elements (or sections) in the structural system, while all other elements need to have adequate capacities in conformation with this inelastic behaviour. For example, **Section 7.3.5.1 of TBEC [3]** states that in structural systems composed of only frames or a combination frames and shear walls, the sum of resisting moments of columns shall be 20% greater than the sum of the resisting moments of beams for each beam-column joint. This provision, which is known as strong-column weak-beam principle, also has an effect on the selection of beam and column sizes.

CHAPTER III

LATERAL LOAD CAPACITY OF RC BUILDINGS WITH DIFFERENT DESIGN PARAMETERS

3.1 Investigated Design Parameters

In this parametric study, 18 different models with and without shear walls were analysed. The effect of different design parameters critical for buildings with filler-joist floor slabs on the seismic performance is evaluated by considering a generic study building with the typical floor plan given in Figures 3.1 and 3.2. Span lengths of 6 m and 5 m are specified in X and Y directions, respectively, which are typical span lengths for reinforced concrete construction. A uniform height of 3.15 m is assumed for all stories. The widths of primary and rib (secondary) beams are taken as 70 cm and 20 cm, respectively. Concrete class is taken as C30 which has a characteristic compressive strength of 30 MPa.

In this thesis, a parametric study is carried out by analysing a total of 18 different variants of the building that are created with respect to the combinations of specified design parameters. The whole set of investigated design parameters are presented in Table 3.1. The flexibility of floor slabs is investigated through slab thickness (t_{slab} = 7cm, 10cm, 12cm) and filler block height (h_{block} = 25cm, 30cm, 36cm). As the Seismic Design Code of Turkey (2018) requires the slab thickness to be greater than at least one third of block height, only three combinations of slab thickness and filler block height are taken into consideration. The effect of building height is investigated under three different cases of number of stories (N_{story}), while two different structural designs, buildings without shear walls (referred with “F: frame system”) and with shear walls (referred with “SW: frames with shear wall”), are also investigated to assess the influence of the use of shear walls on the structural response of the building. Figures 3.1 and 3.2 displays the formwork plans of a typical floor from the study buildings without shear walls and with shear walls, respectively. As can be seen from these figures, all columns and shear walls are symmetrically placed on the plan.

In the generated study building cases, square columns are used for simplicity and column sizes are determined for each group of buildings with 5, 8 and 12 stories. According to the seismic design procedure explained in Section 3.3 is, the column sizes are taken as 50×50 cm for 5-story buildings, 60×60 cm for 8-story buildings and 70×70 cm for 12-story buildings.

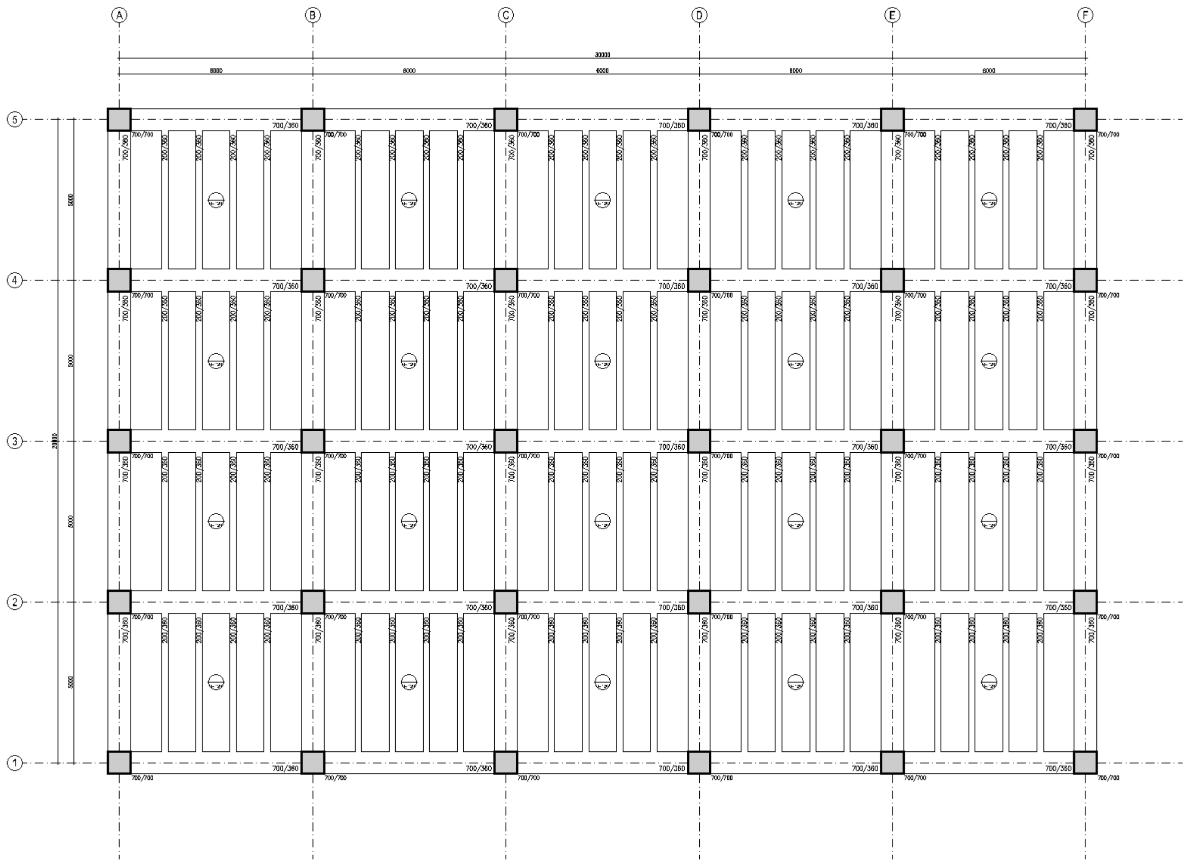

Figure 3.1 Frame only structure formwork plan

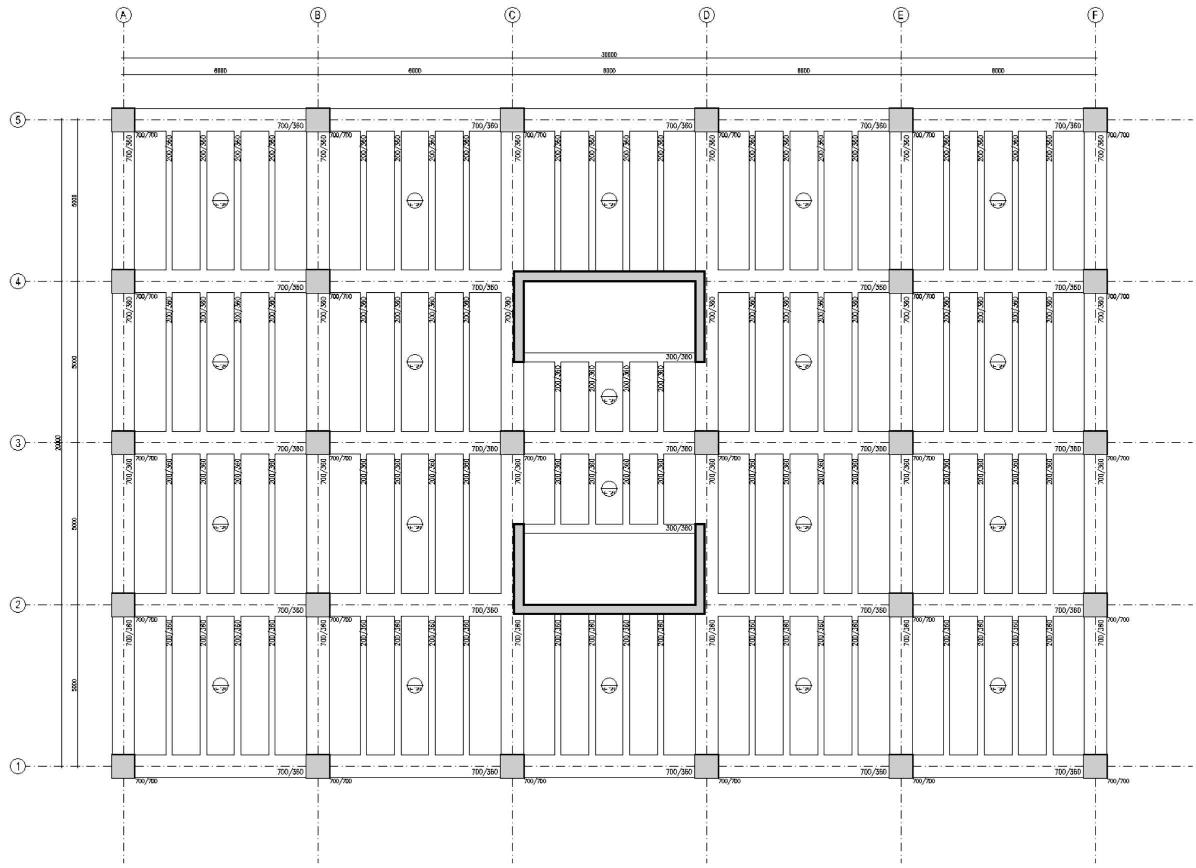

Figure 3.2 Wall frame structure formwork plan

3.2 Finite Element Modeling of the Buildings

Structural analysis software CSI ETABS [24] is used to create three-dimensional structural models of the study building. As an example, the analytical model for the 5-story building case with shear walls is demonstrated in Figure 3.3. Within the analytical models, linear elastic frame elements are used to model column and beam elements, and shell elements are used to model RC slabs and shear walls. Rigidity of nonstructural walls are ignored in the models, but their weights are included for the load and mass calculations. The inelastic behavior of the building is obtained through the use of lumped plasticity plastic hinges defined column and beam ends, as well as the fiber sections defined for shear walls. The details on nonlinear modeling are explained in Section 3.5.

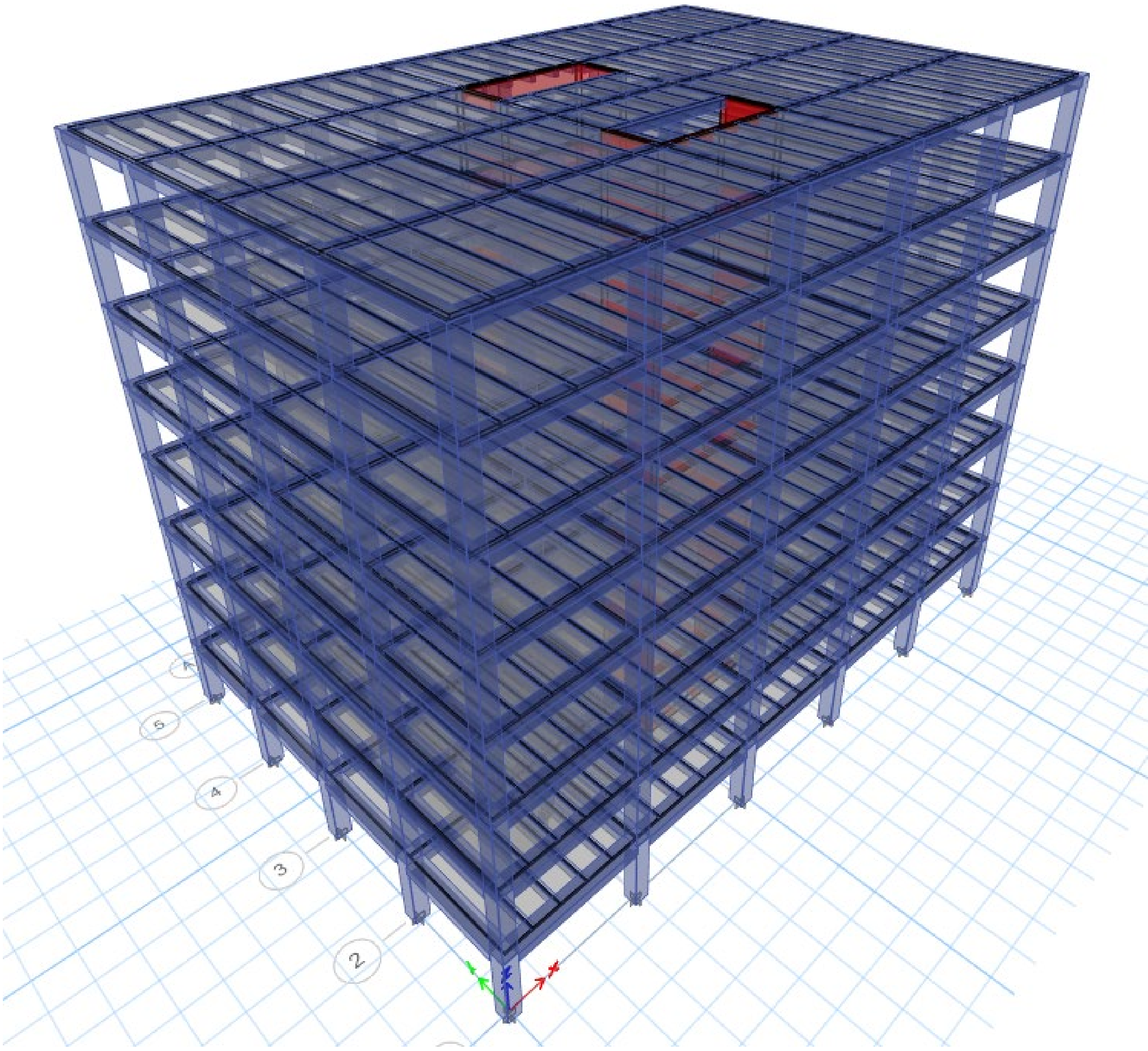

Figure 3.3 Etabs 3D model

Load definitions are as defined below.

- Dead loads which are self-loads of structural elements are taken into consideration by software itself.
- Live Loads 2kN/m^2
- Super Dead Loads (SDL) 2.5kN/m^2
- Partitions 1.5kN/m^2
- Rigidity of non-structural walls ignored while model creation

Definitions of sections:

Each model with different stories are solved linear for decision of column sizes and hence they have changed as mentioned in 3.1.

Table 3.1 Definitions of Sections

Name	Material	Area	Area	As2	As3	J	I33	I22	Mass	Weight
	cm²	cm⁴								
B200/360	C30/37	720	1	1	1	1	1	0.35	1	1
B300/360	C30/37	1080	1	1	1	1	1	0.35	1	1
B700/360	C30/37	2520	1	1	1	1	1	0.35	1	1
C700/700-24T16	C30/37	4900	1	1	1	1	0.7	0.7	1	1

Table 3.2 Table of material definitions

Material	Fc	LtWt Conc	IsUser Fr	SS CurveOpt	SS HysType	SFc	SCap	Final Slope
	MPa					mm/mm	mm/mm	
C30/37	30	No	No	Mander	Concrete	0.001818	0.005	-0.1

Table 3.3 Table of load cases (linear static)

Name	Mass Source	Stiffness Type	Nonlinear Case	Load Type	Load Name	Load SF	Design Type
Dead	MsSrc1	P-Delta		Load	Dead	1	Program Determined
Live	MsSrc1	P-Delta		Load	Live	0.3	Program Determined
Partition	MsSrc1	P-Delta		Load	Partition	1	Program Determined
SDL	MsSrc1	P-Delta		Load	SDL	1	Program Determined
Soil	MsSrc1	Nonlinear Case	None	Load	Soil	1	Program Determined

Table 3.4 Table of load cases (nonlinear static)

Name	Mass Source	Initial Condition	Nonlinear Case	Load Type	Load Name	Load SF	Load App Type	Control Displ	Displ Translational
								mm	
D+03L	Previous	Unstressed		Load	Dead	1	Full		
D+03L				Load	Live	0.3			
D+03L				Load	Partition	1			
D+03L				Load	SDL	1			
PushOverX	Previous	Nonlinear Case	D+03L	Mode	3	1	Displacement Control	Monitored	1000
PushOverY	Previous	Nonlinear Case	D+03L	Mode	1	1	Displacement Control	Monitored	1000

Load combinations are taken into consideration due to TBDY 2018. Vertical earthquake loads and 30% of perpendicular directional spectral forces are included in combinations.

Table 3.5 Table of Effective section stiffness

Reinforced Concrete Bearing Elements	**Effective Section Stiffness Coef.**	
Shear-Plate (in-plane)	**Axial**	**Shear**
Shear Wall	0.50	0.50
Basement Wall	0.80	0.50
Plate	0.25	0.025
Shear-Plate (out of plane)	**Flexure**	**Shear**
Shear Wall	0.25	1.0
Basement Wall	0.50	1.0
Plate	0.25	1.0
Frame Elements	**Flexure**	**Shear**
Tie Beam	0.15	1.0
Frame Beam	0.35	1.0
Frame Column	0.70	1.0
Shear Wall (equvalent frame)	0.50	0.5

3.3 Seismic Design of Study Buildings

Spectral curves are generated from Turkish earthquake hazard map with below latitude and longitude. Soil class is accepted as ZB. Structural analyses are done with DD2 accelerations where story drifts are calculated by DD3 accelerations.

Table 3.6 Table of spectrum values

Earthquake Ground Motion Level	DD2	DD3
Latitude	40.987688	
Longitude	29.036902	
Local Soil Class	ZB	
Spectral acceleration coefficient for Short Period [S_S]	0.975	0.391
1.0 second period for map spectral acceleration coefficient [S_1]	0.267	0.106
PGA [g]	0.399	0.169
PGV [cm/sn]	24.687	10.248

S_{DS}	0.877	0.352
S_{D1}	0.214	0.085

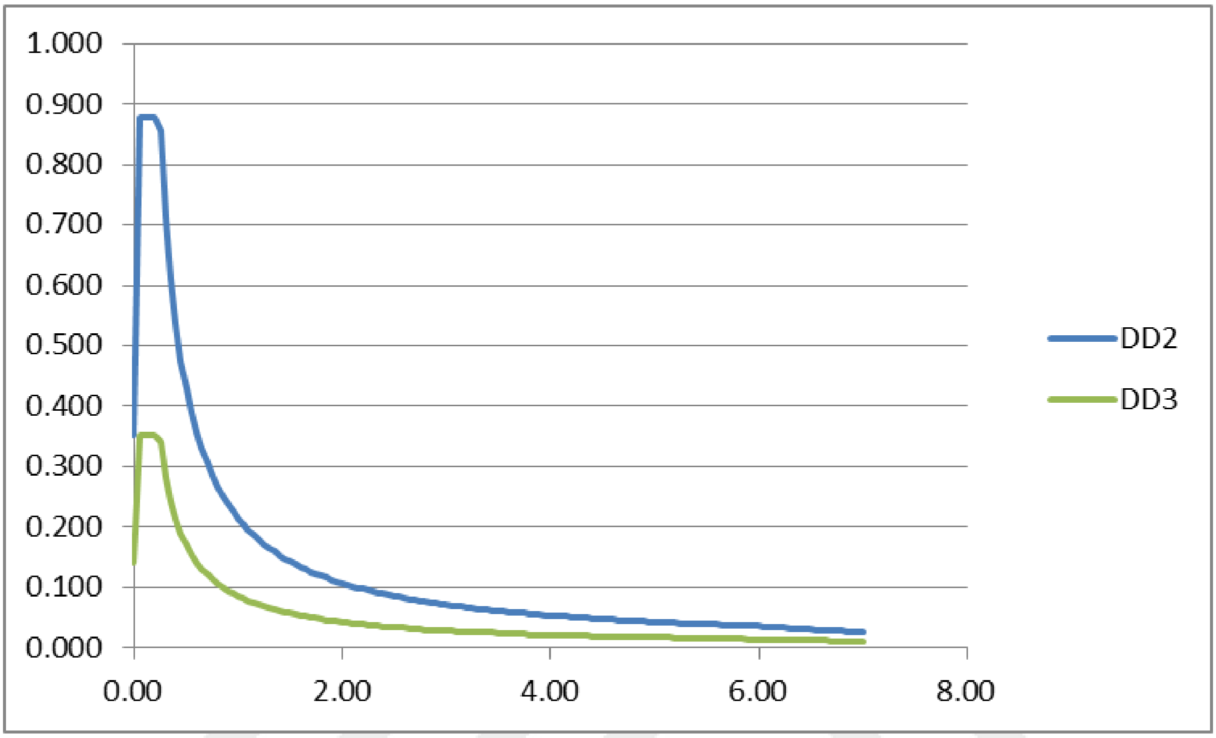

Figure 3.4 Spectral curves

3.4 Modal Analysis Results

The models were designed using modal analysis method. 36 modes were defined with the Eigen method. In order to obtain the effective mass participation rates in accordance with TBDY 2018 article 4.8.1.2, 36-mode solution was performed.

For each model, the following mode values and their dominant directions are indicated. The corresponding values show that the 1st mode of the structure shifts from x-direction to y-direction and the 2nd mode shifts from y-direction to rz, which is the torsional mode, when the shear wall is added. The shear walls, which limit the displacement and period of the structure, also completely changed the behavior of the structure under earthquake effect.

Table 3.7 Table of modal results

Model	**1.Mod**	**2.Mod**	**3.Mod**
F-5-s7-b25	1.722 (x)	1.517 (y)	1.349 (rz)
F-5-s10-b30	1.522 (x)	1.341 (y)	1.207 (rz)
F-5-s12-b36	1.323 (x)	1.172 (y)	1.062 (rz)
F-8-s7-b25	2.754 (x)	2.411 (y)	2.08 (rz)
F-8-s10-b30	2.402 (x)	2.097 (y)	1.856 (rz)
F-8-s12-b36	2.053 (x)	1.795 (y)	1.614 (rz)
F-12-s7-b25	4.225 (x)	3.683 (y)	3.02 (rz)
F-12-s10-b30	3.649 (x)	3.171 (y)	2.715 (rz)
F-12-s12-b36	2.973 (x)	2.593 (y)	2.29 (rz)
SW-5-s7-b25	0.565 (y)	0.495 (rz)	0.287 (x)
SW-5-s10-b30	0.557 (y)	0.502 (rz)	0.3 (x)
SW-5-s12-b36	0.532 (y)	0.499 (rz)	0.309 (x)
SW-8-s7-b25	1.156 (y)	0.949 (rz)	0.575 (x)
SW-8-s10-b30	1.091 (y)	0.947 (rz)	0.597 (x)
SW-8-s12-b36	0.998 (y)	0.918 (rz)	0.608 (x)
SW-12-s7-b25	2.075 (y)	1.708 (rz)	1.136 (x)
SW-12-s10-b30	1.884 (y)	1.653 (rz)	1.159 (x)
SW-12-s12-b36	1.671 (y)	1.547 (rz)	1.153 (x)

3.5 Relative Story Drifts

Relative story drift is the parameter that defines how much a story is displaced compared to the story below it. It is commonly used engineering demand parameter that is correlated with the damages occurring during earthquakes. According to Turkish Seismic Design Code (TSDC, 2018), the maximum value of relative story drift as can be calculated from Equation 3.1 are subjected to some limitations. Effective story drift can be calculated as follows:

$$\delta_i = \frac{R}{I}\Delta_i \tag{3.1}$$

$$\Delta_i = \mathrm{u}_i - \mathrm{u}_{i-1} \tag{3.2}$$

where Δ_i is the relative drift for the i^{th} story; u_i and u_{i-1} are the drifts at the i^{th} and $(i-1)^{th}$ stories, respectively. According to the provisions of TSDC (2018), the maximum drifts are required to limiting values as defined in Equations 3.3 and 3.4. The requirement in Equation 3.3 applies to the case where wall or facade elements are connected to frame elements with flexible joints or infill walls are totally independent from frames; whereas the requirement given in Equation 3.4 applies to all other cases (i.e. infill walls are adjacent to frames).

$$\lambda\frac{\delta_{i,max}}{h_i} \leq 0.016K \tag{3.3}$$

$$\lambda\frac{\delta_{i,max}}{h_i} \leq 0.008K \tag{3.4}$$

In Equations 3.3 and 3.4, the coefficient λ refers to the ratio of spectral acceleration at the predominant modal period obtained from the design seismic event DD-3 (with a return period of 72-year.) to the one obtained from the design seismic event DD-2 (with a return period of 475-years). h_i in the above equations is the height of the i^{th} story. The coefficient K in the above equations are taken as K=1 for reinforced concrete buildings.

If the requirements stated in Equations 3.3 or 3.4 are not met, the structural design has to be revised with updated element sizes and the relative story drift check has to be repeated. The distributions of story drifts along X-direction computed for all studied buildings are presented in Figure 3.5.

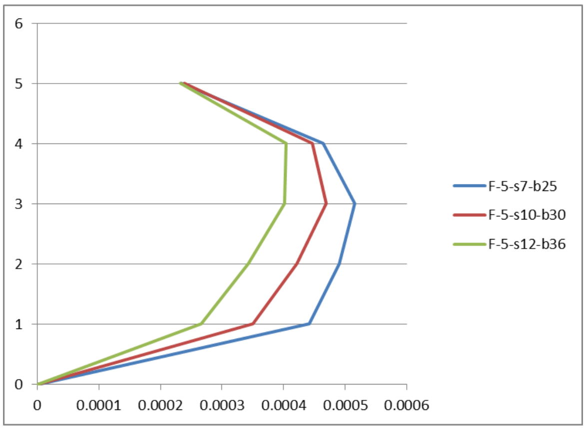

(a) 5-story building without shear walls

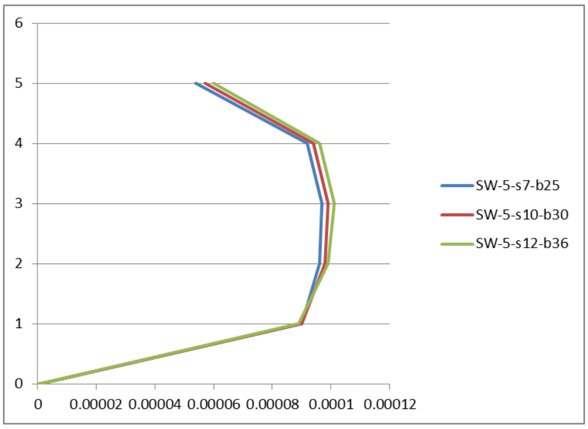

(b) 5-story building with shear walls

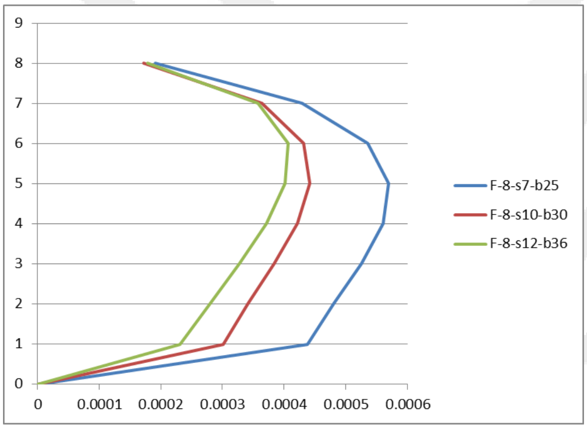

(c) 8-story building without shear walls

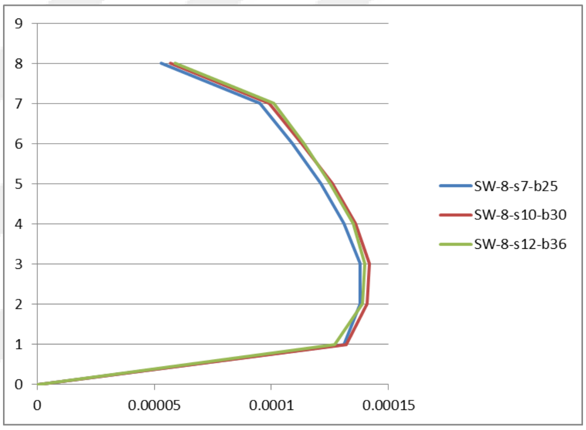

(d) 8-story building with shear walls

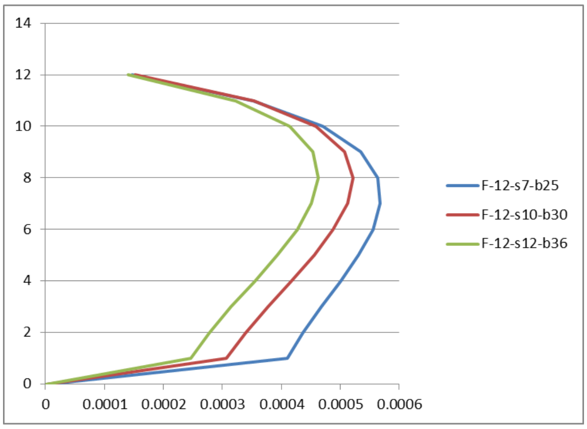

(e) 12-story building without shear walls

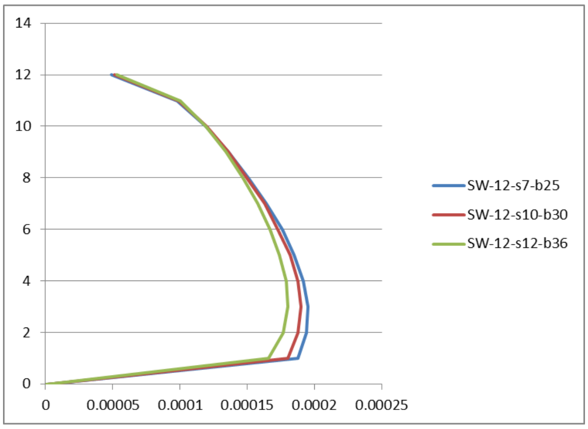

(f) 12-story building with shear walls

Figure 3.5 Distribution of drifts for all studied buildings

As can be seen from Figure 3.5, height of the building system has a significant effect on the behaviour of the structure. It is also observed that shear walls limited drifts considerably, and the difference in drifts due to different slab flexibility is diminished with the use of shear walls. On the other hand, when shear walls are not used, buildings with greater total slab thickness resulted in lower drifts due to the increased floor rigidities. Therefore, the height of the building system has a significant effect on the behaviour of the structure. The contribution of the floor planes to the rigid behaviour was undeniably effective. On the other hand, shear walls limited the periods and displacements of the structures.

3.6 Pushover Analyses

Incremental pushover analysis is a method that can be used to determine the performance targets of structures. Incremental equivalent earthquake method can be used for structures with adequate first mode participation (see TBDY 2018 chapter 5). Modal capacity diagrams can be obtained by defining the dominant mode in the thrust direction. This method can be used to determine the global capacity of a structure and determine the structural performance under lateral loads.

While creating the models, the joint definitions were selected as displacement controlled plastic joints and M2 option was preferred for beams, P-M2-M3 for columns and fiber hinges for shear walls.

Figure 3.6 Hinge assignment of an elevation

Figures 3.7, 3.8, and 3.9 show the resulting pushover curves of 5-story, 8-story and 12-story buildings without shear walls, respectively. On these figures, the pushover curves obtained from the analysis in X-direction and Y-direction are presented separately, also the curves pertinent to the buildings with different combinations of slab thickness and filler block heights are displayed with different colors. It can be said that the lateral displacement capacity of the buildings along X-direction (along the longer side of the building) is generally greater than the one along Y-direction for the 5-story and 8-story buildings, while this difference is insignificant for the 12-story buildings. Another conclusion from these figures is that as the rigidity of floor slabs is increased with the greater sum of slab thickness and block height, base shear capacities of the buildings are enhanced with a lower lateral displacement capacity. This also shows that lower slab flexibility results in increased lateral displacements.

Figures 3.10, 3.11, and 3.12 shows the resulting pushover curves of 5-story, 8-story and 12-story buildings, respectively when shear walls are used. In this case, it is observed that the structural response in X-direction is considerably more rigid than the one in Y-direction, as much larger displacement capacities are obtained for Y-direction. The same conclusions made for the effect of slab rigidity on the pushover curves is also applicable for the 5-story and 12-story buildings with shear walls, but the same trend is not obtained for the 8-story buildings. This outcome may be due to an issue related with nonlinear modeling or a convergence problem.

As a general outcome obtained from the Figure 3.7 to Figure 3.12, it can be said that increased slab rigidities and shear walls has a positive effect in restricting the lateral displacement of buildings.

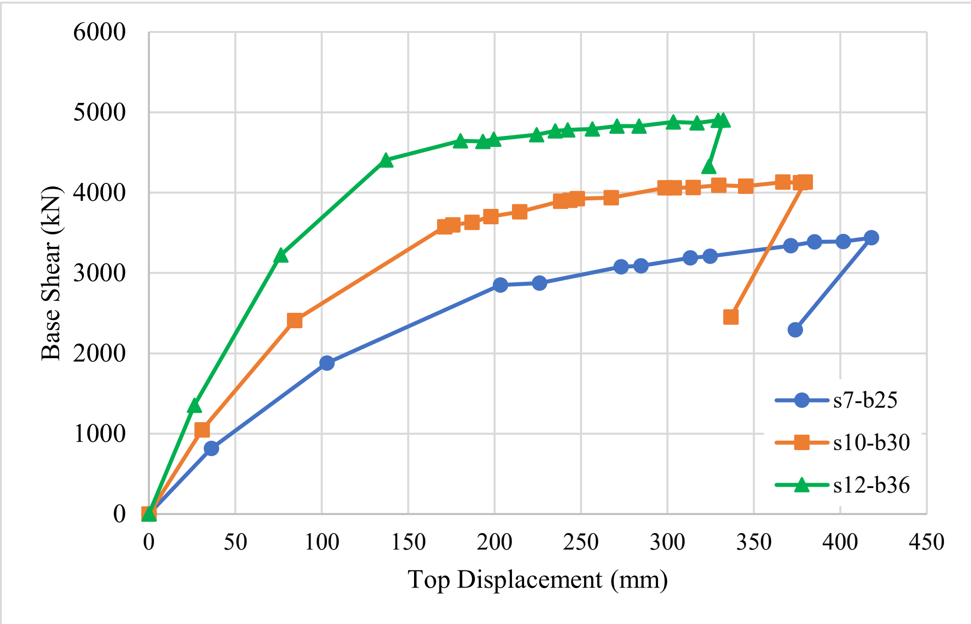

(a) Along X-direction

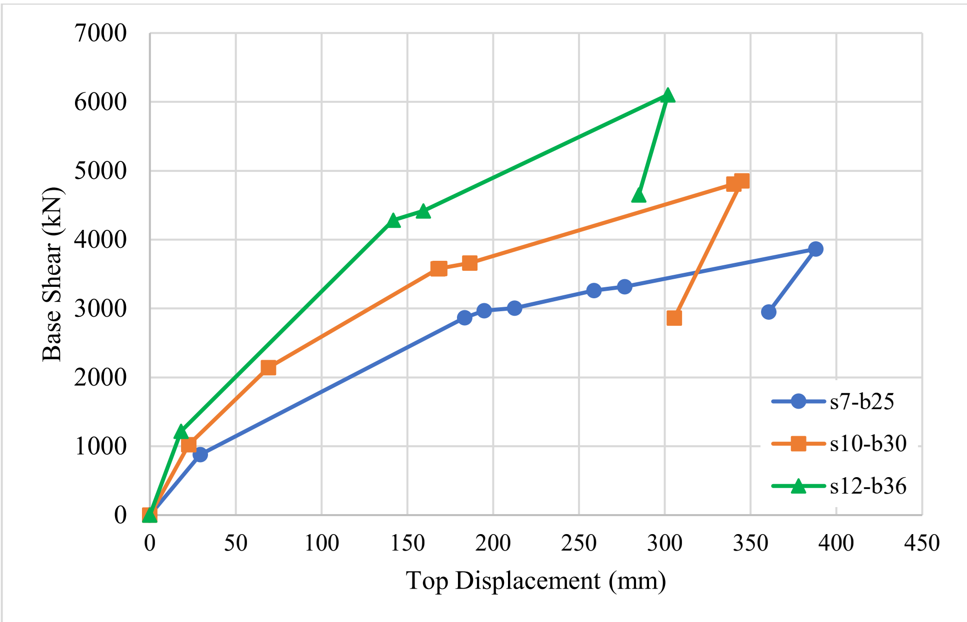

(b) Along Y-direction

Figure 3.7 Pushover curves of the 5-story buildings without shear walls

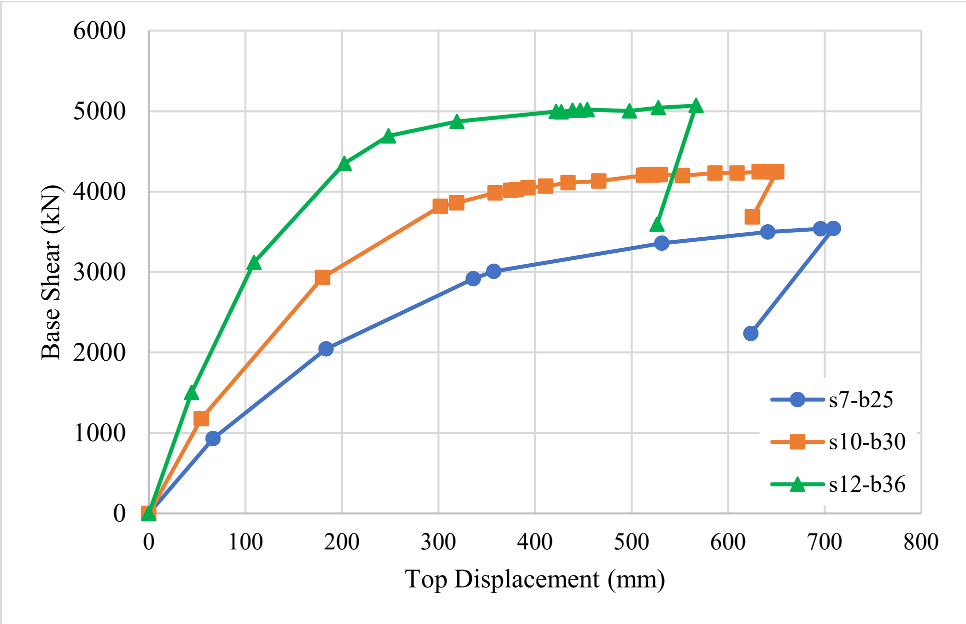

(a) Along X-direction

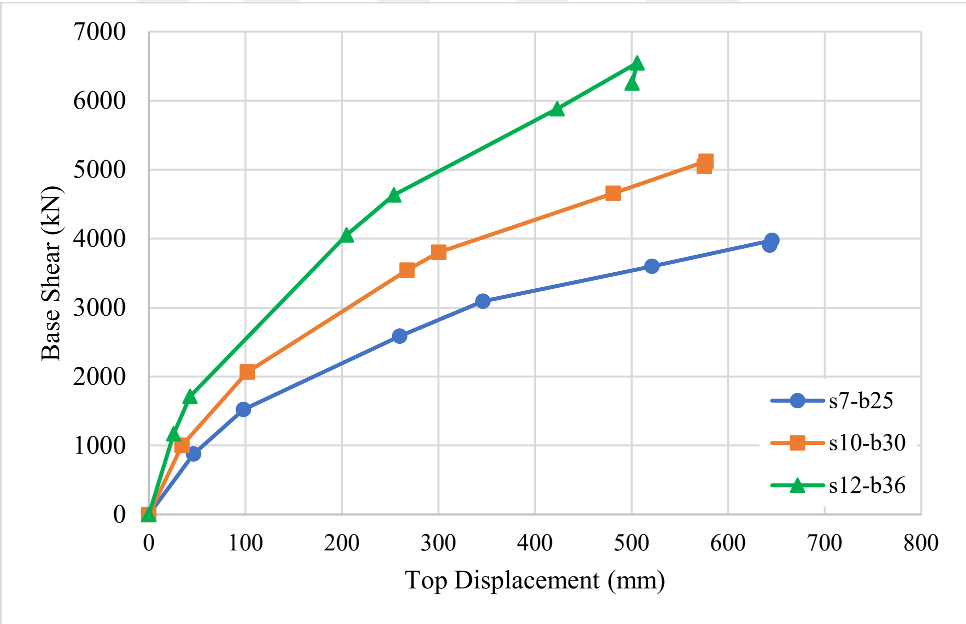

(b) Along Y-direction

Figure 3.8 Pushover curves of the 8-story buildings without shear walls

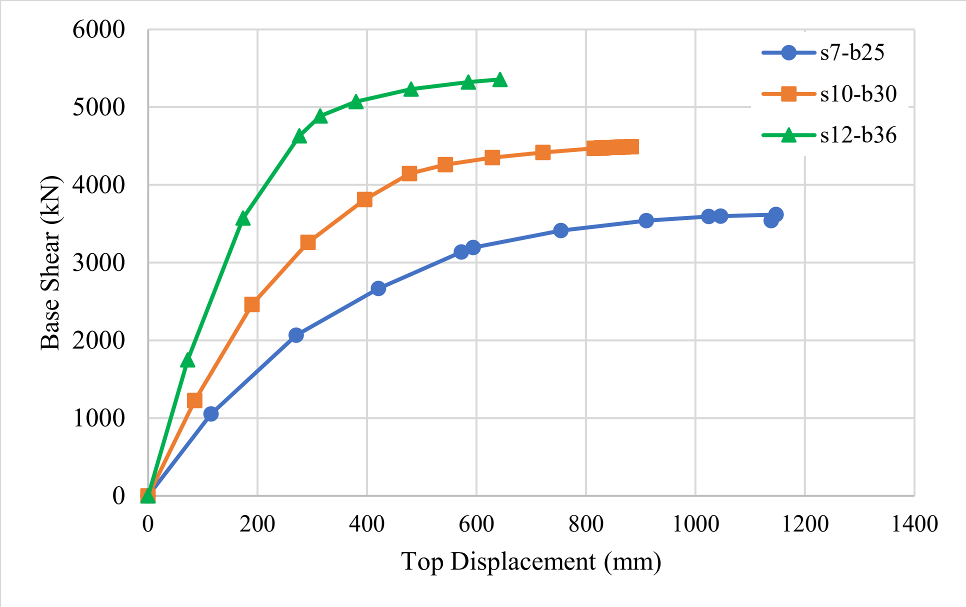

(a) Along X-direction

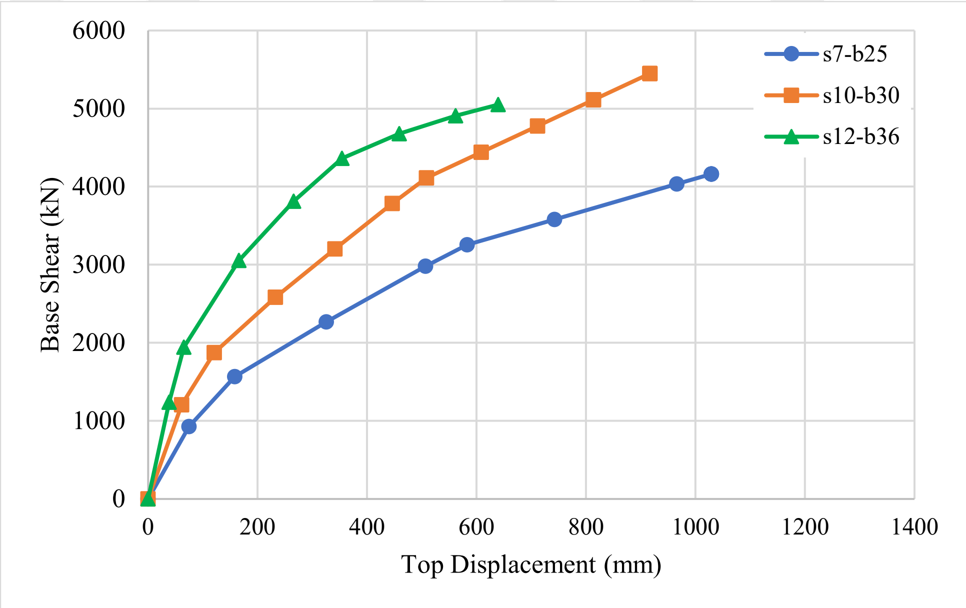

(b) Along Y-direction

Figure 3.9 Pushover curves of the 12-story buildings without shear walls

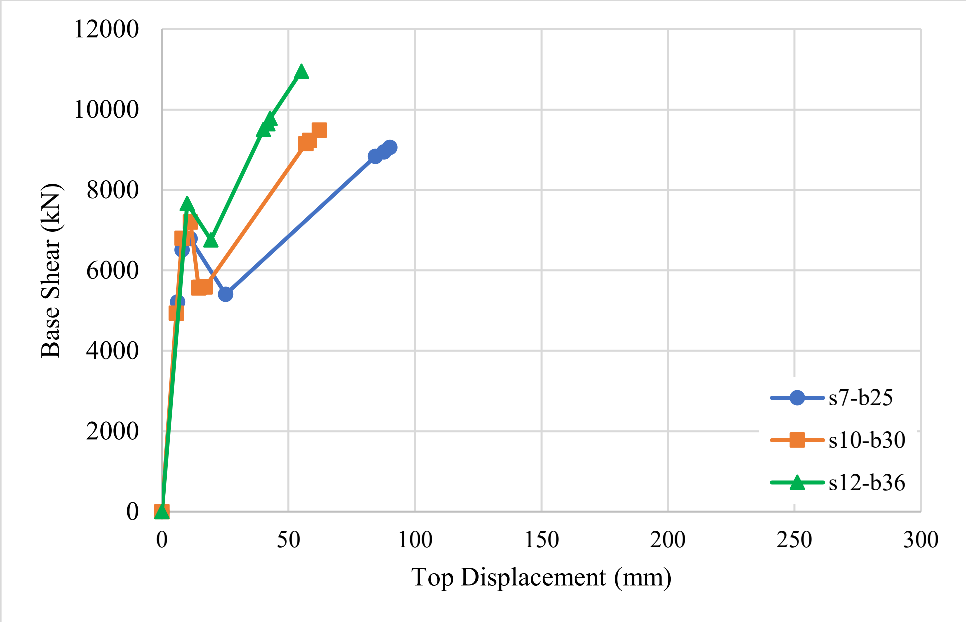

(a) Along X-direction

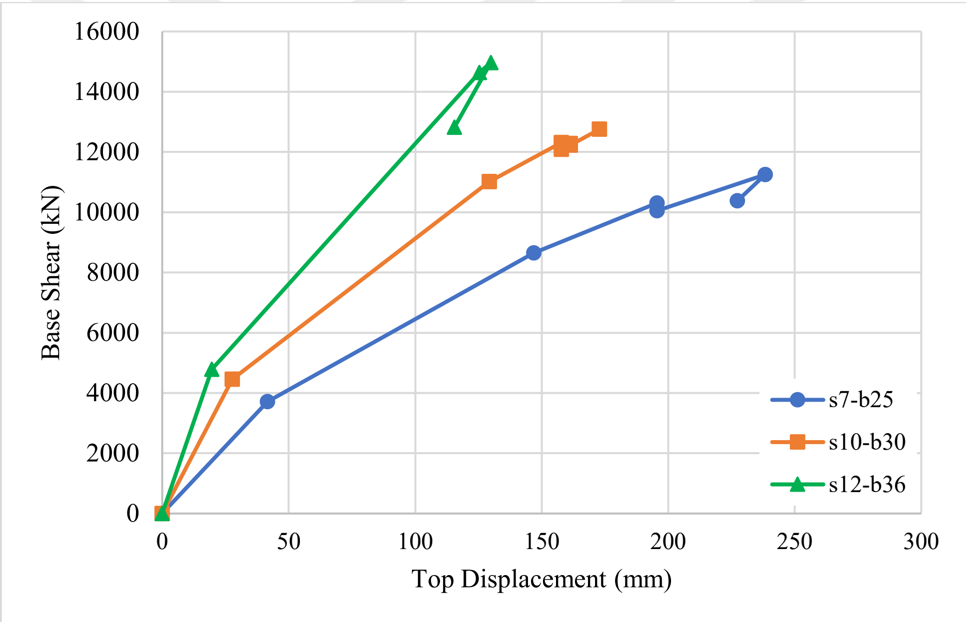

(b) Along Y-direction

Figure 3.10 Pushover curves of the 5-story buildings with shear walls

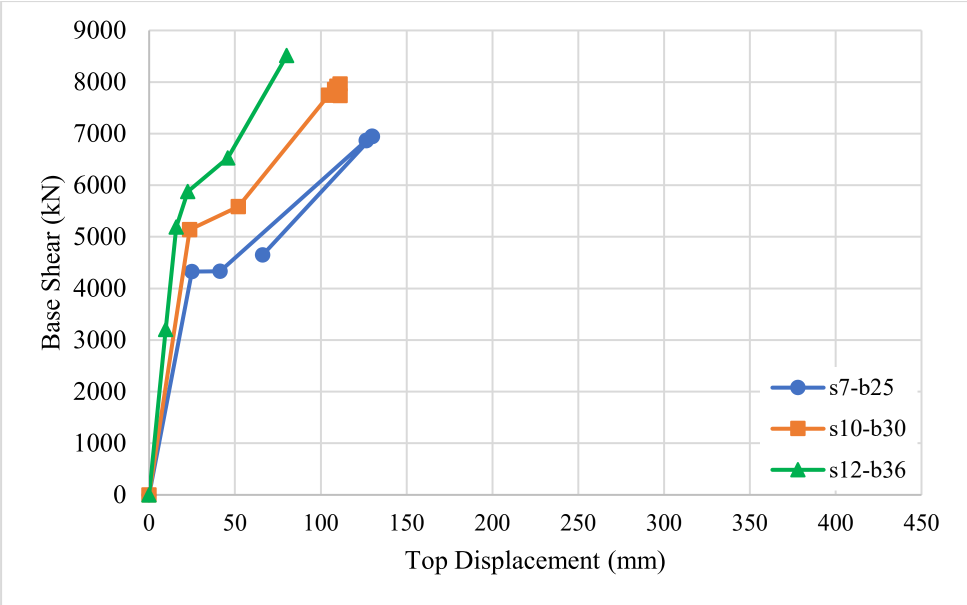

(a) Along X-direction

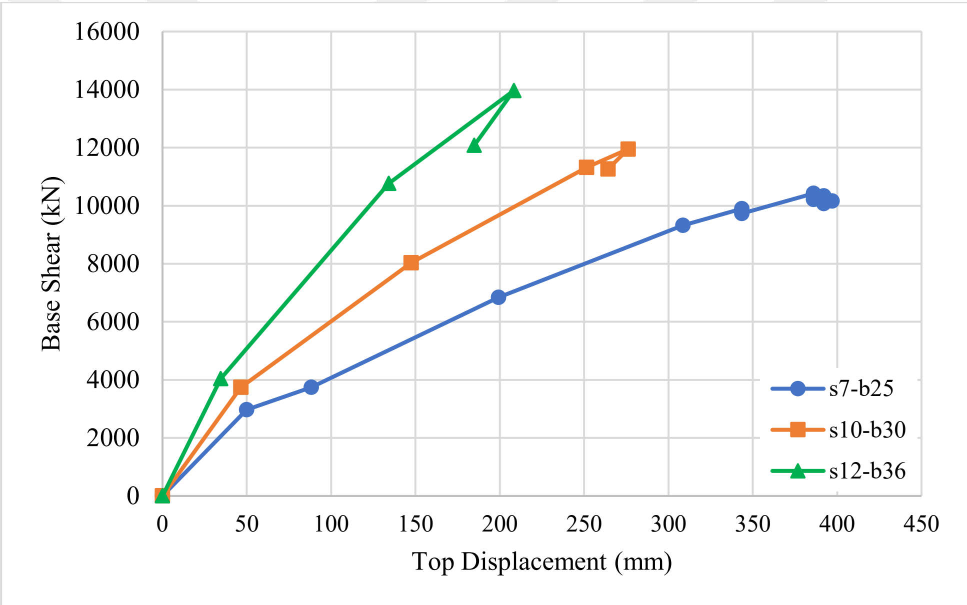

(b) Along Y-direction

Figure 3.11 Pushover curves of the 8-story buildings with shear walls

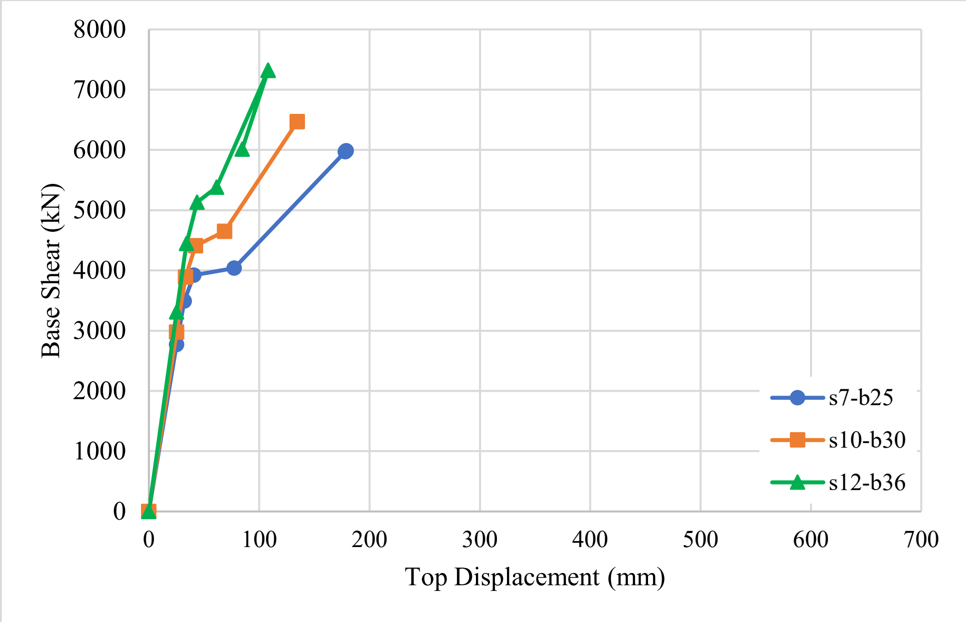

(a) Along X-direction

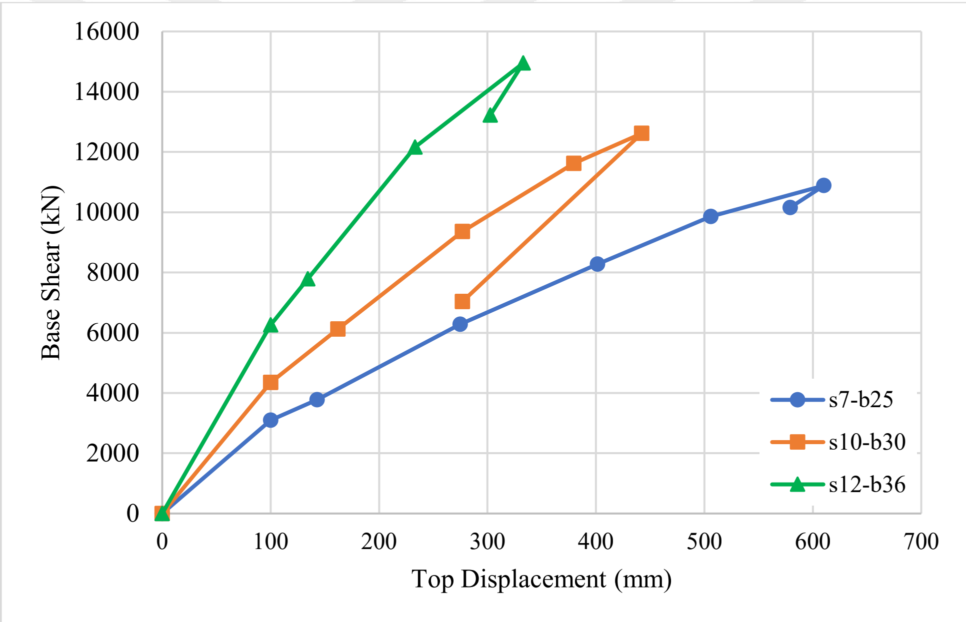

(b) Along Y-direction

Figure 3.12 Pushover curves of the 12-story buildings with shear walls

CHAPTER IV

TIME HISTORY ANALYSIS OF THE BUILDINGS

4.1 Introduction

In this chapter, it is aimed to assess the response of the investigated buildings with different design parameters through nonlinear time-history analyses of the 3-D models of the buildings. Compared to response spectrum and nonlinear static analysis employed in the previous chapter, time-history analysis is the most accurate type of analysis that can be applied to determine the displacement or force response of a structure under earthquake loading. In response spectrum method, earthquake loads acting on the structure are determined from acceleration response spectra and considering the modal periods of the structure, then response (e.g., internal forces) demands are obtained by some modal combination rules such as SRSS and CQC. For design calculations, design acceleration response spectra as described in seismic design codes are utilized where spectral values are modified according to design-basis earthquake level, location, and local site characteristics of the structure. Response spectrum analysis can be convenient for design purposes, as it is a linear elastic analysis and maximum response quantities can be conveniently determined under a certain earthquake loading level without use of any ground motion record. On the other hand, for performance assessment purposes or when more accurate information on the seismic behavior of a structure is needed, nonlinear time-history analysis is a useful tool as it allows for tracing the step-by-step response demand of a structure resulting from a ground acceleration time-history of an earthquake record. However, analysis run times can be significantly longer than single-step elastic analysis and multiple number of analyses are generally required for meaningful interpretation of response demands.

TBEC [3] requires that at least 11 earthquake ground motion records shall be applied in time-history analysis. In addition, both orthogonal horizontal components of these records should be applied to the X and Y axes of the structure at the same time, while another analysis shall be run when horizontal components acting along X and Y are interchanged, leading to two analyses for a single ground motion record.

In the following paragraphs, some of the past studies in literature that used time-history analysis method for performance evaluation of buildings are reviewed.

Bagheri [25] conducted response spectrum and time-history analyses of 20-story buildings having irregularities at different heights for different shear wall groups by using ETABS and SAP2000 analysis software and concluded that story displacements obtained from response spectrum analysis method are larger compared to time-history analysis, thus leading uneconomical results.

Patil [26] made time-history analyses on a 10-story building by using five different earthquake ground motion record and found out that time-history analysis method gave safer results.

Harshita [27] compared response spectrum analysis and time-history analysis methods on the seismic response of multi-story symmetrical structures by using the structural analysis software Staad-Pro and observed that base shear forces obtained from time-history analysis is slightly higher than the ones obtained from response spectrum analysis method.

Bhagwat [28] compared the results of response spectrum and time-history analyses of two different earthquakes using the structural analysis software ETABS and concluded that the response spectrum analysis results were 50% higher than the results obtained from time-history analysis.

Padol [29] used time-history analysis method to evaluate structures with mass irregularities and concluded that the best way to deal with such irregularities would be to add shear walls or base isolators.

Dubey [30] compared time-history analysis and response spectrum analysis in the structural analysis software Staad-Pro on a 20-story structure. It was observed that the response spectrum analysis results yielded lower story drifts for tall buildings, while story shear forces being larger. In this case, the study recommended the use of time-history analysis method, especially for high-rise buildings, for achieving safer and more economical structures.

4.2 Ground Motion Dataset

An earthquake ground motion dataset is generated by selecting real ground acceleration time-histories available in PEER NGA [31] database. TBEC [3] recommends that accelerograms in the dataset should be selected from earthquake events that have a magnitude range compatible with design earthquake ground motion level and considering fault-to-site distance, source mechanism and local site conditions of the building of interest. In this regard, the criteria shown in Table 4.1 is taken into consideration for selecting the ground motion records in the dataset. In addition, during the selection process, the design lateral acceleration response spectrum (5% damping) for the accepted building site location and local soil condition is set as the target spectrum for matching the spectral acceleration values. The PEER NGA [31] database website has the feature of selecting the appropriate records from its database in accordance with the criteria and target spectrum set by the user. The names of the selected 11 ground motion records and scaling coefficients used for spectral matching are given in Table 4.2. The ground acceleration versus time histories of each ground motion record in the data set are presented in Figures 4.1 to 4.22.

Table 4.1 Searching criteria for selection of ground motion records from PEER NGA database.

Criteria	**Selection range**
Earthquake magnitude, M_w	6.5 - 7.5
Rupture distance	10 - 30 km
Shear wave velocity, VS30	360 - 760 m/sec
Effective duration	15 - 60 sec
Scale factor (for spectral matching)	0.1 - 4
Fault type	Strike slip (SS)

Table 4.2 Ground motion records selected in the dataset.

Ground Motion Number	PEER NGA number	Earthquake Name	Year	Station Name	Magnitude	Scale Factor
1	0164	Imperial Valley-06	1979	Cerro Prieto	6.53	0.8543
2	0864	Landers	1992	Joshua Tree	7.28	0.5533
3	0881	Landers	1992	Morongo Valley Fire Station	7.28	0.7712
4	1614	Duzce - Turkey	1999	Lamont 1061	7.14	1.5519
5	1633	Manjil - Iran	1990	Abbar	7.37	0.3183
6	3753	Landers	1992	Fun Valley	7.28	0.8487
7	3757	Landers	1992	North Palm Springs Fire Sta #36	7.28	1.1042
8	3759	Landers	1992	Whitewater Trout Farm	7.28	1.5118
9	3907	Tottori - Japan	2000	OKY004	6.61	0.6593
10	6915	Darfield - New Zealand	2010	Heathcote Valley Primary School	7	0.5114
11	6971	Darfield - New Zealand	2010	SPFS	7	0.832

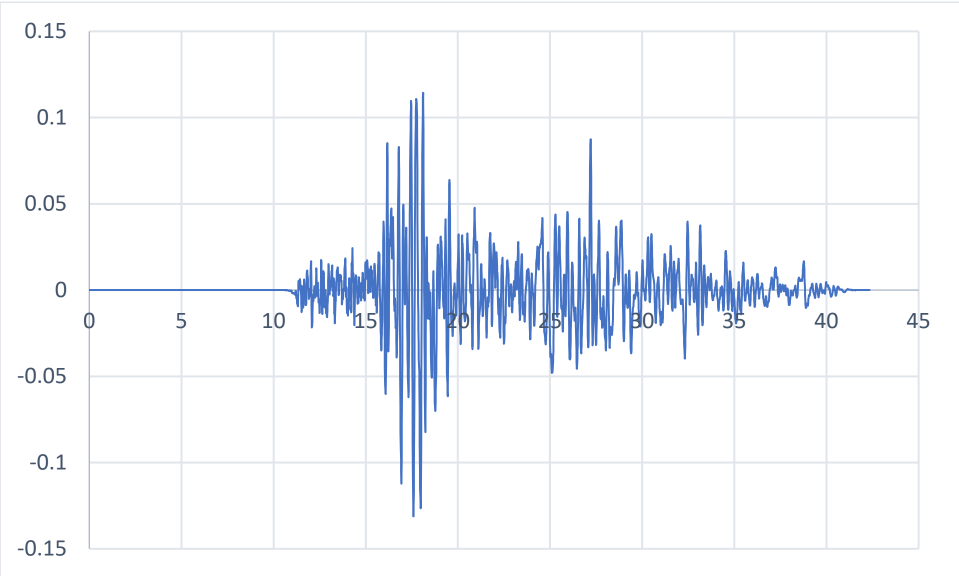

Figure 4.1 Time History Data for RSN1614_Duzce_1061-E

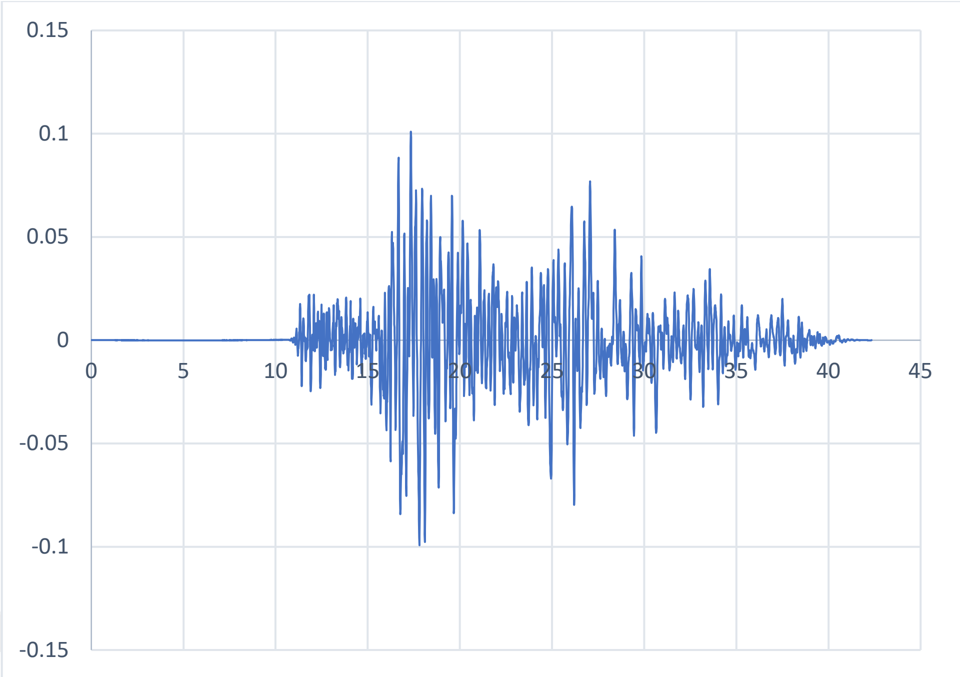

Figure 4.2 Time History Data for RSN1614_Duzce_1061-N

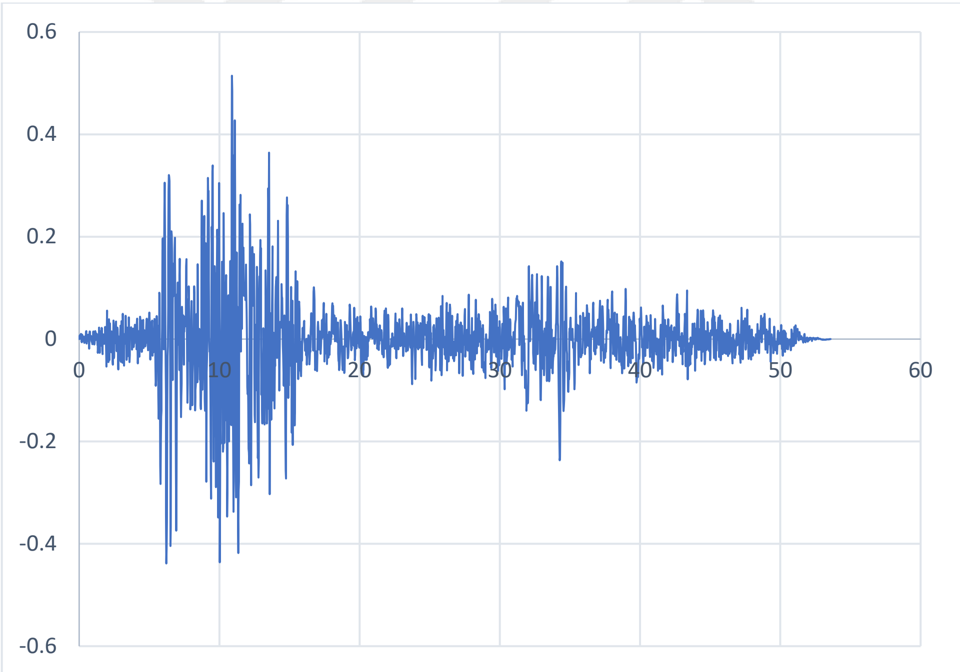

Figure 4.3 Time History Data for RSN1633_Manjil_Abbar--L

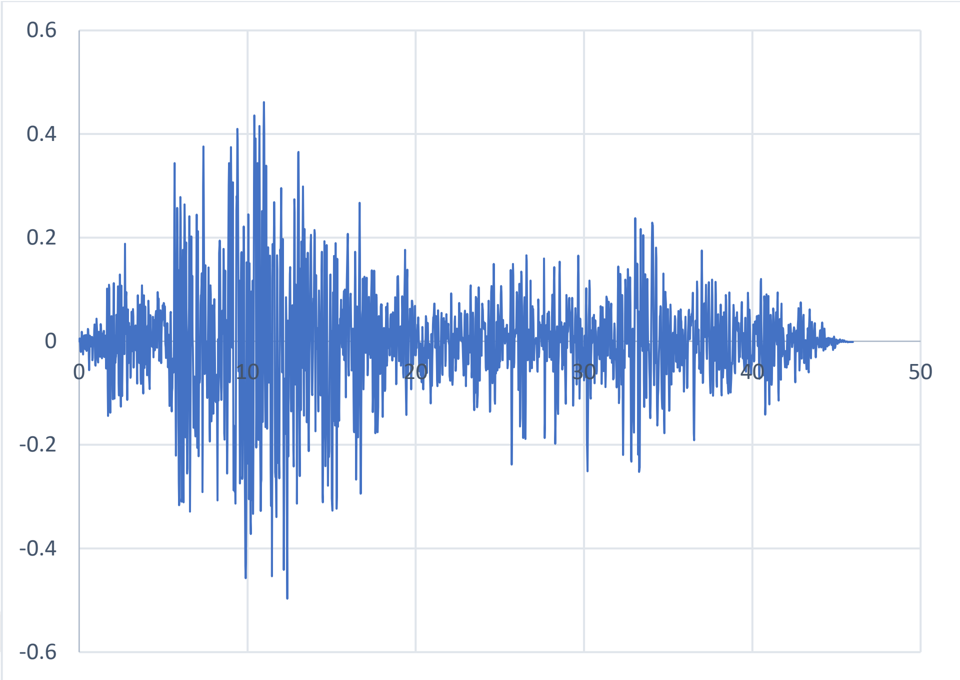

Figure 4.4 Time History Data for RSN1633_Manjil_Abbar—T

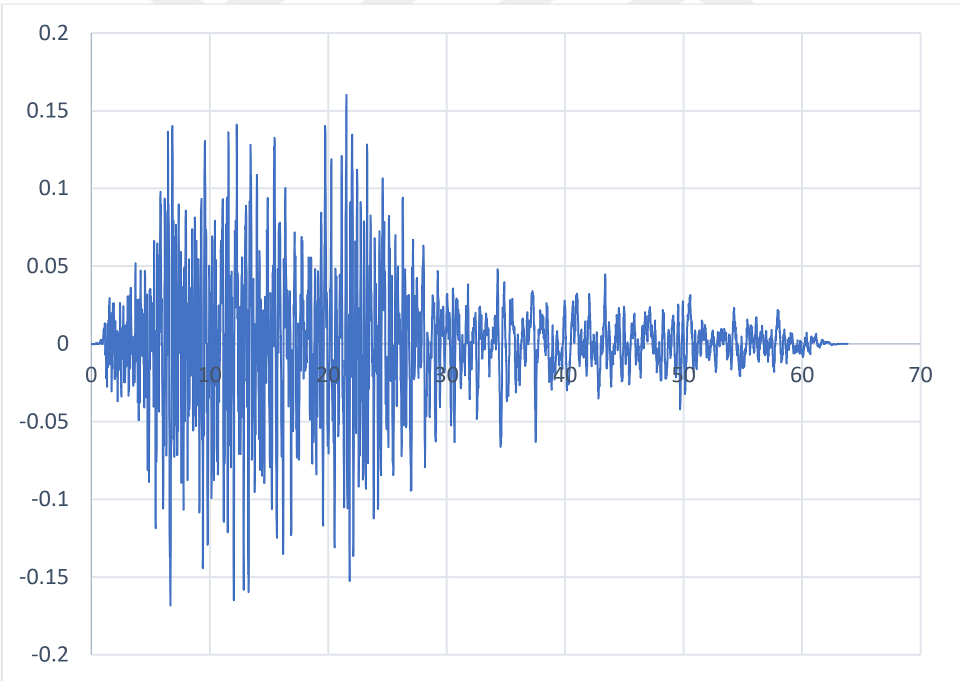

Figure 4.5 Time History Data for RSN164_Impall.h-CPE147

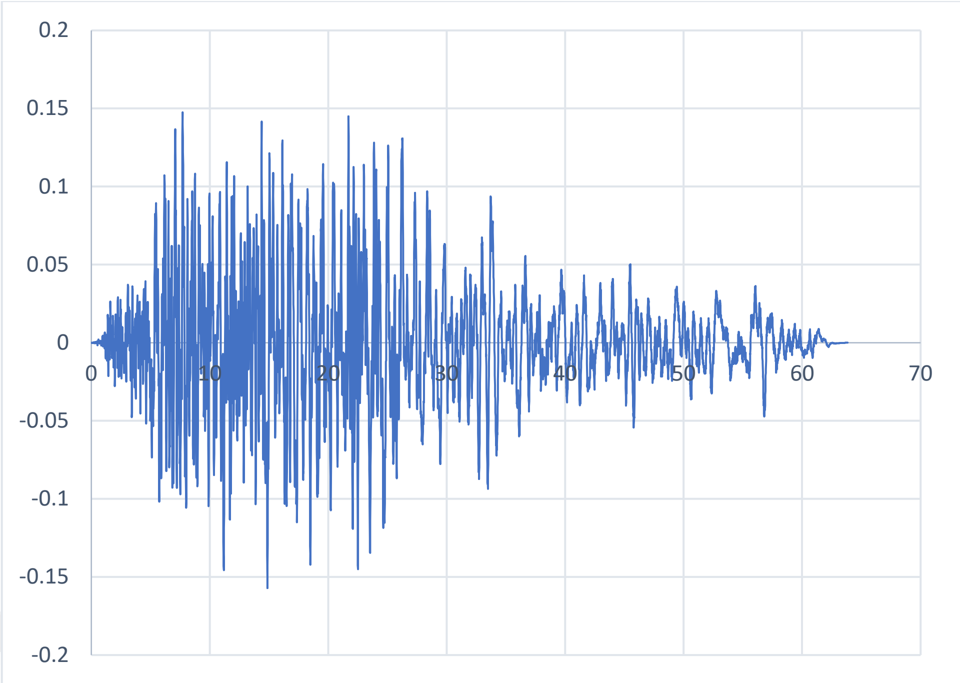

Figure 4.6 Time History Data for RSN164_Impall.h-CPE237

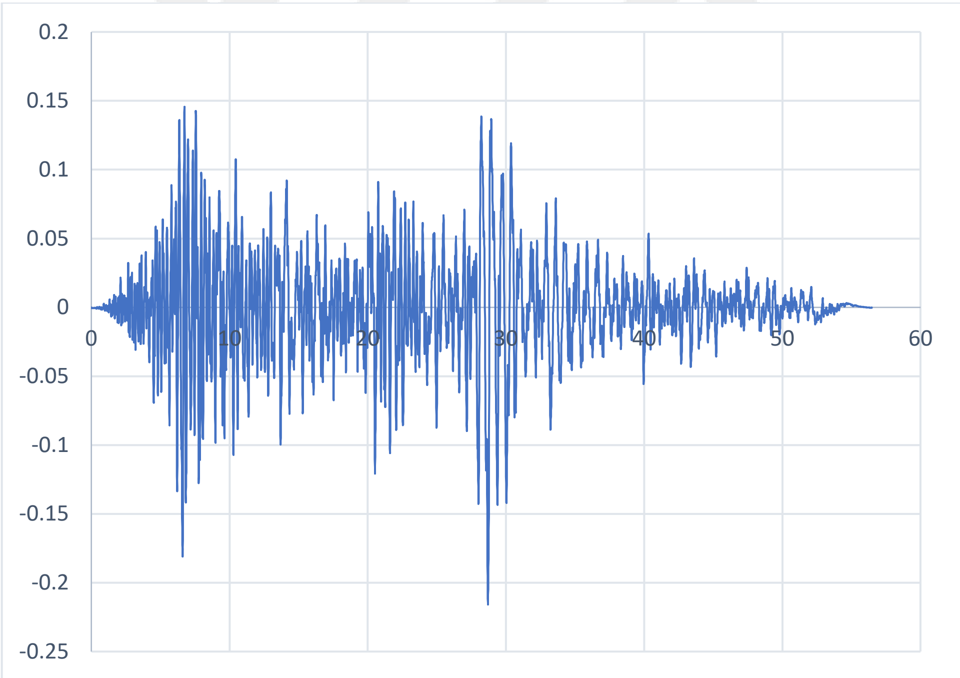

Figure 4.7 Time History Data for RSN3753_Landers_FVR045

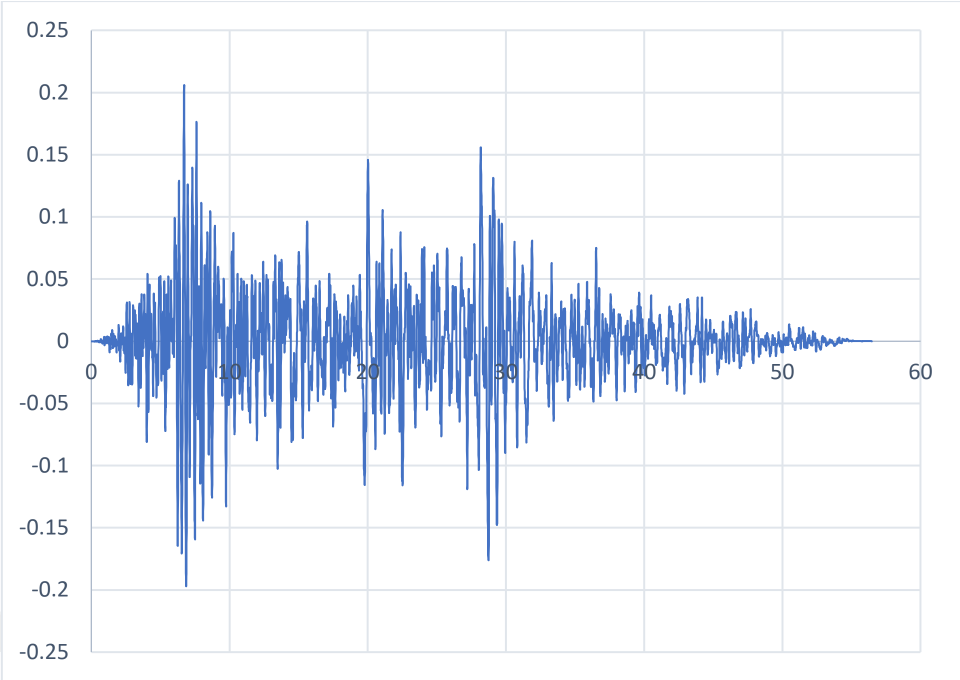

Figure 4.8 Time History Data for RSN3753_Landers_FVR135

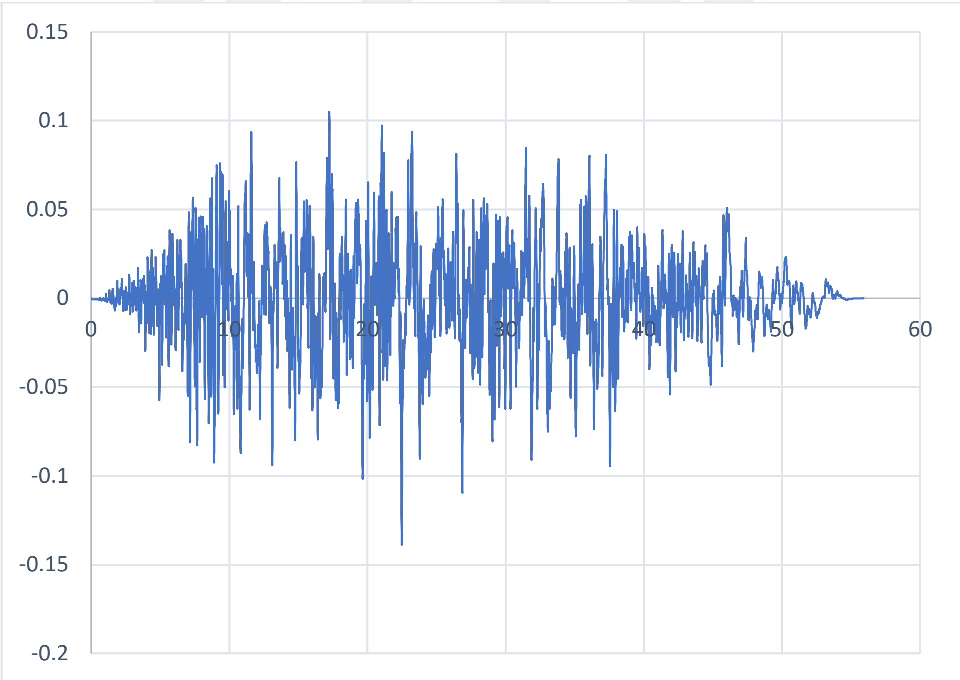

Figure 4.9 Time History Data for RSN3757_Landers_NPF090

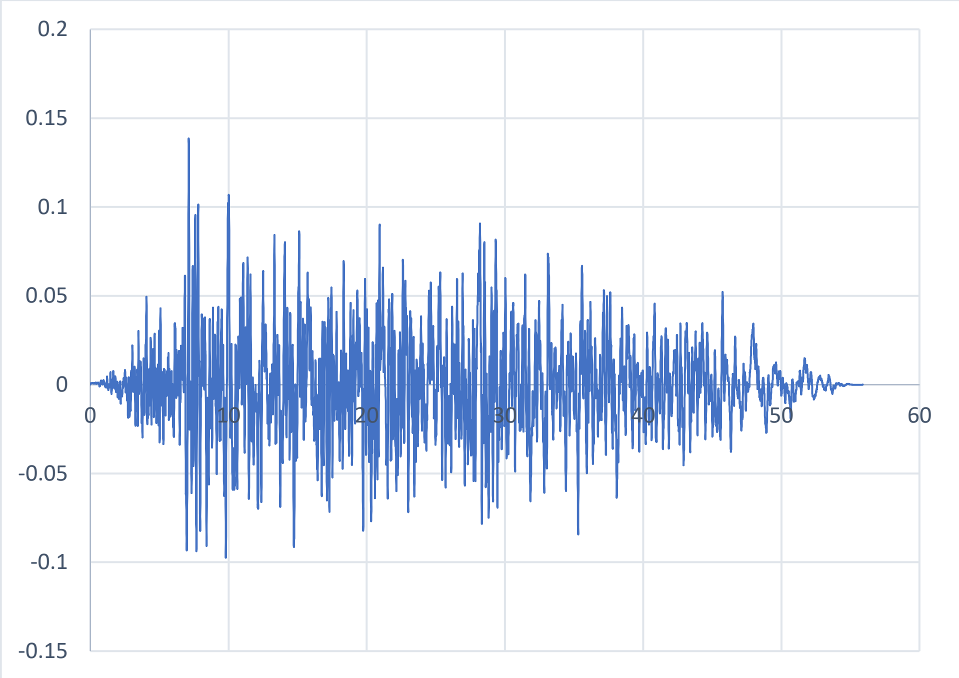

Figure 4.10 Time History Data for RSN3757_Landers_NPF180

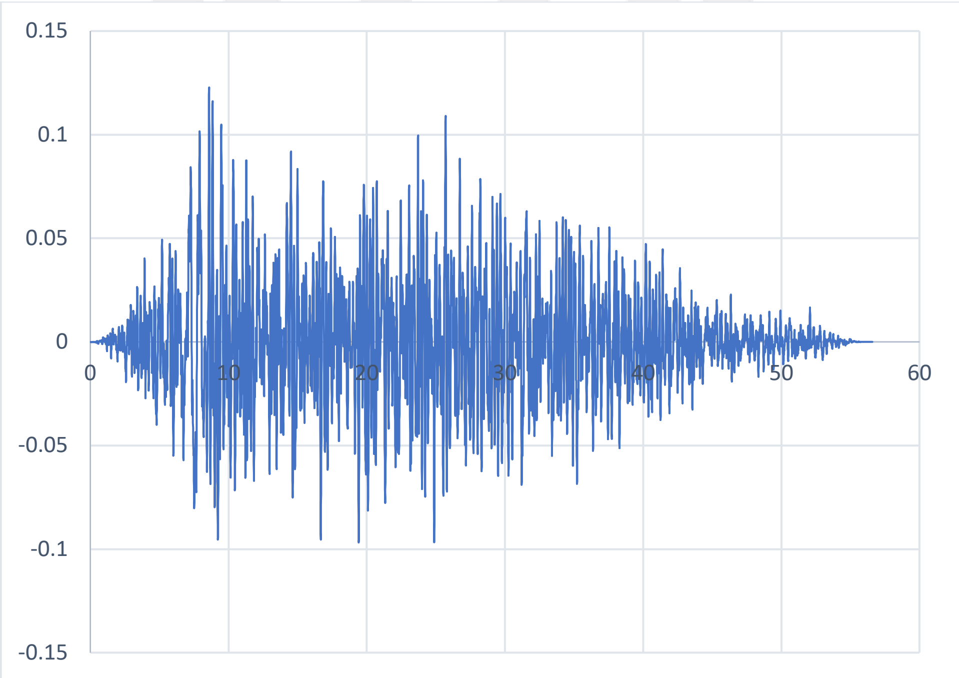

Figure 4.11 Time History Data for RSN3759_Landers_WWT180

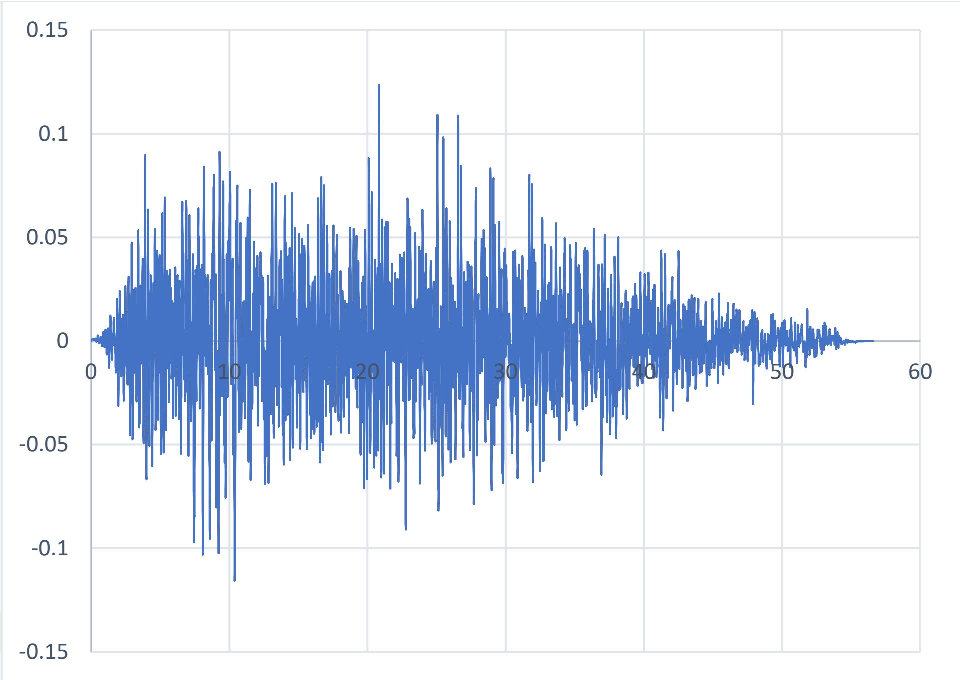

Figure 4.12 Time History Data for RSN3759_Landers_WWT270

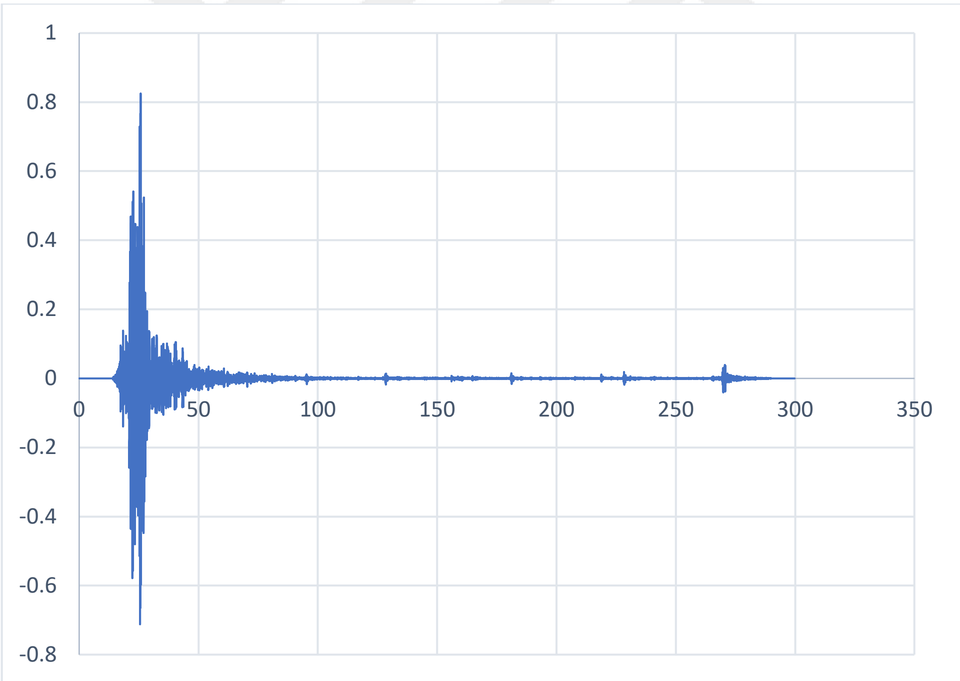

Figure 4.13 Time History Data for RSN3907_Tottori_OKY004EW

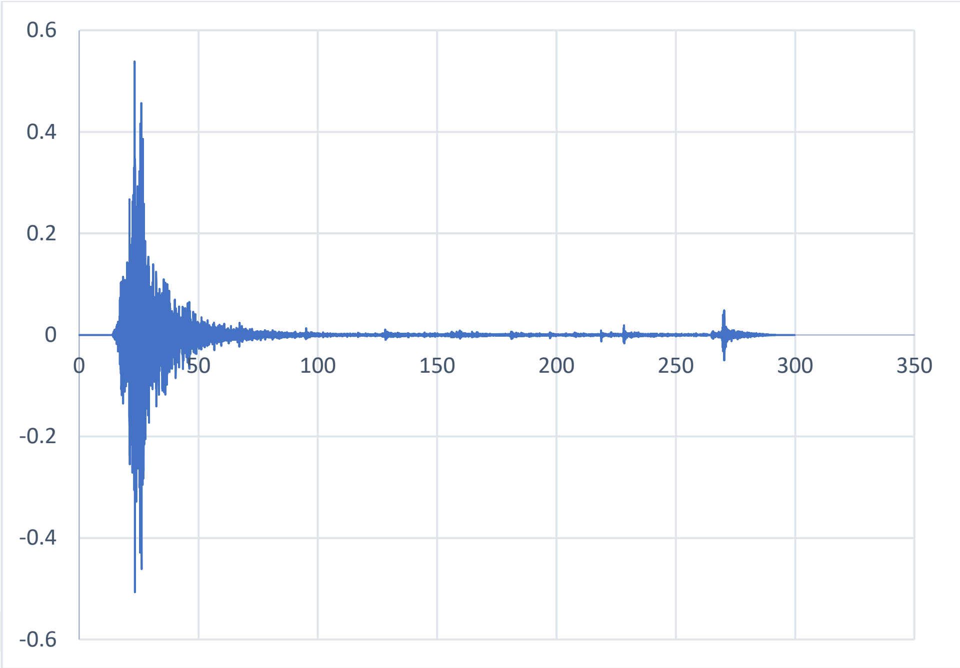

Figure 4.14 Time History Data for RSN3907_Tottori_OKY004NS

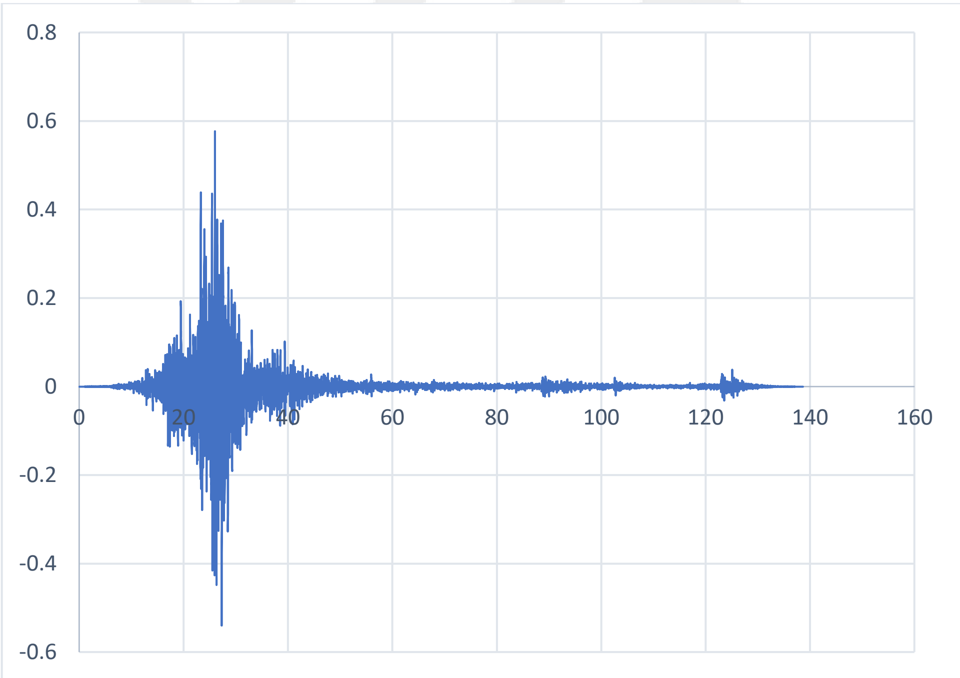

Figure 4.15 Time History Data for RSN6915_Darfield_HVSCS26W

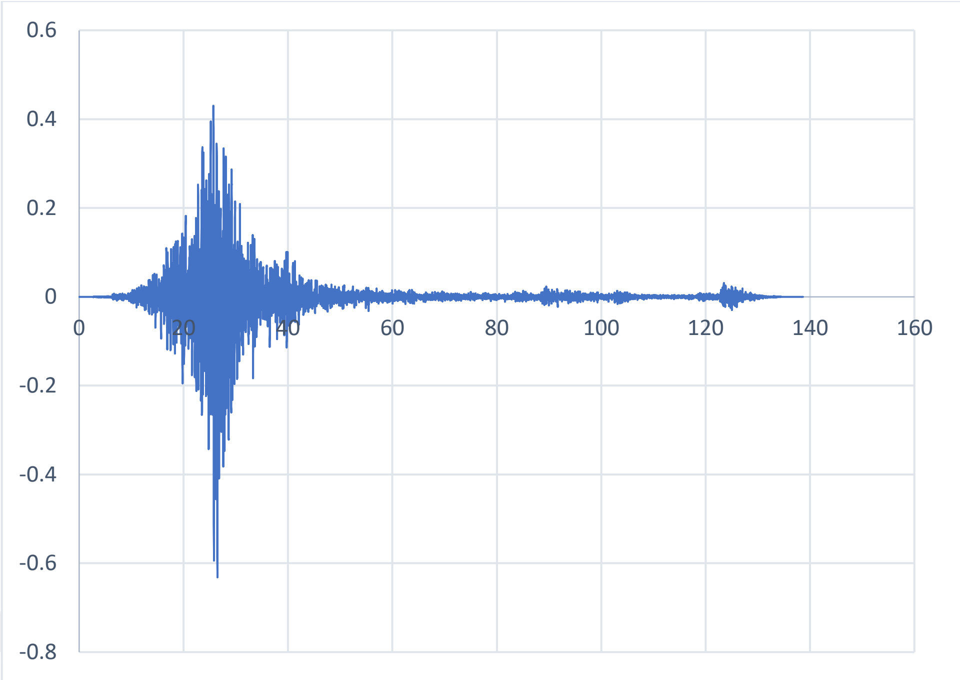

Figure 4.16 Time History Data for RSN6915_Darfield_HVSCS64E

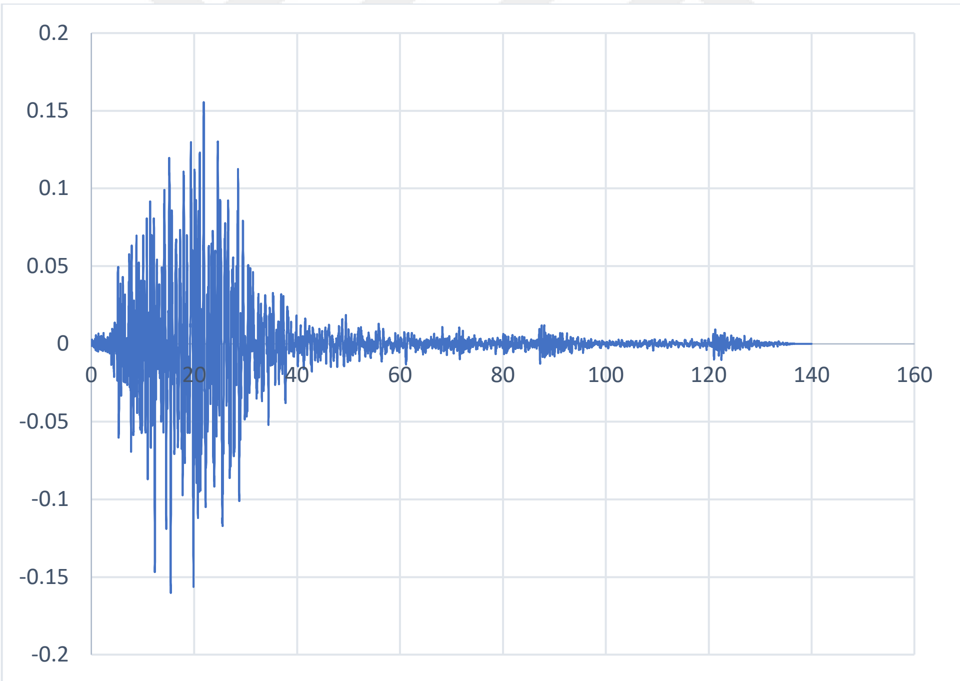

Figure 4.17 Time History Data for RSN6971_Darfield_SPFSN17E

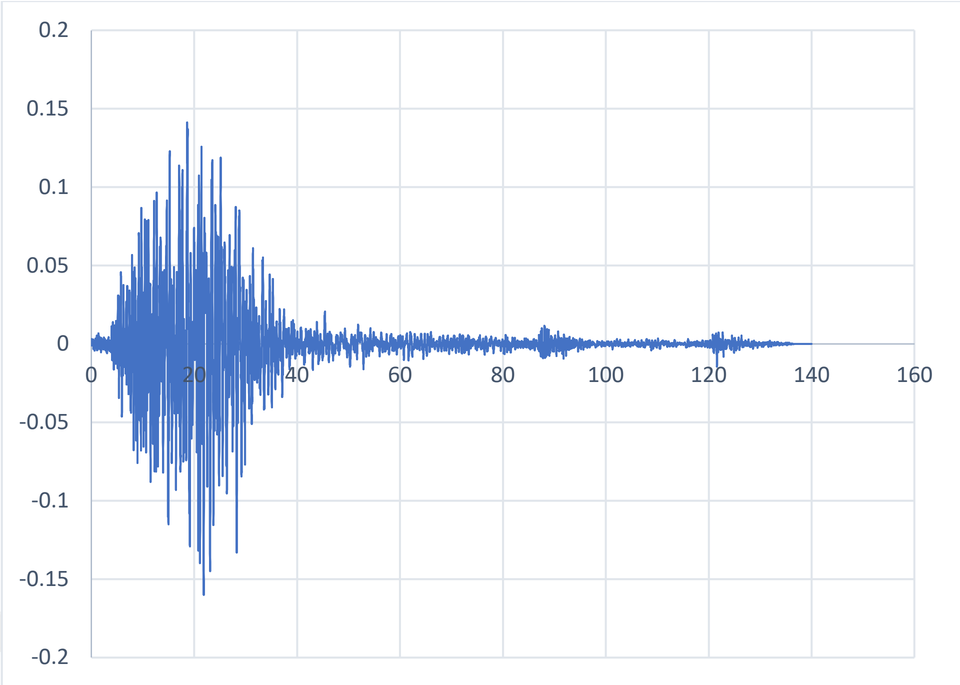

Figure 4.18 Time History Data for RSN6971_Darfield_SPFSN73W

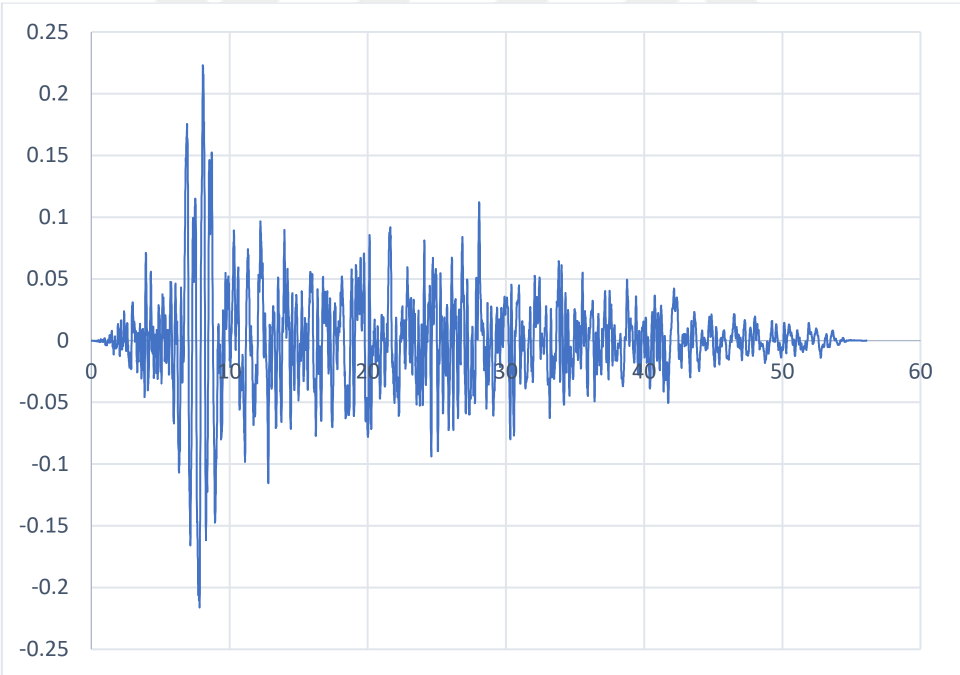

Figure 4.19 Time History Data for RSN881_Landers_MVH045

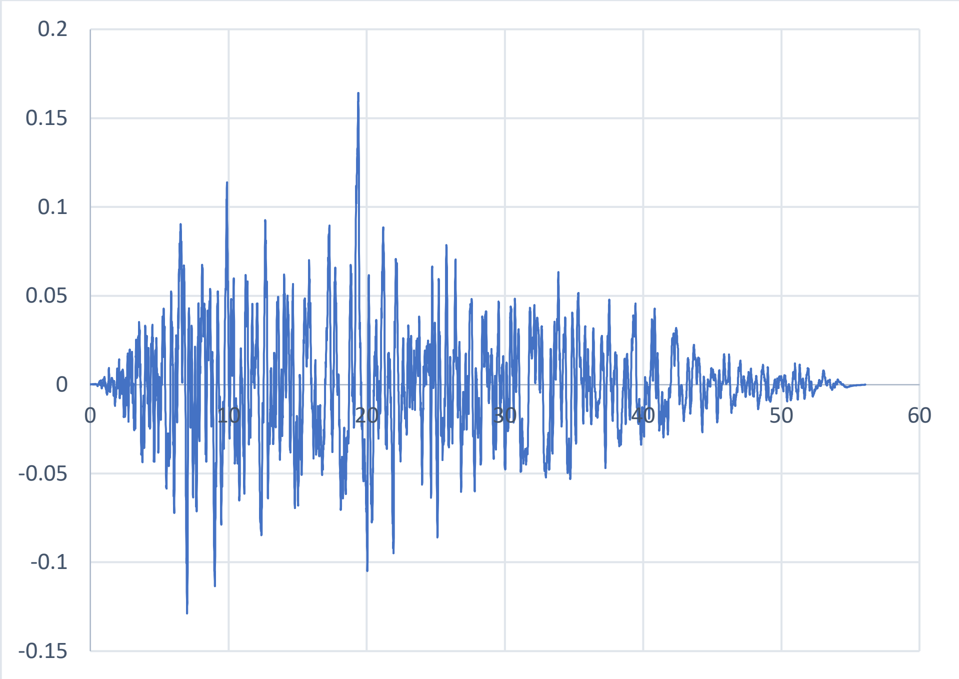

Figure 4.20 Time History Data for RSN881_Landers_MVH135

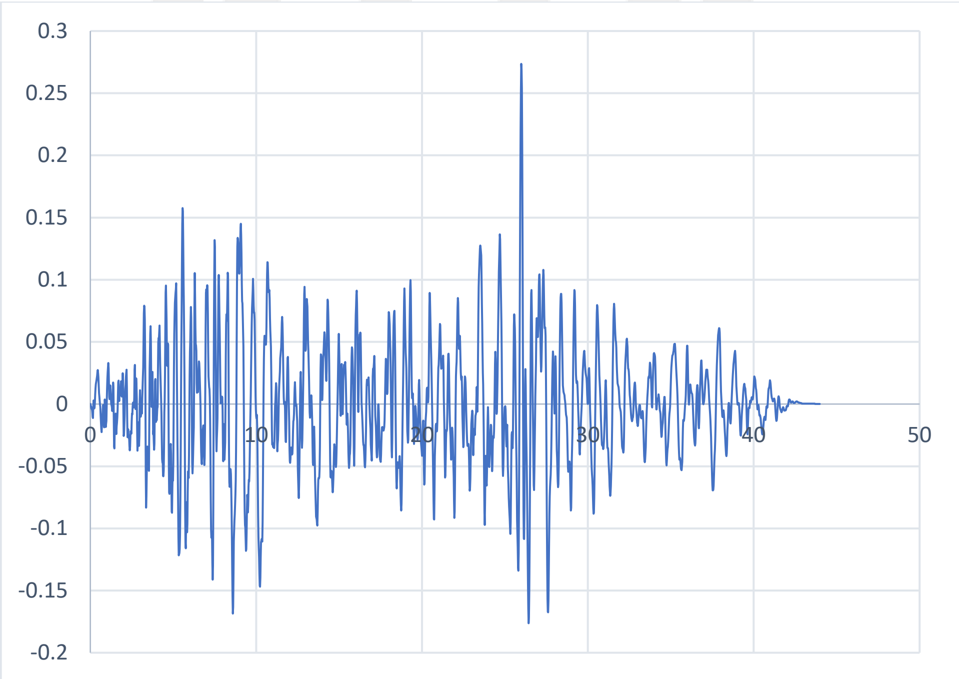

Figure 4.21 Time History Data for RSN864_Landers_JOS000

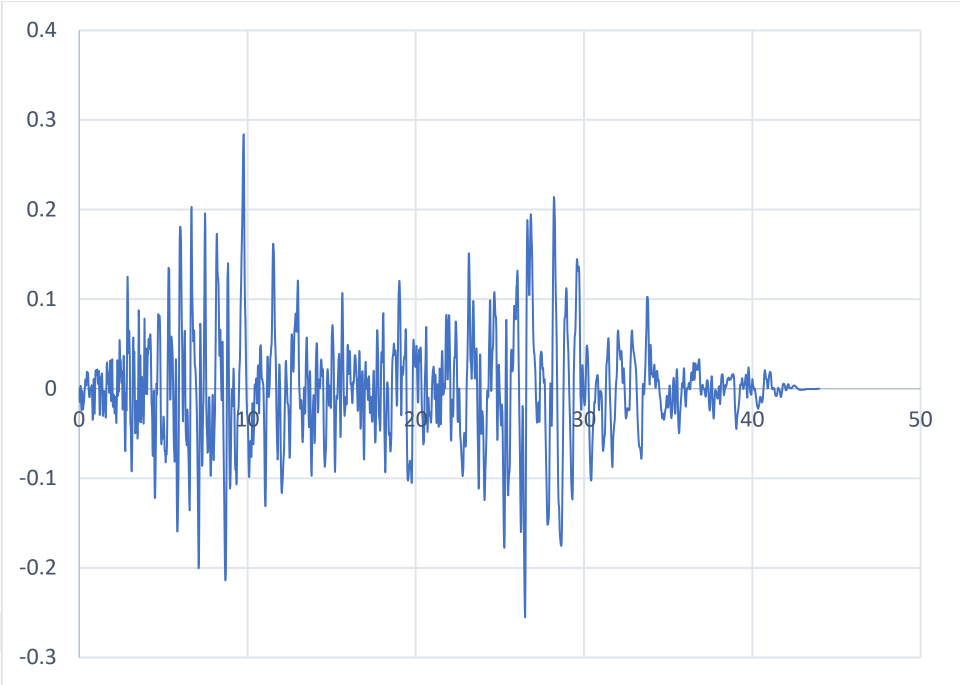

Figure 4.22 Time History Data for RSN864_Landers_JOS090

4.3 Relative Story Drifts

In this section, it is tried to determine the order of the relative story drifts by time-history analysis. The maximum drift values resulting from the identification of 11 earthquake records and 2 components are presented graphically. In Section 3.5 of this study, the definition and calculation method for storey drifts were given. In this section, the related method is unchanged, but the storey drift values are obtained with the time-history analysis method. The comparison of the values obtained according to the analysis method is shared in the conclusion section. The study by Dok and Aktaş [32] supports the data in this study where it also proves that the concern at the study by A. Benavent-Climent, R. Zahran [4] need more attention.

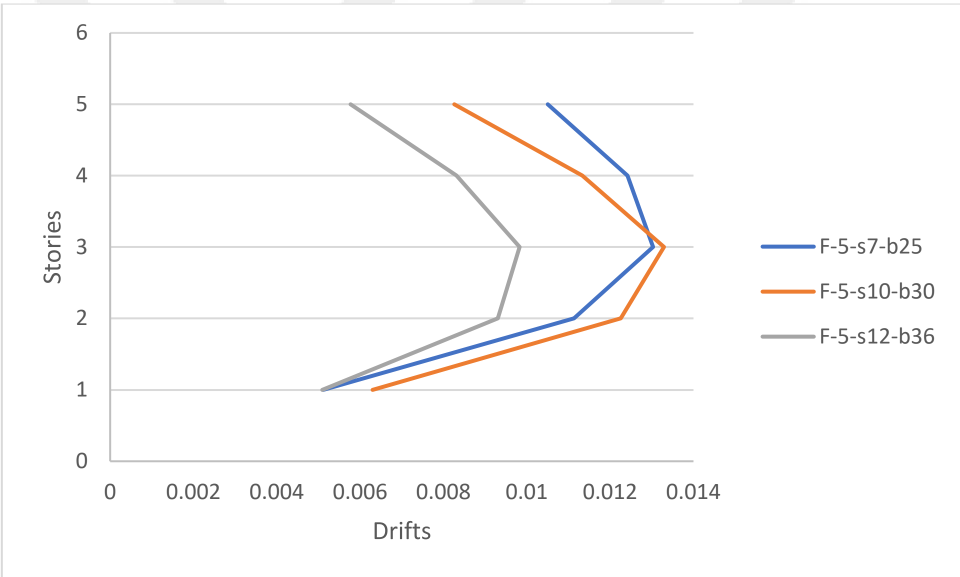

Figure 4.23 Story Drifts for 5 Floors Framed Only Structure X Direction

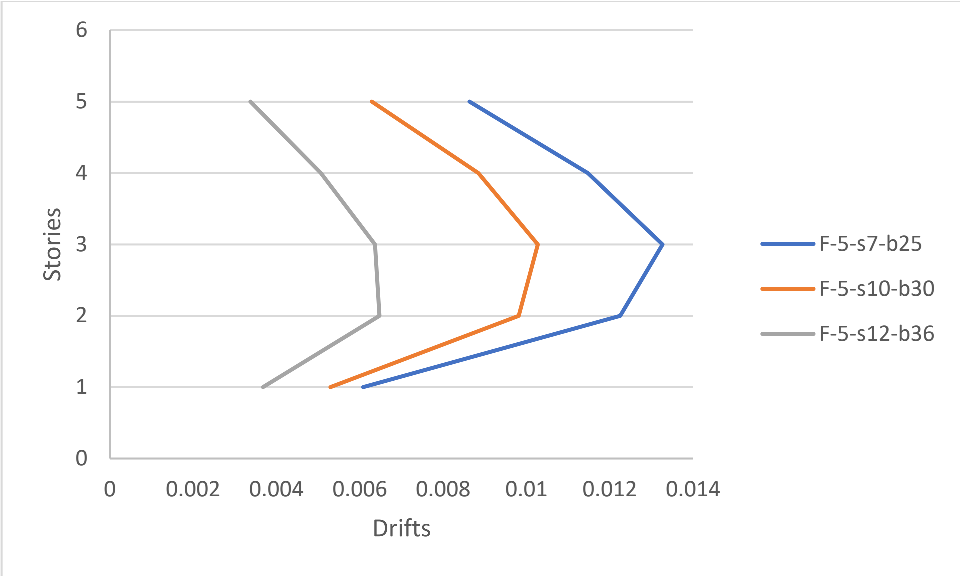

Figure 4.24 Story Drifts for 5 Floors Framed Only Structure Y Direction

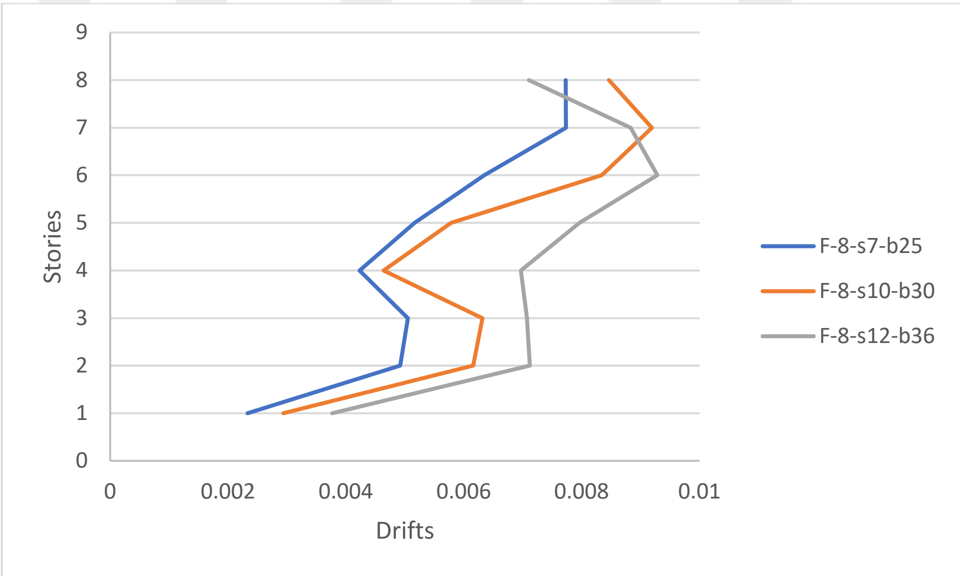

Figure 4.25 Story Drifts for 8 Floors Framed Only Structure X Direction

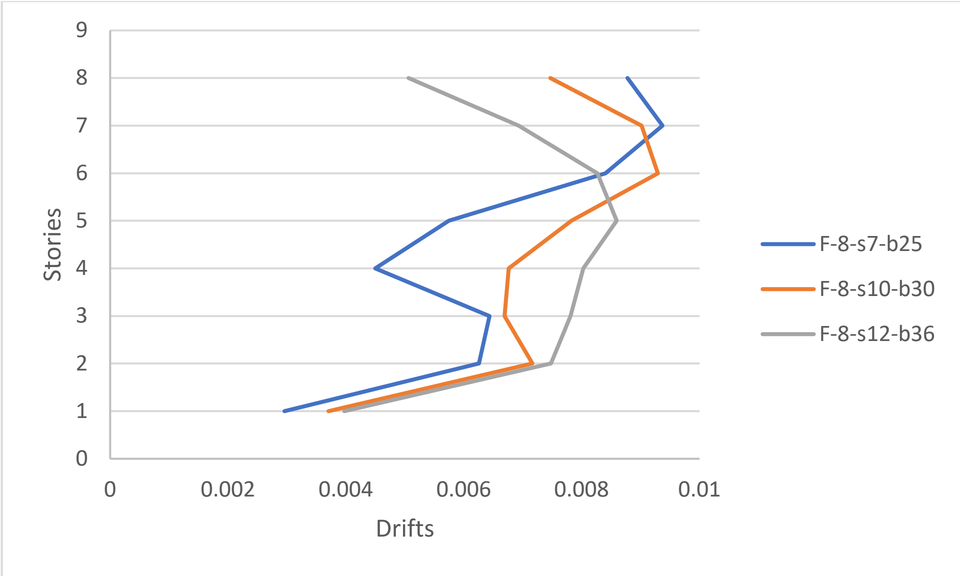

Figure 4.26 Story Drifts for 8 Floors Framed Only Structure Y Direction

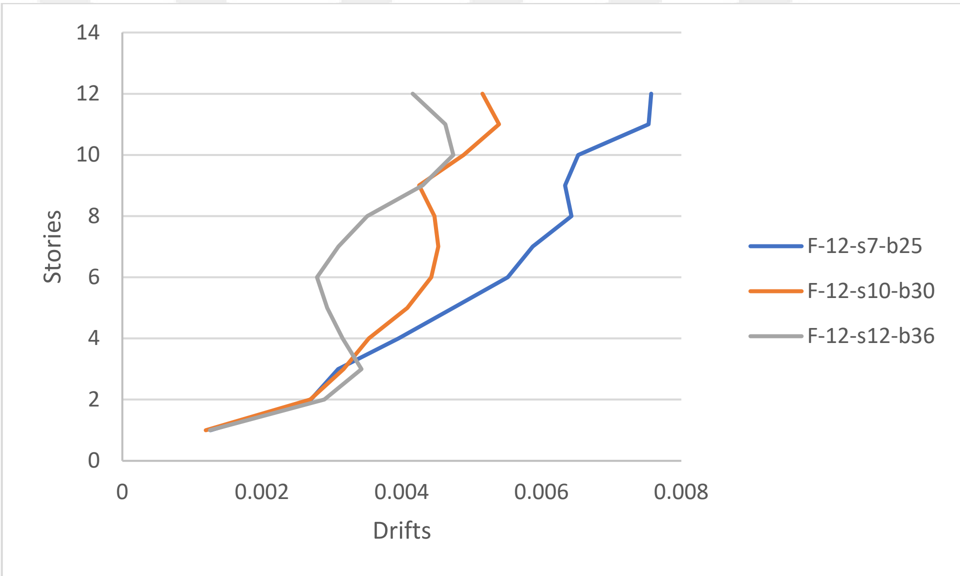

Figure 4.27 Story Drifts for 12 Floors Framed Only Structure X Direction

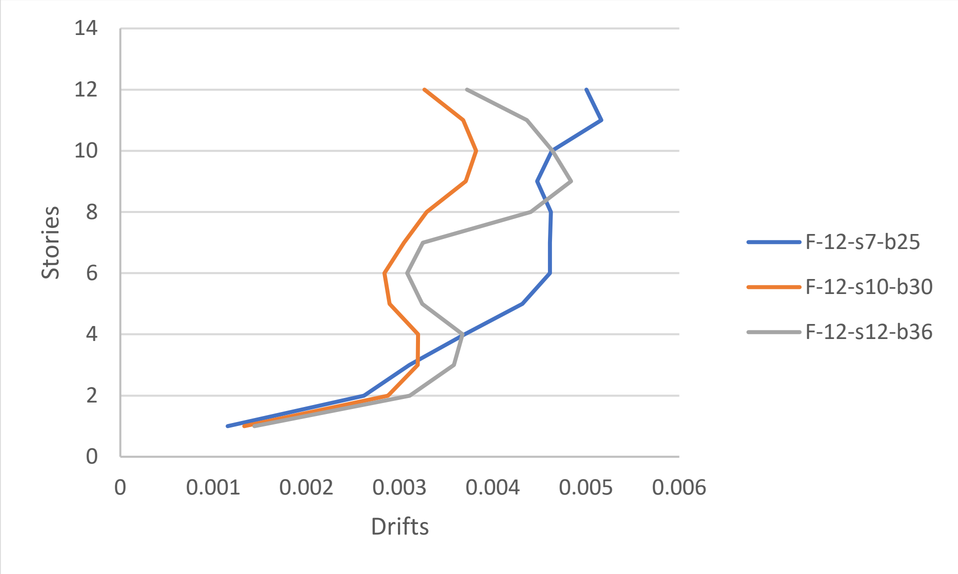

Figure 4.28 Story Drifts for 12 Floors Framed Only Structure Y Direction

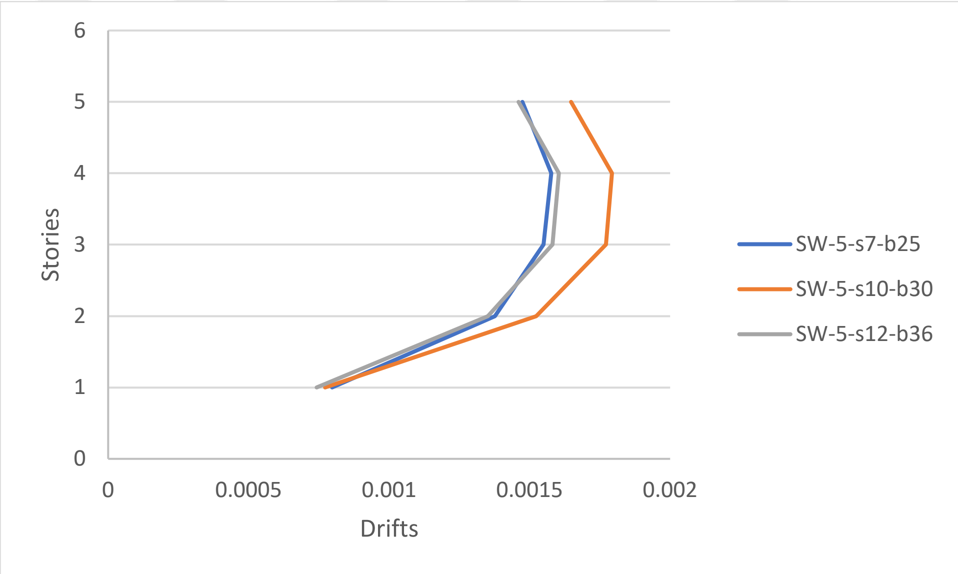

Figure 4.29 Story Drifts for 5 Floors Frame & Shear Wall Structure X Direction

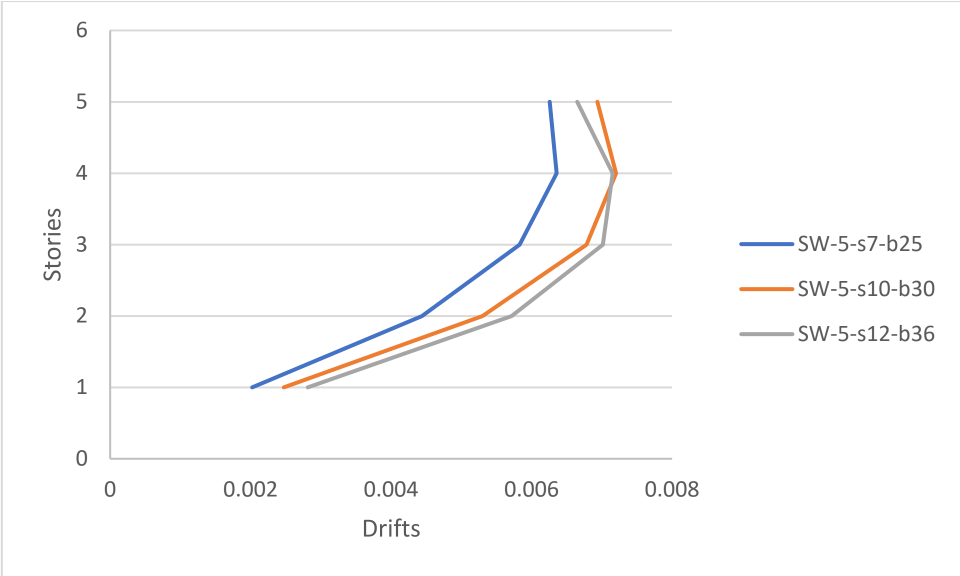

Figure 4.30 Story Drifts for 5 Floors Frame & Shear Wall Structure Y Direction

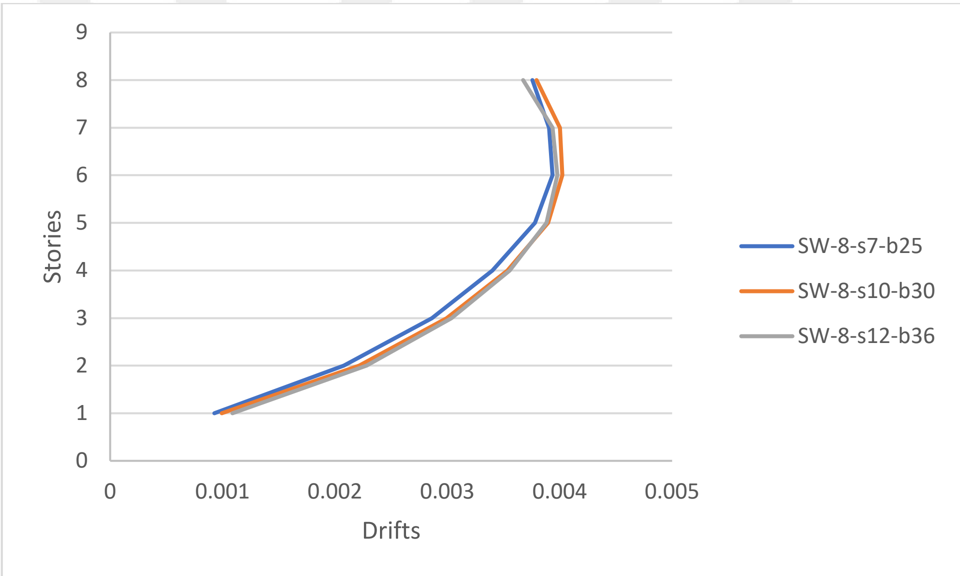

Figure 4.31 Story Drifts for 8 Floors Frame & Shear Wall Structure X Direction

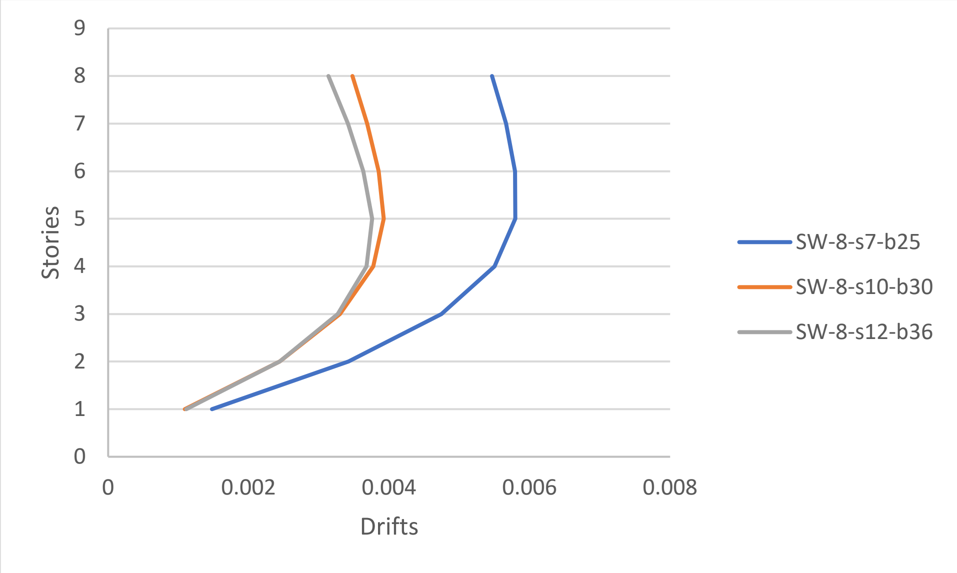

Figure 4.32 Story Drifts for 8 Floors Frame & Shear Wall Structure Y Direction

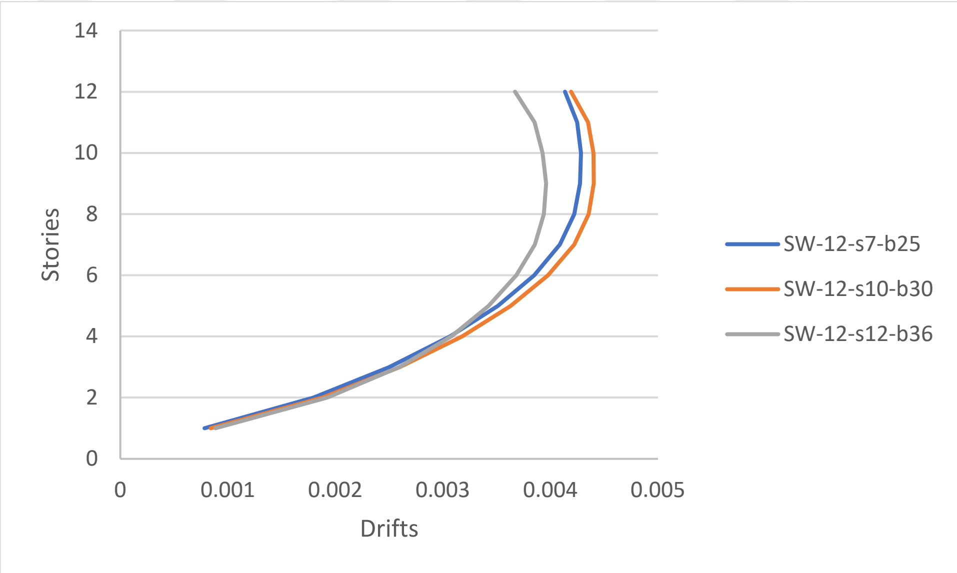

Figure 4.33 Story Drifts for 12 Floors Frame & Shear Wall Structure X Direction

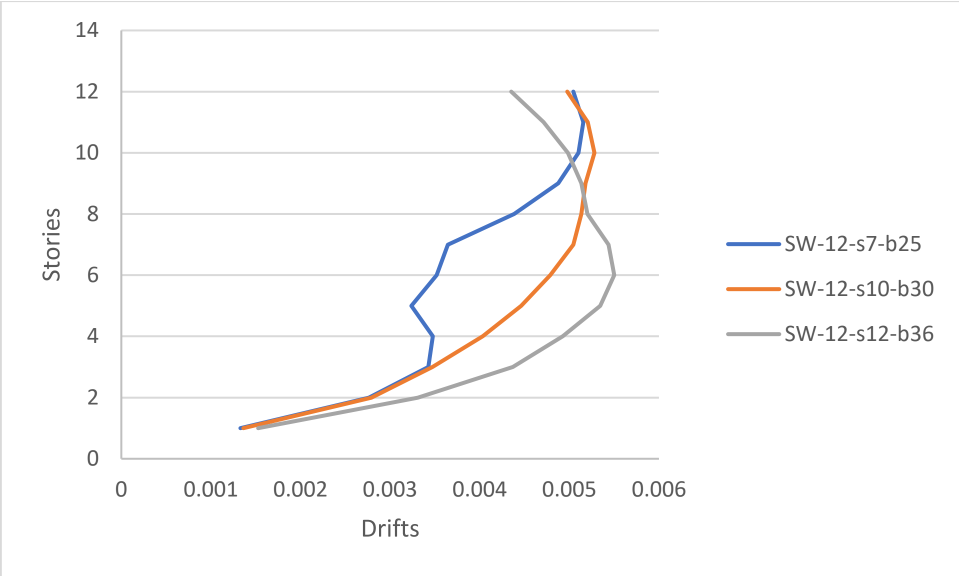

Figure 4.34 Story Drifts for 12 Floors Frame & Shear Wall Structure Y Direction

4.4 Story Forces Values

The horizontal forces induced in the structure by the earthquake accelerations are analysed for each t in time and the results are presented in this section. Each diagram is presented with positive and negative values for structures with the same number of storeys. Diagrams are separated according to x and y directions.

As in all nonlinear methods, a nonlinear incremental static calculation under non-earthquake loading is performed in the initial step of the calculation. As stated in 5.7.4, internal force demands will be calculated as the average of the largest absolute values of the results obtained from each of the analyses (2x11 = 22 analyses). In the graphs you will see below, the analyses were made on a system basis, not on an element basis where worst scenario is searching in this study. For this reason, the largest values obtained from 22 analyses are used to determine the limit values and to facilitate comparisons with other analysis methods.

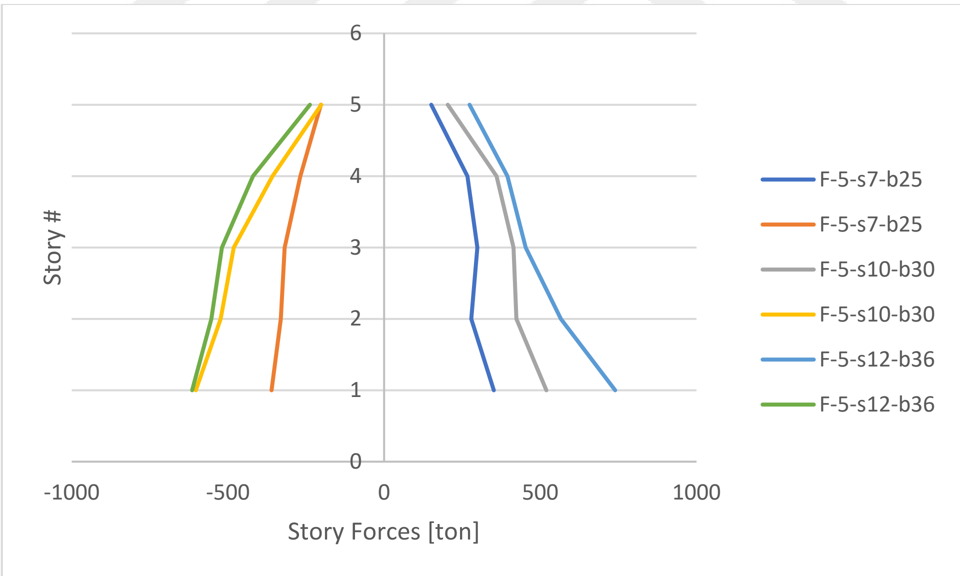

Figure 4.35 Story Forces for 5 Floors Frame Only Structure X Direction

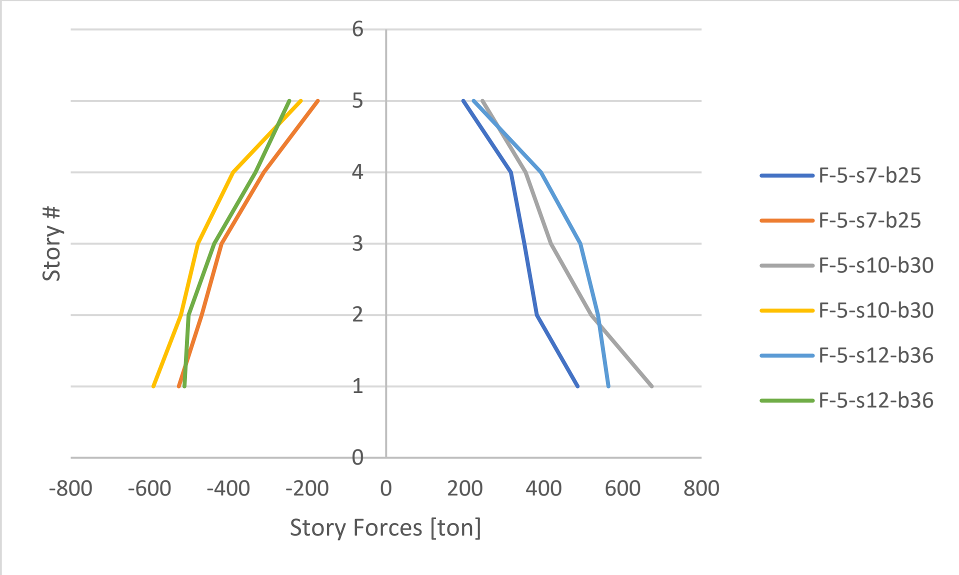

Figure 4.36 Story Forces for 5 Floors Frame Only Structure Y Direction

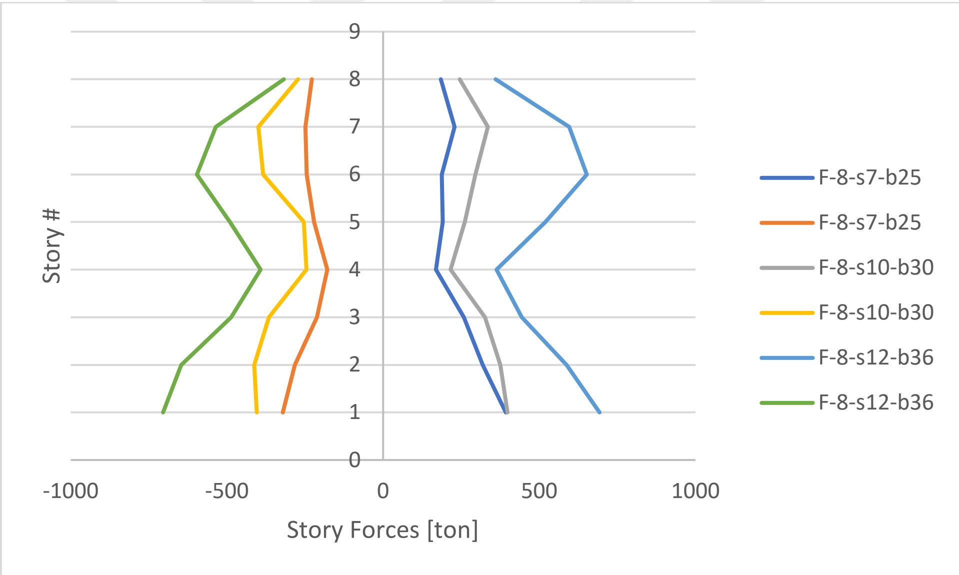

Figure 4.37 Story Forces for 8 Floors Frame Only Structure X Direction

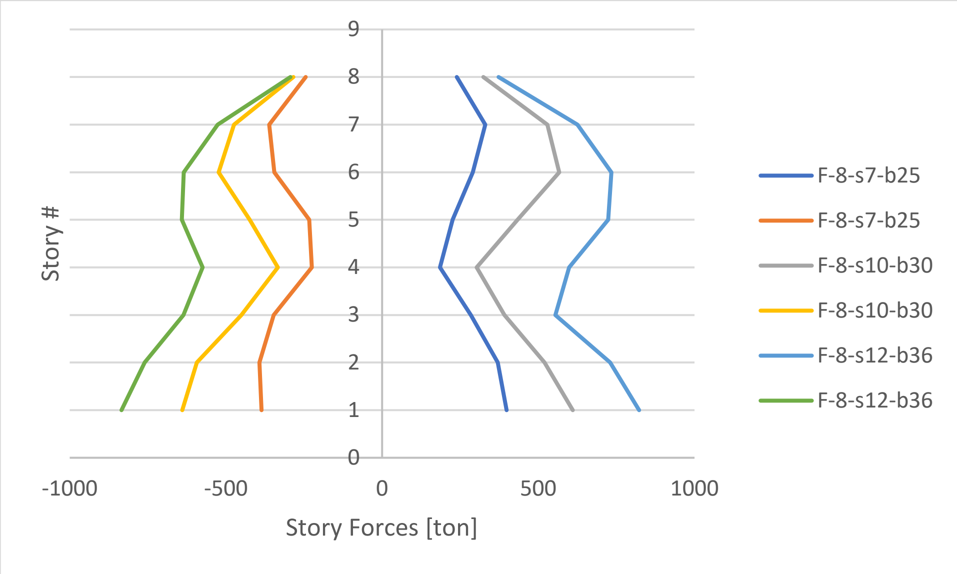

Figure 4.38 Story Forces for 8 Floors Frame Only Structure Y Direction

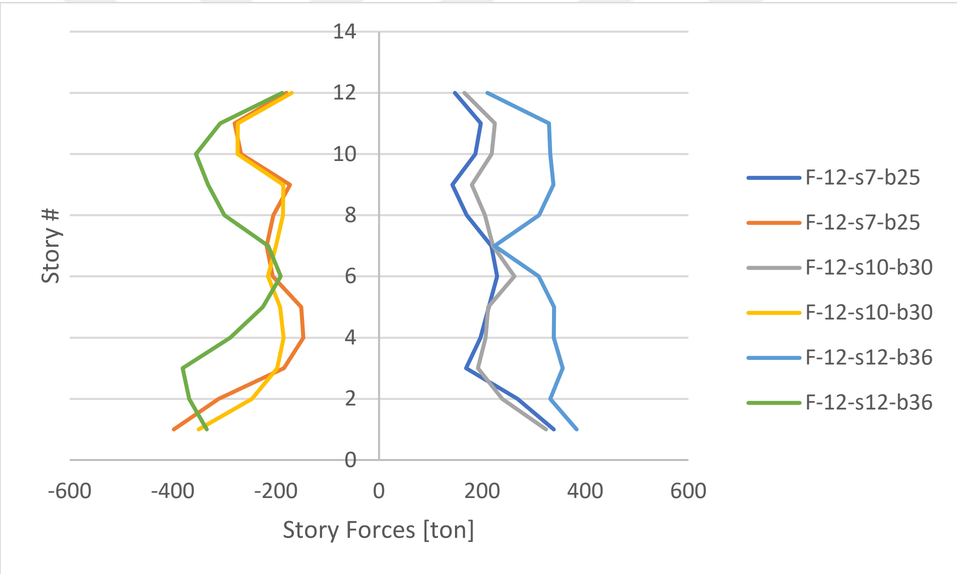

Figure 4.39 Story Forces for 12 Floors Frame Only Structure X Direction

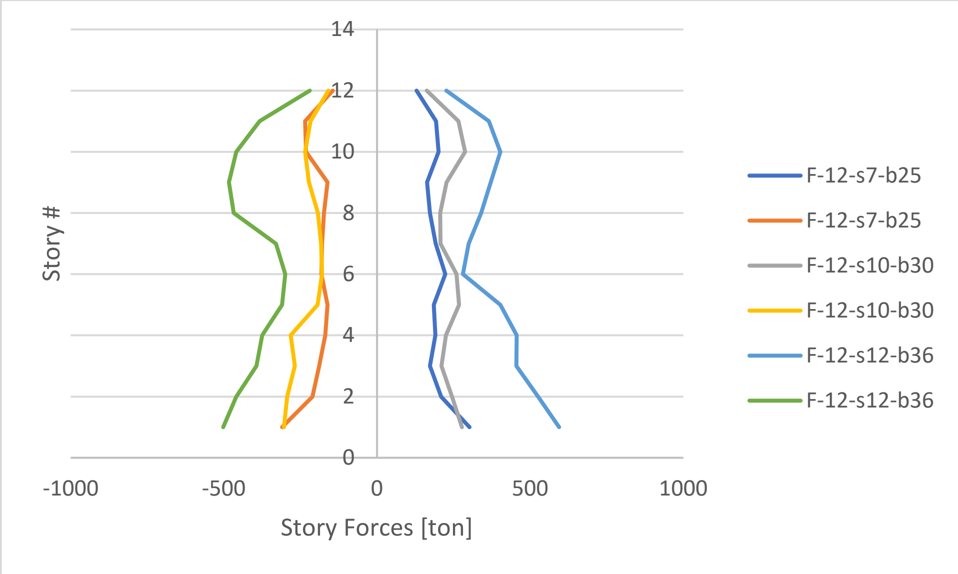

Figure 4.40 Story Forces for 12 Floors Frame Only Structure Y Direction

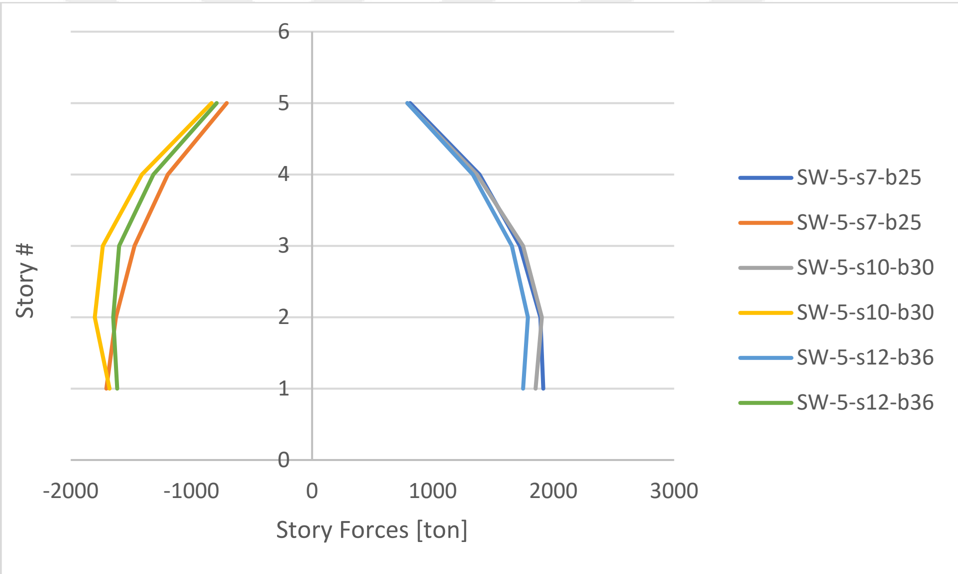

Figure 4.41 Story Drifts for 5 Floors Frame & Shear Wall Structure X Direction

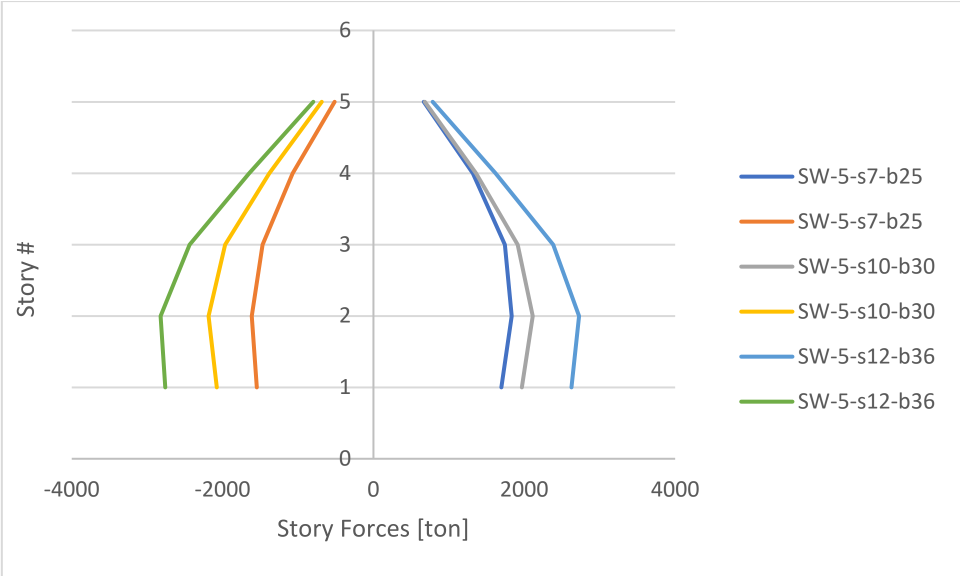

Figure 4.42 Story Drifts for 5 Floors Frame & Shear Wall Structure Y Direction

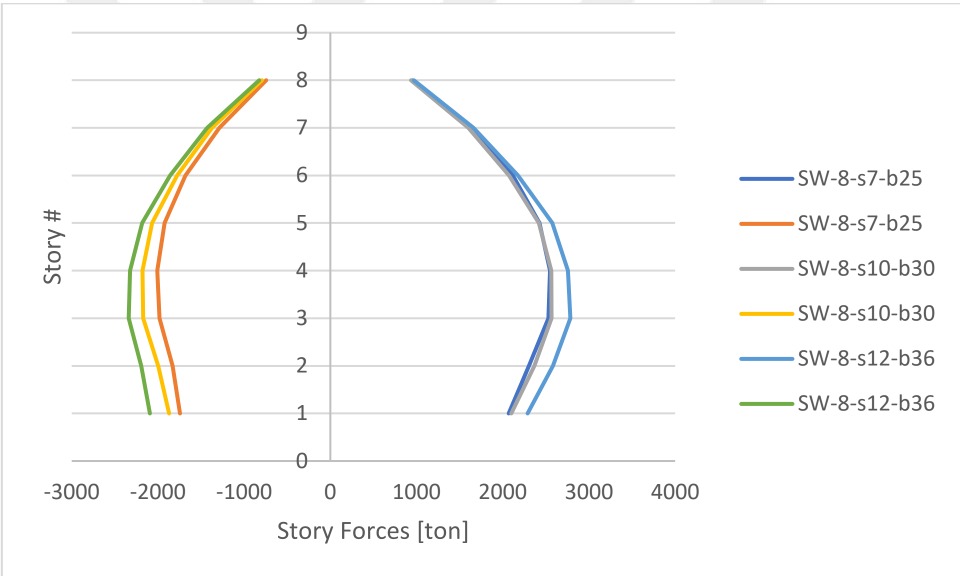

Figure 4.43 Story Drifts for 8 Floors Frame & Shear Wall Structure X Direction

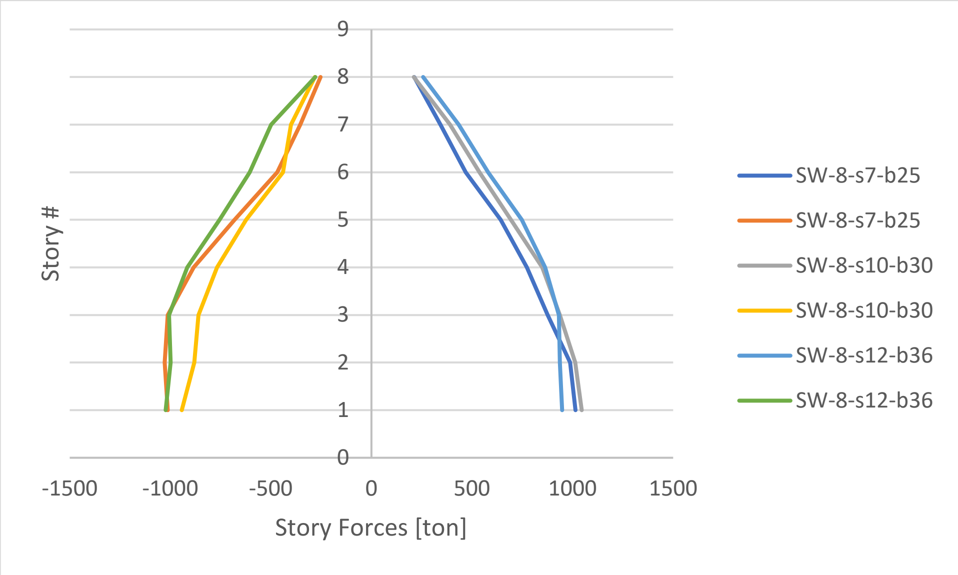

Figure 4.44 Story Drifts for 8 Floors Frame & Shear Wall Structure Y Direction

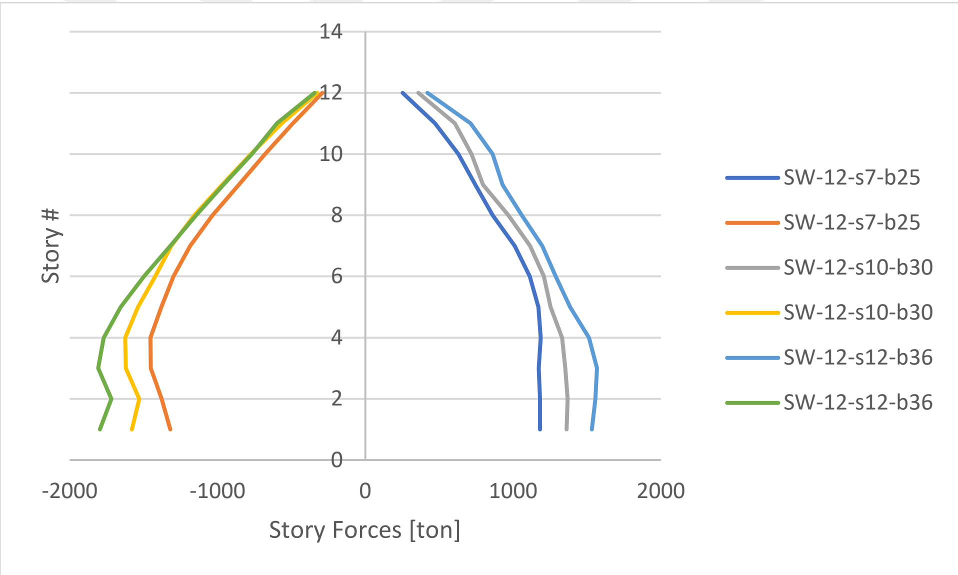

Figure 4.45 Story Drifts for 12 Floors Frame & Shear Wall Structure X Direction

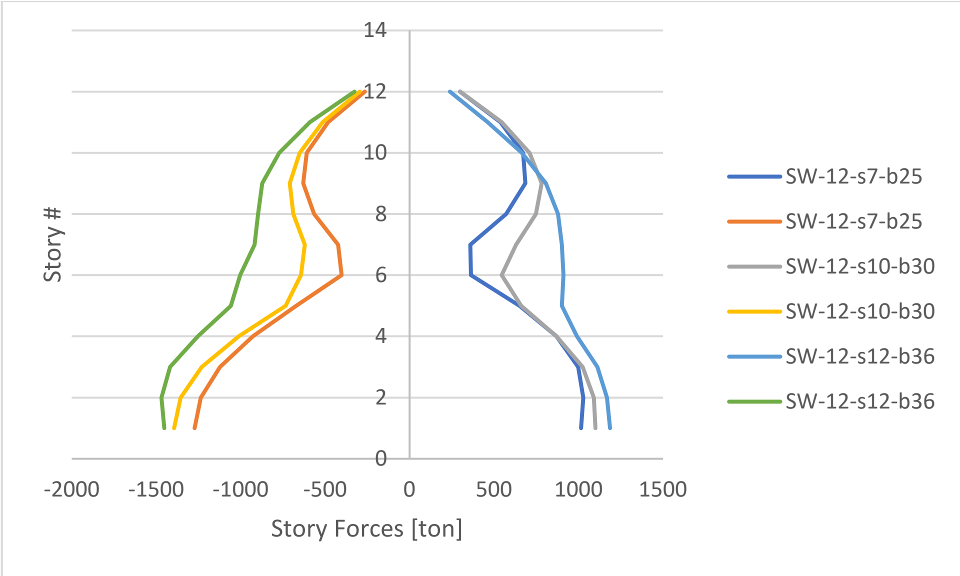

Figure 4.46 Story Drifts for 12 Floors Frame & Shear Wall Structure Y Direction

CHAPTER V

DEVELOPMENT OF SEISMIC FRAGILITY CURVES OF THE BUILDINGS

5.1 Introduction

In the previous chapters of this thesis, lateral force-displacement capacities of the investigated buildings were evaluated by nonlinear static (i.e. pushover) analysis, while force and displacement demand of these buildings under design-level earthquake loads were obtained through response spectrum and nonlinear time-history analyses. These analyses provide valuable insight on the seismic behavior of RC buildings with FJF systems, however performance assessment of these type of buildings under a wide range of seismic intensities would also be useful for future studies towards design and risk assessment of such structures. For this purpose, seismic fragility curves of the investigated buildings are generated in this chapter. Fragility curves are conditional probability functions that give the likelihood that the structure will meet or exceed a specified level of damage for a given ground motion intensity measure [33].

Fragility curves are convenient tools to provide the probabilities that seismic demands resulting from a range of earthquake intensities exceed structural capacities defined according to several performance levels. There are various methods in literature for producing seismic fragility curves of structures or group of structures, including empirical, expert-based, or analytical methods. In the present study, analytical method is utilized to generate the seismic fragility curves of the investigated buildings. The analytical method is mainly based on determining displacement (or deformation) demands of structures through nonlinear time-history analyses under a large number of earthquake ground motion records. The parameters of fragility function, which is generally taken as a cumulative lognormal function, can be estimated from alternative probabilistic approaches. Among these approaches, cloud analysis and incremental dynamic analysis (IDA) are the most used approaches for generating seismic fragility curves [34].

In cloud analysis approach, structural analyses are performed under a ground motion dataset that consists of a large number of earthquake records, where each record has a different amplitude (e.g. PGA) and frequency content. On the other hand, in IDA, a smaller size ground motion dataset is created, but each earthquake record is incrementally scaled up to a certain level based on the ground motion intensity parameter that is taken into consideration. In this thesis, IDA method is adopted, and the ground motion dataset constituted in Chapter 4 is used for time-history analyses.

The horizontal axis of a seismic fragility curve represents the intensity measure of earthquake hazard. Different seismic intensity measures have been tried out in literature for different types of structures based on various criteria such as practicality and efficiency of the intensity of a seismic event. For example, Donmez et al. [22] used peak ground velocity (PGV) for the seismic fragility curves that they produced for RC buildings with filler-joist floor systems. Nevertheless, in the present study, peak ground acceleration (PGA) is used for the intensity measure of seismic fragility curves, since it is a more practical parameter to represent the seismic hazard level at a building site. In addition, unlike the methodologies which utilizes probabilistic seismic demand models that constructs a regression relationship between intensity measure of earthquake records and resulting seismic demands, herein fragility parameters are directly obtained from the method of maximum likelihood as will be explained in Section 5.2.

5.2 Methodology for Generating Seismic Fragility Curves

A time-history analysis of the 3-D model of the building under a single ground motion record can be computationally expensive, thus performing such analysis for dozens of times (according to the size of the ground motion dataset) and under different design combinations of the investigated building needs significant time and computational power. For this reason, a simplified approach is rather employed in this thesis to attain nonlinear seismic displacement demands of the investigated buildings during the process of producing seismic fragility curves. This approach, which is schematically demonstrated in Figure 5.1, is mainly based on the assumption that the dynamic response of building is represented with an equivalent single-degree-of-freedom (SDOF) system, and lateral response under an earthquake excitation is governed with the first mode response of the building. This assumption can be said to be reasonable for the investigated buildings in this thesis, since these structures are known to have no structural irregularity. However, it would be necessary to perform nonlinear time-history analyses on 3-D structural models to get seismic demands when the structure of interest has some irregular features such as torsional irregularity.

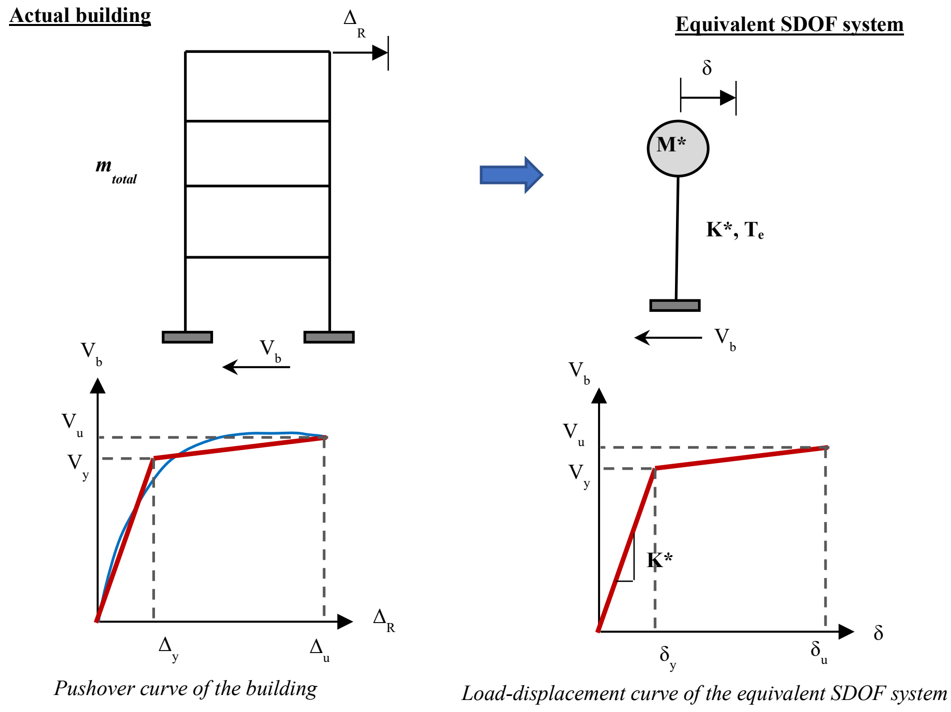

Figure 5.1 Representation of the dynamic response of the building by equivalent SDOF system.

In Figure 5.1, V_b stands for the base shear force or the total pushing force in the capacity curve of the building. Δ_R represents the roof displacement of the actual building in the horizontal direction under consideration and δ is the corresponding lateral displacement of the equivalent SDOF system. The relationship between Δ_R and δ are given in Equation 5.1.

$$\delta = \frac{\Delta_R}{\Gamma_1 \phi_{1r}} \tag{5.1}$$

where; Γ_1 is the modal participation factor for the first mode, ϕ_{1r} is the amplitude of lateral displacement at the roof level for first mode deformed shape. In the present study, the factor $\Gamma_1 \phi_{1r}$ is simply taken as 1.3 as recommended in ASCE 41-13 [35]. Effective mass (M^*) of the equivalent SDOF system is determined from Equation 5.2.

$$M^* = C_m \, m_{total} \tag{5.2}$$

where; C_m is the mass participation factor for the first mode, m_{total} is the total mass of the building.The effective period of the equivalent SDOF system can be computed from Equation 5.3 below.

$$T_{eff} = \frac{2\pi}{\sqrt{K^*/_{M^*}}} \tag{5.3}$$

where; K^* is the initial stiffness of the load-displacement curve of the equivalent SDOF system.

The overall procedure followed for generating seismic fragility curves is summarized in the following four step:

Step 1: The actual pushover curve of a building, which was obtained in Chapter 3.6 of the thesis) is converted into idealized (bilinear representation) load-displacement curve as shown in Figure 5.2. In finding the idealized force-displacement curve, the principle given in ASCE 41-13 [35] is taken into consideration. According to this principle, the areas under the load-displacement curves of the actual pushover curve and idealized curve must be approximately the same. Also, an iterative process is carried out to determine the yield displacement and force of the idealized curve so that 60% of the yielding base shear force must intersect the actual pushover curve. The schematic demonstration of the bilinearization of the capacity curve and application of it on the pushover curve belonging to the building “F-5-s07-b25” for X-direction is shown in Figure 5.2.

Idealized pushover curves of all investigated buildings are shown in Figures 5.3 to 5.8. The yield and ultimate displacement and forces of the idealized pushover curves, building mass, first mode participation ratio, and effective period of equivalent SDOF system are also presented in Table 5.1 and 5.2 for X and Y directions, respectively.

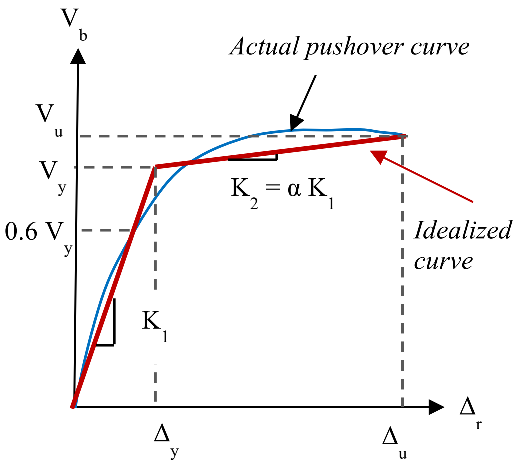

(a) Idealization of pushover curve

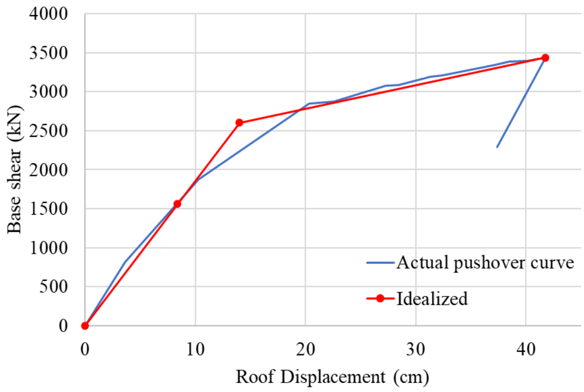

(b) Pushover curve idealization for the building F-5-s07-b25 along X-direction

Figure 5.2 Process of creating idealized pushover curves.

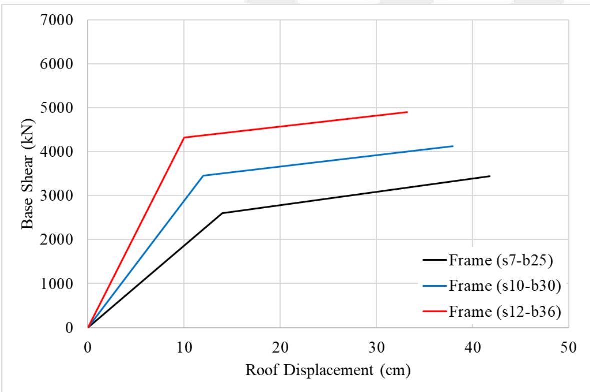

(a) Along X-direction

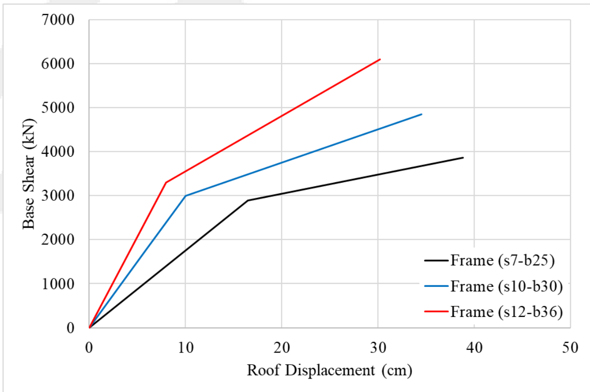

(b) Along Y-direction

Figure 5.3 Idealized pushover curves of 5-story buildings with frames only.

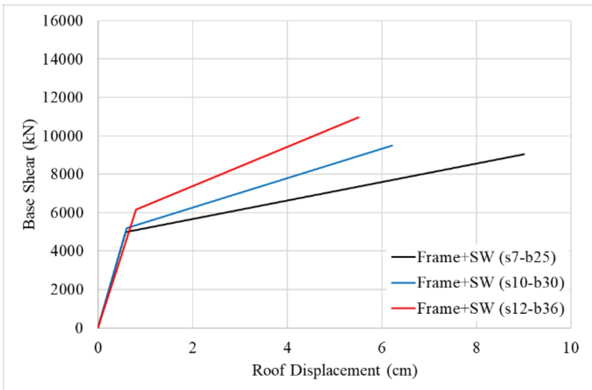

(a) Along X-direction

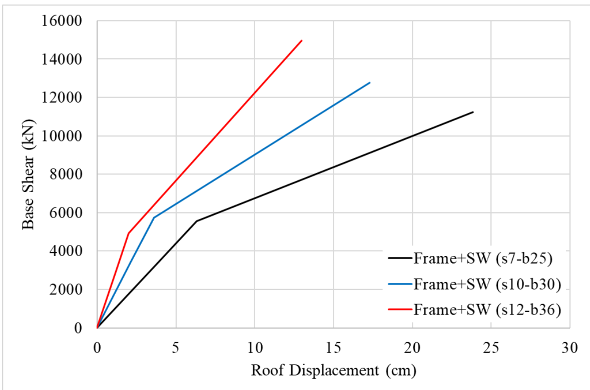

(b) Along Y-direction

Figure 5.4 Idealized pushover curves of 5-story buildings with frames and shear walls.

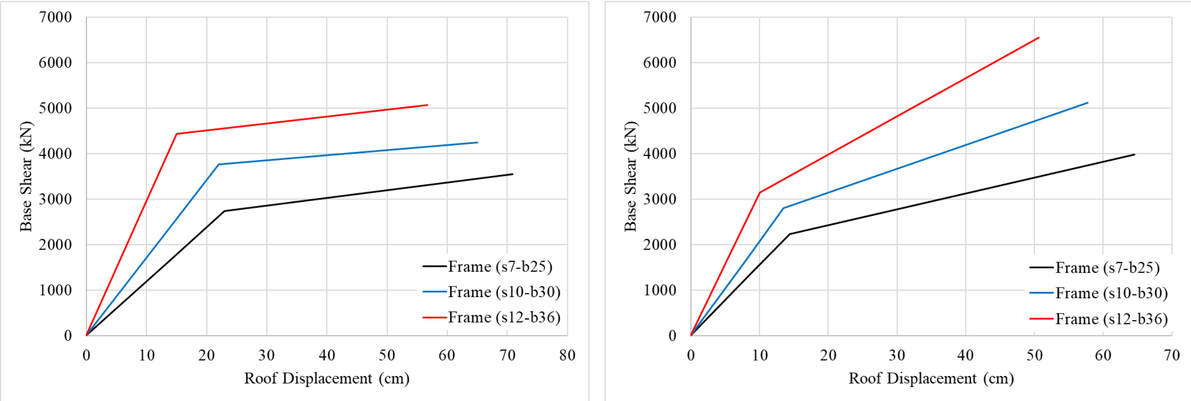

(a) Along X-direction (b) Along Y-direction

Figure 5.5 Idealized pushover curves of 8-story buildings with frames only.

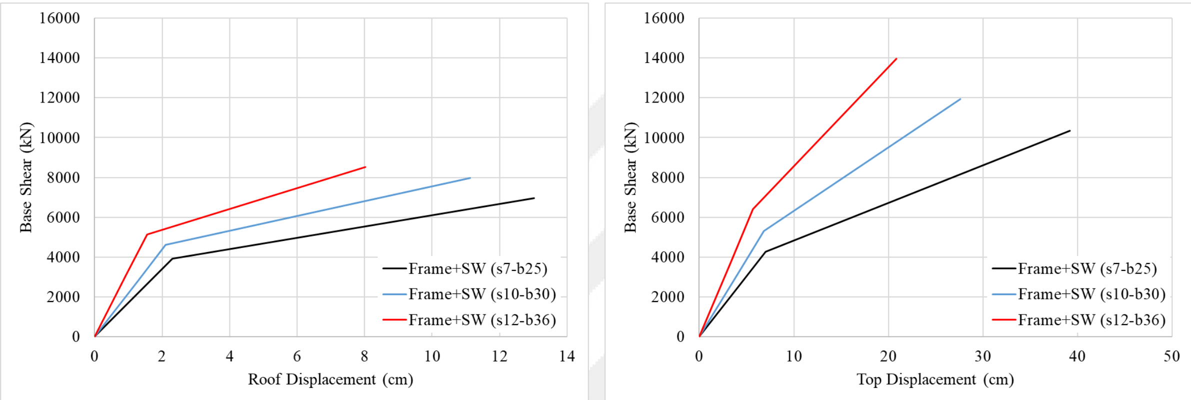

(a) Along X-direction (b) Along Y-direction

Figure 5.6 Idealized pushover curves of 8-story buildings with frames and shear walls.

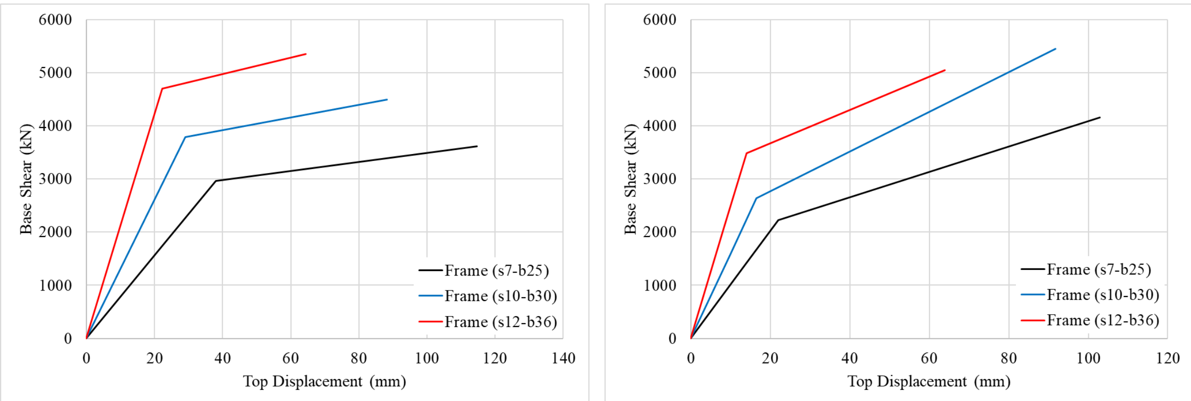

(a) Along X-direction (b) Along Y-direction

Figure 5.7 Idealized pushover curves of 12-story buildings with frames only.

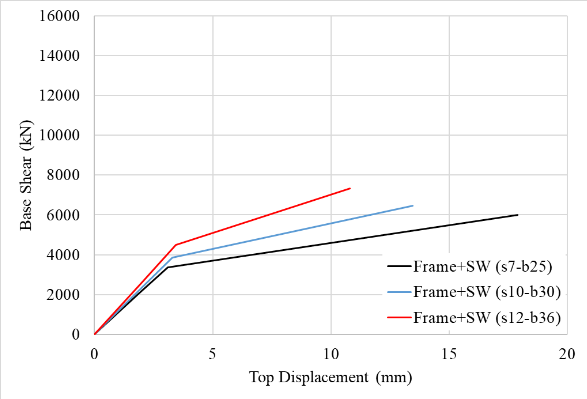

(a) Along X-direction

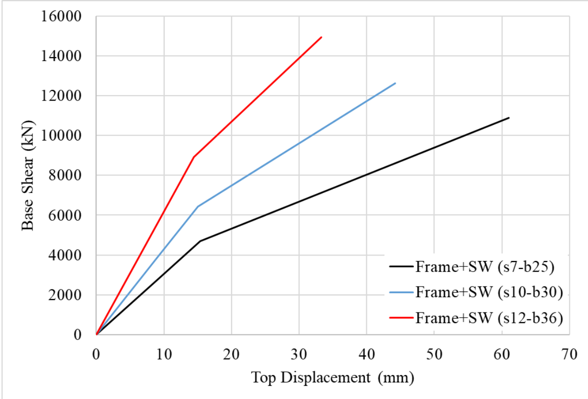

(b) Along Y-direction

Figure 5.8 Idealized pushover curves of 12-story buildings with frames and shear walls.

Table 5.1 Necessary building parameters for generating equivalent SDOF systems in X-direction.

Model ID	m_{total} (ton)	C_m	Δ_y (cm)	F_y (kN)	Δ_u (cm)	F_u (kN)	T_{eff} (sec)
F-5-s07-b25	3016	0.754	14.0	2600	41.8	3437	1.93
F-5-s10-b30	3405	0.775	12.0	3450	38.0	4130	1.90
F-5-s12-b36	3751	0.794	10.0	4320	33.2	4905	1.65
SW-5-s07-b25	3174	0.762	0.6	5000	9.0	9055	0.33
SW-5-s10-b30	3542	0.765	0.6	5190	6.2	9492	0.35
SW-5-s12-b36	3868	0.768	0.8	6170	5.5	10953	0.39
F-8-s07-b25	5024	0.733	23.0	2730	70.9	3542	3.07
F-8-s10-b30	5645	0.753	22.0	3760	65.0	4247	3.13
F-8-s12-b36	6193	0.771	15.0	4435	56.7	5068	2.52
SW-8-s07-b25	5116	0.708	2.3	3920	13.0	6946	0.92
SW-8-s10-b30	5705	0.711	2.1	4620	11.1	7964	0.85
SW-8-s12-b36	6226	0.715	1.6	5150	8.0	8512	0.73
F-12-s07-b25	7892	0.724	38.0	2963	114.7	3619	4.72
F-12-s10-b30	8817	0.743	29.0	3785	88.3	4489	4.45
F-12-s12-b36	9634	0.750	22.2	4705	64.3	5357	3.67
SW-12-s07-b25	7996	0.673	3.1	3365	17.9	5987	1.40
SW-12-s10-b30	8876	0.677	3.3	3870	13.5	6470	1.42
SW-12-s12-b36	9652	0.683	3.5	4500	10.8	7318	1.41

Table 5.2 Necessary building parameters for generating equivalent SDOF systems in Y-direction.

Model ID	m_{total} (ton)	C_m	Δ_y (cm)	F_y (kN)	Δ_u (cm)	F_u (kN)	T_{eff} (sec)
F-5-s07-b25	3016	0.768	16.5	2890	38.8	3864	2.00
F-5-s10-b30	3405	0.787	10.0	3000	34.5	4853	1.88
F-5-s12-b36	3751	0.805	8.0	3300	30.2	6104	1.70
SW-5-s07-b25	3174	0.701	6.3	5550	23.8	11249	1.00
SW-5-s10-b30	3542	0.711	3.6	5750	17.3	12754	0.79
SW-5-s12-b36	3868	0.723	2.0	4930	13.0	14969	0.67
F-8-s07-b25	5024	0.747	14.4	2230	64.6	3974	2.71
F-8-s10-b30	5645	0.765	13.5	2795	57.7	5122	2.87
F-8-s12-b36	6193	0.781	10.0	3145	50.6	6548	2.46
SW-8-s07-b25	5116	0.681	7.0	4260	39.2	10334	1.50
SW-8-s10-b30	5705	0.693	6.8	5300	27.6	11949	1.42
SW-8-s12-b36	6226	0.710	5.7	6410	20.8	13967	1.25
F-12-s07-b25	7892	0.737	22.0	2224	102.9	4162	4.18
F-12-s10-b30	8817	0.755	16.5	2635	91.7	5449	4.06
F-12-s12-b36	9634	0.760	14.0	3490	63.9	5051	3.40
SW-12-s07-b25	7996	0.678	15.4	4700	61.0	10885	2.65
SW-12-s10-b30	8876	0.695	15.0	6445	44.2	12613	2.38
SW-12-s12-b36	9652	0.714	14.4	8910	33.3	14950	2.10

Step 2: For each investigated building, load-displacement curves of the equivalent SDOF systems are generated from the idealized pushover curves of actual buildings by computing the yield and ultimate displacements as presented in Equation 5.1. By doing that, initial stiffness, post-yield stiffness, and strain hardening ratio (the ratio of post-yield stiffness to initial stiffness) that are needed for the hysteresis model of equivalent SDOF are obtained. A bilinear hysteresis model is assumed within the scope of this thesis. At the mean time, effective masses of equivalent SDOF systems are computed as described in Equation 5.2.

Step 3: A simple OpenSees [36] model is created to conduct nonlinear time-history analysis of a SDOF system. The bilinear hysteresis model and effective mass that are computed in the previous step are assigned in the OpenSees model. Then for a given earthquake record, time-history analysis is performed for 5% damping and resulting maximum displacement is determined to be the inelastic displacement demand of the equivalent SDOF under that earthquake record. This model is adopted for a batch analysis of the SDOF model that is of interest under a large set of ground motion records. To generate seismic fragility curves, multiple-strip analysis as explained in Baker [37] is applied. In this regard, an incremental analysis is performed for varying levels of PGA values ranging from 0.1g to 2.0 g with an increment of 0.1g. Therefore, for each PGA level, all earthquake records within the ground motion dataset are scaled according to the PGA value under consideration, and inelastic displacement demands are computed under all scaled ground motion records in the dataset. For a ground motion dataset that consists of 22 earthquake records (two components from 11 unique earthquake events), a total of 440 analyses are performed for all PGA levels. The inelastic displacement demands obtained from the analyses of equivalent SDOF systems are back converted to the corresponding roof displacement demands of actual buildings by Equation 5.4.

$$\Delta_R = \delta\,(\Gamma_1 \phi_{1r}) \tag{5.4}$$

<u>Step 4:</u> Seismic fragility curves are produced for three levels of performance limits, namely immediate occupancy (IO), life safety (LS), and collapse prevention (CP). Within the scope of this thesis, performance of buildings is assessed with respect to the engineering demand parameter of building lateral roof displacement (Δ_R), which can also be translated into global drift ratio. During the process of generating fragility curves, roof displacement demands resulting from 22 analyses at each PGA level within the incremental analysis are compared with respect to the threshold limits defined for the performance limit under consideration, and probability of exceedance (probability of failure) is calculated. This calculation process is repeated for all PGA levels, and a cumulative lognormal distribution curve is fitted onto the exceedance probabilities that are calculated for each PGA levels. The method of maximum likelihood is utilized to estimate the median and dispersion values that define the cumulative lognormal distribution (fragility curve) during the process of fitting fragility curve onto the computed probability of exceedance values.

Since the building performance is defined globally based on building lateral roof displacements, the critical displacements on the idealized pushover curves of buildings are taken into consideration for determining performance limit threshold values. For frame buildings, the threshold value for IO performance limit is taken as the yield displacement (Δ_y), while the threshold value for CP performance limit is taken as the ultimate displacement (Δ_u) of the idealized pushover curve. The threshold limit for LS performance limit is assumed as the average of the limiting values accepted for IO and CP. The same principle is applied for buildings with shear walls with an exception in X-direction. In this case, instead of taking the yield displacement of the idealized curve, the threshold limit for IO performance limit is assumed as the displacement at which the actual pushover curve starts to increase after the initial yielding portion. The performance threshold limits accepted in this study are summarized in Table 5.3 and 5.4 for X and Y directions of the buildings, respectively. For buildings with frames only (i.e. Type F buildings), the average threshold limit values in X-direction are 0.008, 0.017, and 0.026 for IO, LS, and CP, respectively, while these values are 0.006, 0.015, and 0.024 for Y-direction. On the other hand, for buildings with frames and shear walls (i.e. type SW buildings), the average threshold limit values in X-direction are 0.002, 0.003, and 0.004 for IO, LS, and CP, respectively, while these values are 0.003, 0.008, and 0.012 for Y-direction.

It is worth to note that seismic fragility curves could be more accurately produced if component level performance assessments are performed instead of a global level performance assessment as applied in this thesis.

Table 5.3 Performance limits threshold values in X-direction.

	Roof Displacement			Drift Ratio		
Model ID	IO (cm)	LS (cm)	CP (cm)	IO	LS	CP
F-5-s07-b25	14.0	27.9	41.8	0.009	0.019	0.028
F-5-s10-b30	12.0	25.0	38.0	0.008	0.017	0.025
F-5-s12-b36	10.0	21.6	33.2	0.007	0.014	0.022
SW-5-s07-b25	2.5	5.8	9.0	0.002	0.004	0.006
SW-5-s10-b30	1.7	4.0	6.2	0.001	0.003	0.004
SW-5-s12-b36	1.9	3.7	5.5	0.001	0.002	0.004
F-8-s07-b25	23.0	47.0	70.9	0.010	0.020	0.030
F-8-s10-b30	22.0	43.5	65.0	0.009	0.018	0.027
F-8-s12-b36	15.0	35.8	56.7	0.006	0.015	0.024
SW-8-s07-b25	4.1	8.6	13.0	0.002	0.004	0.005
SW-8-s10-b30	4.8	8.0	11.1	0.002	0.003	0.005
SW-8-s12-b36	4.6	6.3	8.0	0.002	0.003	0.003
F-12-s07-b25	38.0	76.4	114.7	0.011	0.021	0.032
F-12-s10-b30	29.0	58.7	88.3	0.008	0.016	0.025
F-12-s12-b36	22.2	43.3	64.3	0.006	0.012	0.018
SW-12-s07-b25	7.7	12.8	17.9	0.002	0.004	0.005
SW-12-s10-b30	6.9	10.2	13.5	0.002	0.003	0.004
SW-12-s12-b36	6.1	8.5	10.8	0.002	0.002	0.003

Table 5.4 Performance limits threshold values in Y-direction.

	Roof Displacement			Drift ratio		
Model ID	IO **(cm)**	**LS (kN)**	CP **(cm)**	IO	**LS**	CP
F-5-s07-b25	16.5	27.7	38.8	0.011	0.018	0.026
F-5-s10-b30	10.0	22.3	34.5	0.007	0.015	0.023
F-5-s12-b36	8.0	19.1	30.2	0.005	0.013	0.020
SW-5-s07-b25	6.3	15.1	23.8	0.004	0.010	0.016
SW-5-s10-b30	3.6	10.4	17.3	0.002	0.007	0.012
SW-5-s12-b36	2.0	7.5	13.0	0.001	0.005	0.009
F-8-s07-b25	14.4	39.5	64.6	0.006	0.016	0.027
F-8-s10-b30	13.5	35.6	57.7	0.006	0.015	0.024
F-8-s12-b36	10.0	30.3	50.6	0.004	0.013	0.021
SW-8-s07-b25	7.0	23.1	39.2	0.003	0.010	0.016
SW-8-s10-b30	6.8	17.2	27.6	0.003	0.007	0.012
SW-8-s12-b36	5.7	13.3	20.8	0.002	0.006	0.009
F-12-s07-b25	22.0	62.5	102.9	0.006	0.017	0.029
F-12-s10-b30	16.5	54.1	91.7	0.005	0.015	0.025
F-12-s12-b36	14.0	39.0	63.9	0.004	0.011	0.018
SW-12-s07-b25	15.4	38.2	61.0	0.004	0.011	0.017
SW-12-s10-b30	15.0	29.6	44.2	0.004	0.008	0.012
SW-12-s12-b36	14.4	23.8	33.3	0.004	0.007	0.009

5.3 Seismic Fragility Curves

The procedure used for generating seismic fragility curves is repeated for three performance limits (IO, LS, CP) and for all investigated buildings with different design parameter combinations and for each orthogonal direction (X and Y directions). All seismic fragility curves generated are graphically presented between Figure 5.9 and 5.14. For comparison, the median and dispersion values of each investigated building are given in Table 5.5 and 5.6 for X and Y directions, respectively.

Table 5.5 Fragility curve parameters for X-direction of the buildings.

Model ID	Performance Limits					
	IO		LS		CP	
	Median (g)	Dispersion	Median (g)	Dispersion	Median (g)	Dispersion
F-5-s07-b25	0.28	1.16	0.73	0.73	1.11	0.52
F-5-s10-b30	0.26	1.19	0.62	0.82	1.02	0.55
F-5-s12-b36	0.26	1.08	0.63	0.82	0.93	0.61
SW-5-s07-b25	0.39	0.46	0.67	0.60	0.88	0.55
SW-5-s10-b30	0.26	0.41	0.50	0.57	0.68	0.59
SW-5-s12-b36	0.26	0.42	0.45	0.52	0.60	0.60
F-8-s07-b25	0.46	0.83	0.95	0.56	1.37	0.40
F-8-s10-b30	0.43	0.95	0.93	0.62	1.22	0.51
F-8-s12-b36	0.32	1.05	0.79	0.64	1.29	0.55
SW-8-s07-b25	0.19	0.83	0.40	1.04	0.61	0.78
SW-8-s10-b30	0.25	0.87	0.41	1.01	0.57	0.82
SW-8-s12-b36	0.30	0.76	0.39	0.88	0.47	0.88
F-12-s07-b25	0.53	0.80	1.14	0.56	1.68	0.40
F-12-s10-b30	0.43	0.85	0.95	0.56	1.45	0.46
F-12-s12-b36	0.41	0.87	0.78	0.64	1.16	0.46
SW-12-s07-b25	0.27	0.97	0.46	0.97	0.65	0.75
SW-12-s10-b30	0.26	0.91	0.38	0.96	0.48	0.96
SW-12-s12-b36	0.22	0.87	0.31	0.98	0.41	0.95

Table 5.6 Fragility curve parameters for Y-direction of the buildings.

Model ID	Performance Limits					
	IO		LS		CP	
	Median (g)	Dispersion	Median (g)	Dispersion	Median (g)	Dispersion
F-5-s07-b25	0.32	1.13	0.71	0.70	1.05	0.55
F-5-s10-b30	0.20	1.23	0.64	0.78	1.02	0.58
F-5-s12-b36	0.18	1.14	0.60	0.85	0.93	0.62
SW-5-s07-b25	0.24	0.91	0.67	0.74	1.01	0.57
SW-5-s10-b30	0.14	1.12	0.61	0.85	0.94	0.59
SW-5-s12-b36	0.10	0.79	0.51	0.79	0.79	0.64
F-8-s07-b25	0.27	1.06	0.91	0.59	1.37	0.43
F-8-s10-b30	0.28	1.01	0.87	0.63	1.33	0.47
F-8-s12-b36	0.22	1.03	0.80	0.68	1.30	0.51
SW-8-s07-b25	0.18	1.01	0.81	0.72	1.23	0.58
SW-8-s10-b30	0.18	1.01	0.63	0.80	0.95	0.65
SW-8-s12-b36	0.16	0.97	0.49	0.92	0.82	0.67
F-12-s07-b25	0.30	1.06	1.10	0.59	1.69	0.41
F-12-s10-b30	0.24	1.15	1.01	0.49	1.62	0.39
F-12-s12-b36	0.26	1.00	0.81	0.59	1.28	0.47
SW-12-s07-b25	0.31	1.04	0.94	0.64	1.39	0.49
SW-12-s10-b30	0.32	1.11	0.77	0.66	1.16	0.61
SW-12-s12-b36	0.28	1.20	0.58	0.85	0.88	0.69

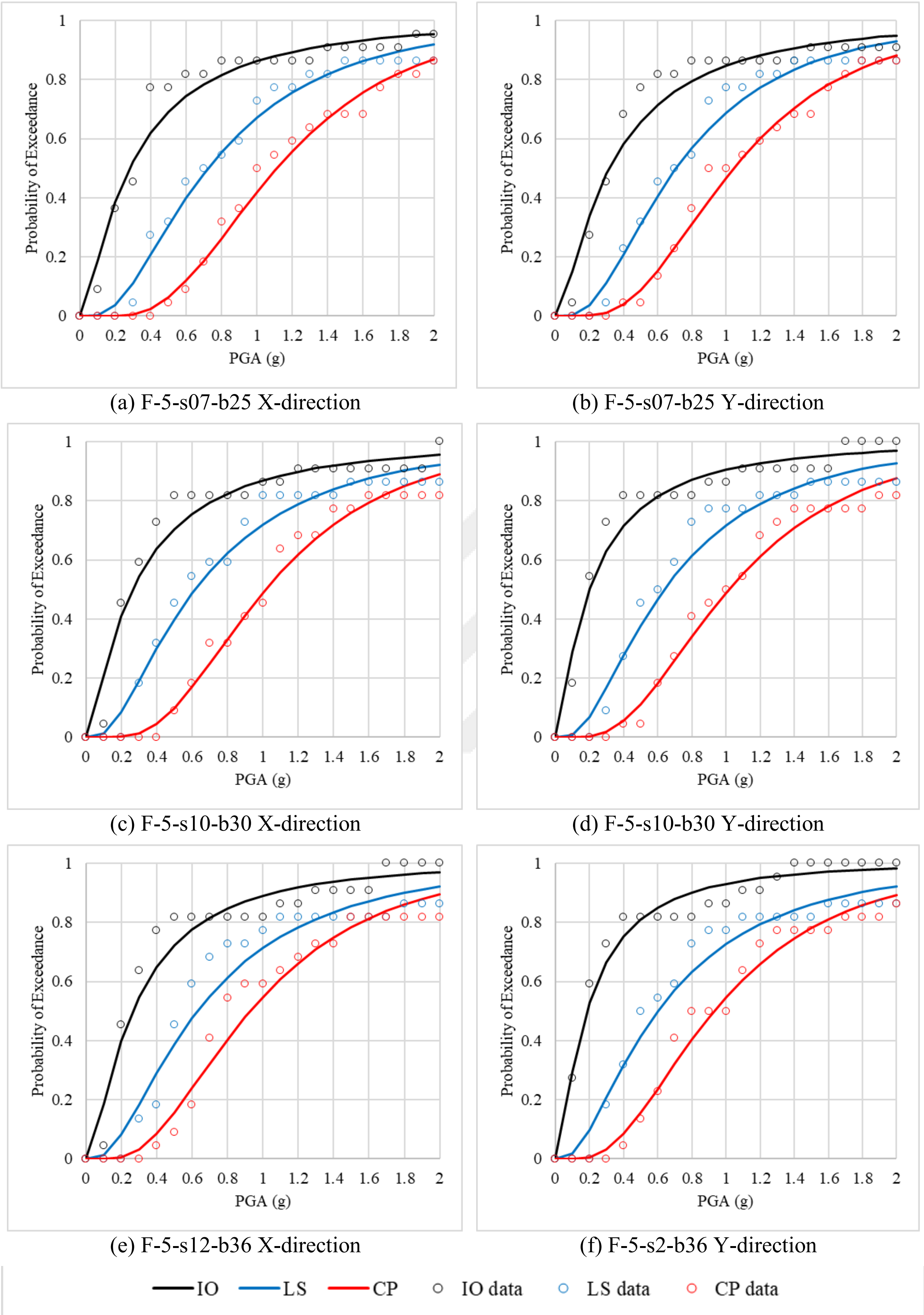

(a) F-5-s07-b25 X-direction
(b) F-5-s07-b25 Y-direction
(c) F-5-s10-b30 X-direction
(d) F-5-s10-b30 Y-direction
(e) F-5-s12-b36 X-direction
(f) F-5-s2-b36 Y-direction

Figure 5.9 Seismic fragility curves of the 5-story buildings with frames only.

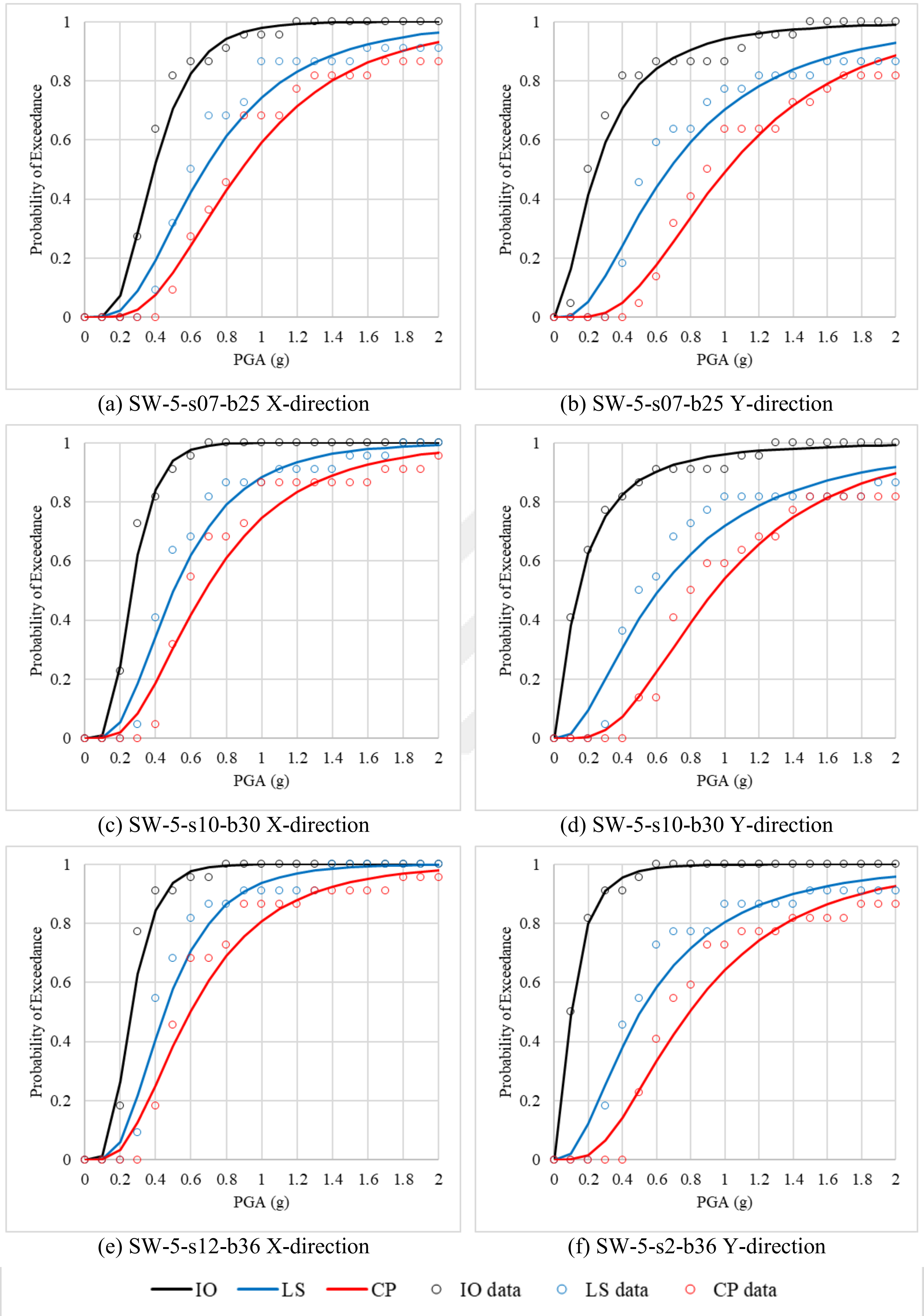

(a) SW-5-s07-b25 X-direction

(b) SW-5-s07-b25 Y-direction

(c) SW-5-s10-b30 X-direction

(d) SW-5-s10-b30 Y-direction

(e) SW-5-s12-b36 X-direction

(f) SW-5-s2-b36 Y-direction

Figure 5.10 Seismic fragility curves of the 5-story buildings with frames and shear walls.

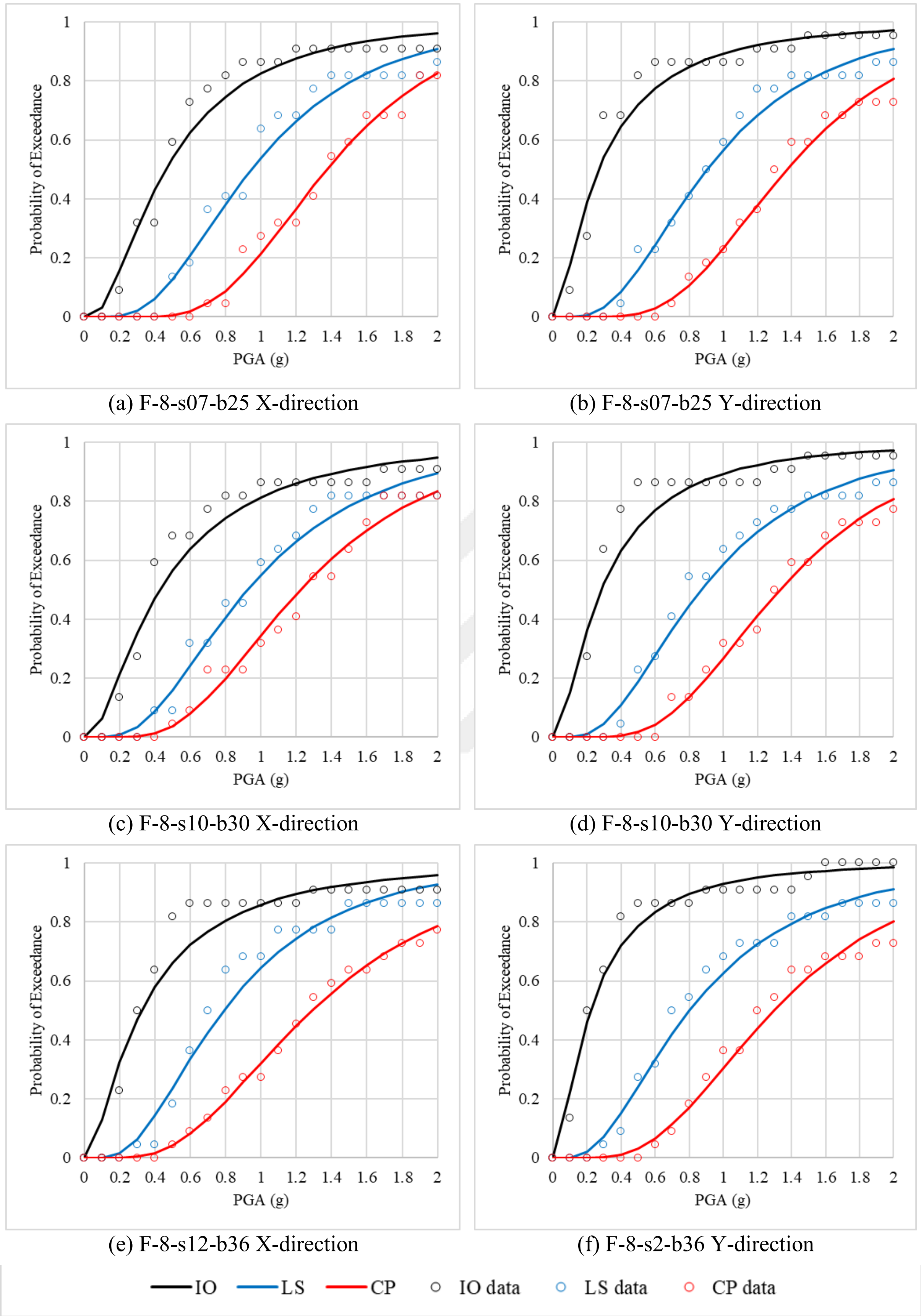

Figure 5.11 Seismic fragility curves of the 8-story buildings with frames only.

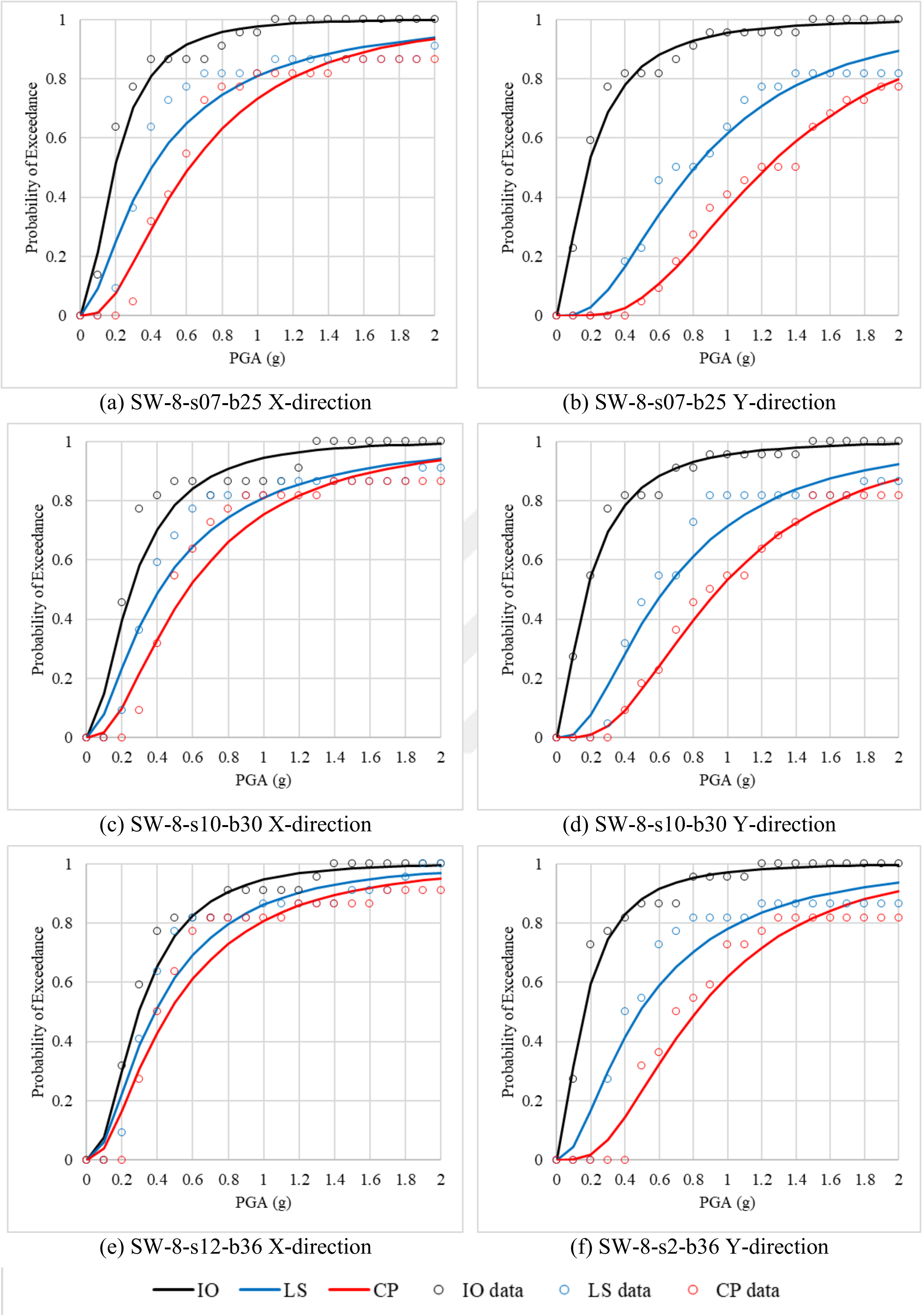

(a) SW-8-s07-b25 X-direction
(b) SW-8-s07-b25 Y-direction
(c) SW-8-s10-b30 X-direction
(d) SW-8-s10-b30 Y-direction
(e) SW-8-s12-b36 X-direction
(f) SW-8-s2-b36 Y-direction

Figure 5.12 Seismic fragility curves of the 8-story buildings with frames and shear walls.

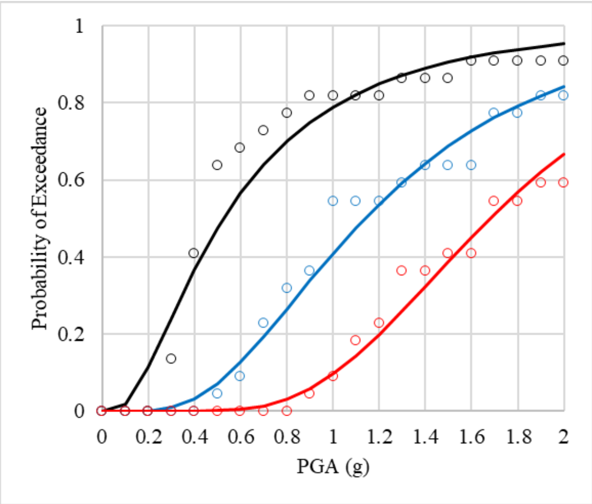

(a) F-12-s07-b25 X-direction

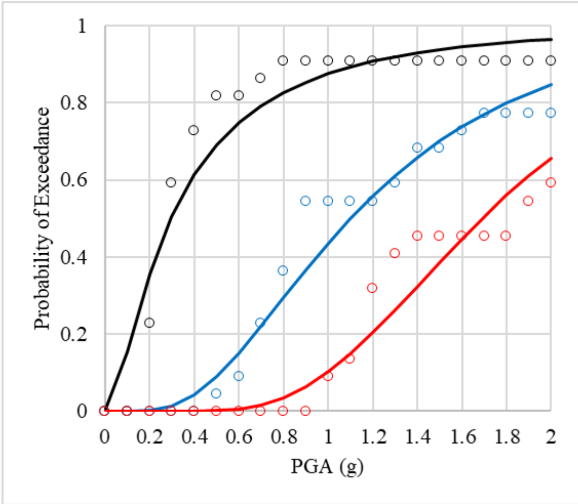

(b) F-12-s07-b25 Y-direction

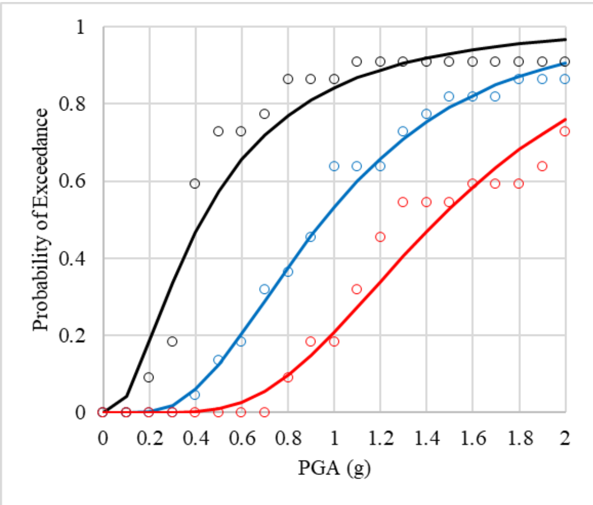

(c) F-12-s10-b30 X-direction

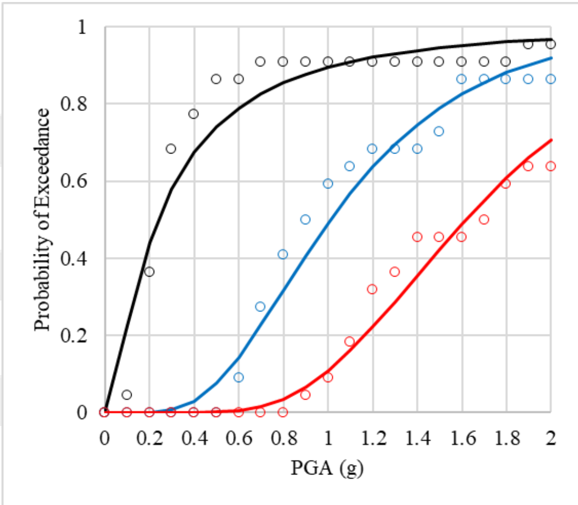

(d) F-12-s10-b30 Y-direction

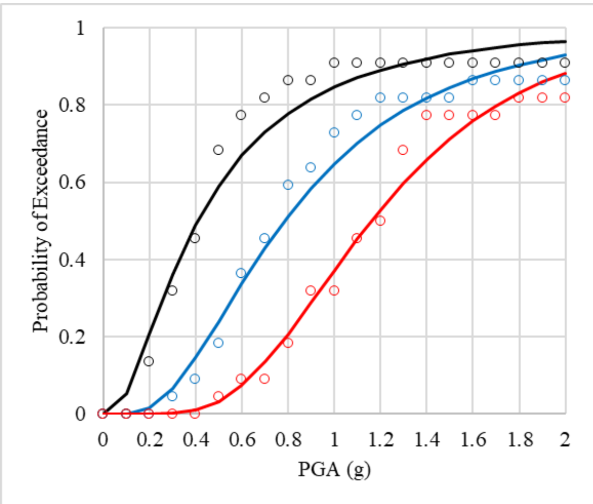

(e) F-12-s12-b36 X-direction

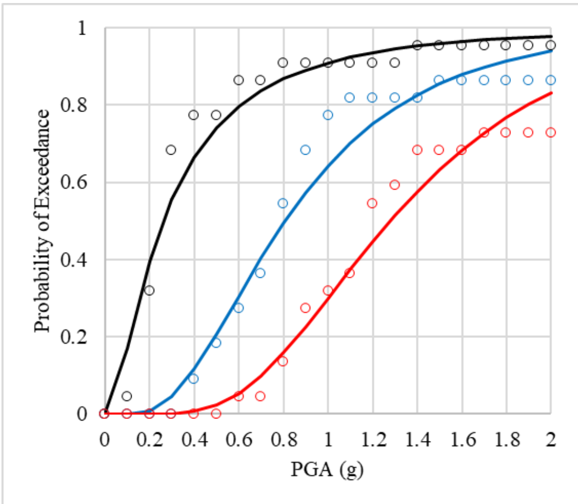

(f) F-12-s2-b36 Y-direction

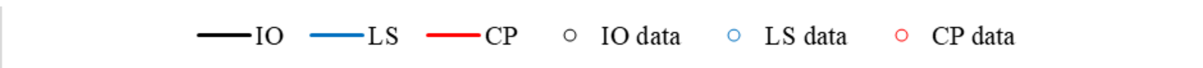

Figure 5.13 Seismic fragility curves of the 12-story buildings with frames only.

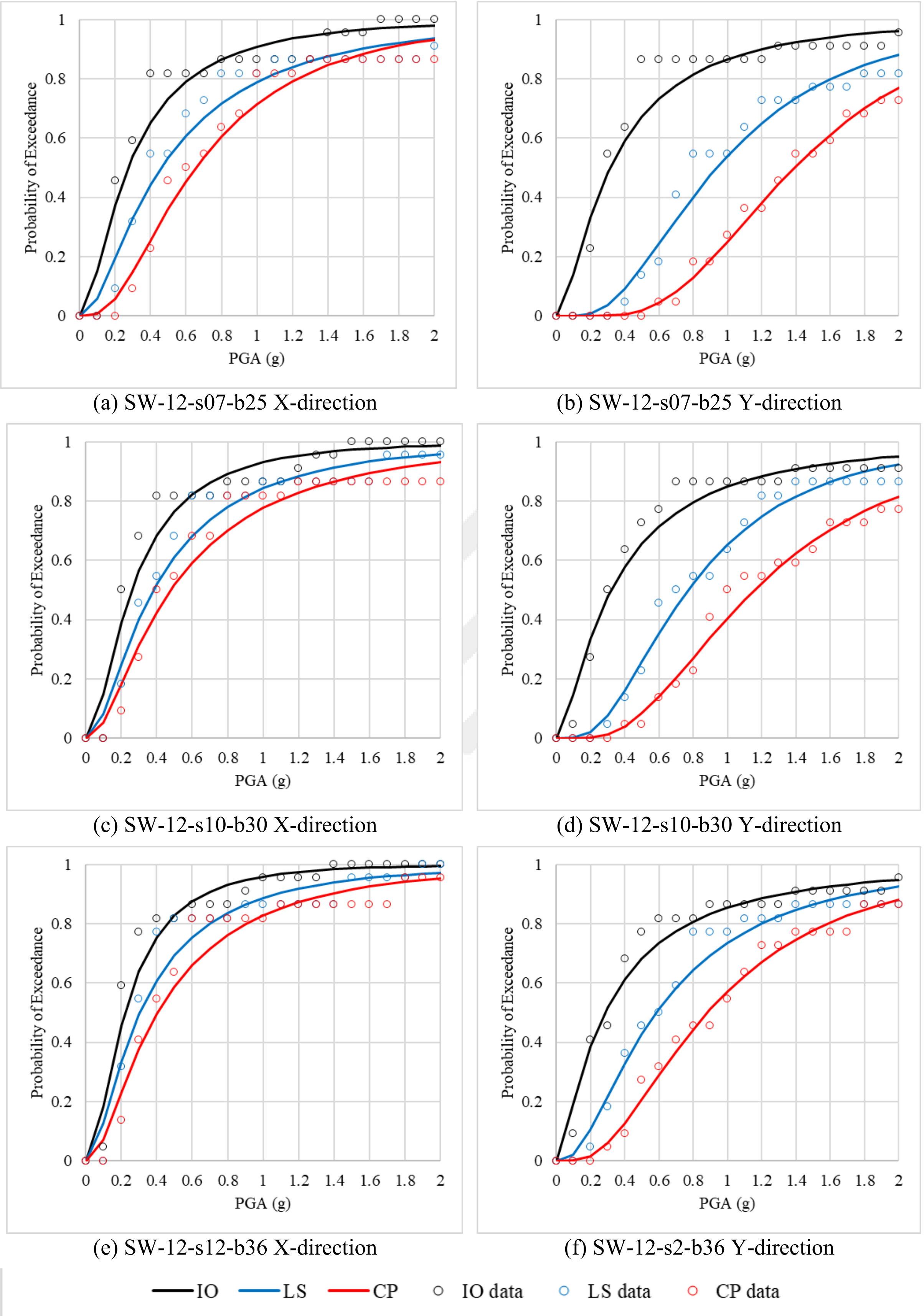

Figure 5.14 Seismic fragility curves of the 12-story buildings with frames and shear walls.

CHAPTER VI

CONCLUSION

6.1 Summary

The current Turkish building earthquake code [3] presents several provisions on the restrictions of the use of filler-joist type floor systems in reinforced concrete buildings. This thesis aims to investigate the effect of floor rigidity, building height and use of shear walls on the seismic performance of these types of buildings, and assess the validity of the provisions stated by the code based on the outcomes obtained from a parametrical study. In accordance with this purpose; finite element models of a generic reinforced concrete building with a typical floor plan are developed in the structural analysis software ETABS considering three different slab thicknesses, three different number of stories and absence and presence of shear walls in the structural system.

As the first part of the analyses performed within this thesis, each of the generated 18 building models are subjected to modal spectrum analysis under the design earthquake hazard level to obtain elastic force demands. Then, nonlinear static analyses are conducted for each building model to plot the pushover curves of the buildings and the influence of each investigated parameter on the lateral load capacity of the building is assessed. After capacities are found, a ground motion data set that consists of 11 real earthquake ground motion records matching with the design earthquake response spectrum is formed and a total of 22 nonlinear time-history analyses of the building models are performed to estimate the seismic demands of each investigated building, which are further compared for each investigated building to evaluate the effect of design parameters on the structural performance.

As the last step of this research, each building model is idealized with equivalent single-degree-of-freedom systems and their load-displacement relationships are represented with the previously obtained pushover curves. Then, multiple-strip analysis is adopted for generating seismic fragility curves of the buildings having a different combination of the considered design parameters. Within this method, each SDOF system is subjected to a series of nonlinear time-history analysis to estimate inelastic displacement demands of the buildings, and the resulting building drift ratio demands are assessed with respect to the drift capacities corresponding to different performance limits, and seismic fragility curve parameters are obtained. Peak ground acceleration is taken into consideration for the seismic intensity measure of the developed seismic fragility curves.

6.2 Major Outcomes

Based on the comparison of the structural performance of the studied RC building with filler-joist floors under different design parameters, the following major outcomes are reached:

1. As the thickness of floor slabs gets reduced, higher lateral drift demands are resulted under earthquake loadings, both from elastic modal spectrum analysis and inelastic time-history analysis. This outcome proves that damage probability, which is directly correlated with inter-story drift ratios, can be lowered by avoiding extremely flexible floor slabs.
2. Lateral drift demands of the RC buildings with filler-joist floors under earthquake loads can be considerably limited by the use of shear walls in the structural systems. So that occurrence of extensive seismic damage can be prevented for the case of having floor slabs with low rigidity.
3. While it is found out that the investigated buildings perform better when shear walls are used, it should be underlined that the transfer of shear forces from slabs to shear walls can be critical. It should be noted that the actual structural behavior can be completely different than what is predicted during the design stage if shear forces are not transmitted safely.

Besides the above listed major outcomes, the following conclusions are drawn based on the comparison of analysis results obtained from the elastic modal spectrum analysis and inelastic time-history analysis:

- The difference between the maximum base shear forces from the time-history analysis and modal spectrum analysis are observed to be not exceeding 10%.

- Relative story drifts resulting from time-history analysis are greater than the ones resulting from linear elastic modal spectrum analyses. This shows that simple analysis methods may not be sufficient for determining the accurate structural behavior of investigated type of structures under high intensity seismic loading conditions such structures in earthquake zones.

When Fragility curve analysis was performed, data supporting other analyzes were obtained in the controlled damage range. However, due to the selection of PGA values or earthquake records, healthy values for life safety and failure intervals could not be established. For the controlled damage range, when the 4 structures are compared to each other, it is clearly shown with graphics that the probability of damage to the shear walled structures is lower. When the effect of building heights is examined between buildings with the same characteristics, there is a clear difference in the slopes of the curves where smaller heights are performed better. The data obtained from this study supports the understandings of TBEC 2018.

6.3 Recommendations for Future Studies

The knowledge-base on the seismic response and performance of RC buildings with filler-joist floors can be expanded with the following future studies:

1. Seismic performance evaluation study presented in Chapter 4 of this thesis can be repeated under a higher-level earthquake hazard (e.g., design earthquake event with a return period of 2475 years).
2. Analyzes can be repeated and structures can be examined by the effects on different soil classes and different earthquake forces where new datasets to be created by increasing the seismicity diversity.
3. Development of seismic fragility curves can be improved by an increase in PGA and earthquake data set. Therefore, seismic performance of such type of buildings can be expressed probabilistically for various limit states.

4. The effect of the use of filler-joist floor systems on RC buildings with irregular plans can be analyzed.

REFERENCES

[1] Afet ve Acil Durum Yönetimi Başkanlığı (AFAD), “Türkiye Deprem Tehlike Haritası.” afad.gov.tr. http://tdth.afad.gov.tr/TDTH (accessed September 05, 2021)

[2] C. Dönmez, “Türkiye'deki asmolen yapıların deprem yeterliliği konusunda bir irdeleme” presented at Proceedings of 2nd Turkish Earthquake Engineering and Seismology Conference, Hatay, Turkey, Sep., 2013, pp 1-11.

[3] İçişleri Bakanlığı, Afet ve Acil Durumlar Başkanlığı, “Türkiye Bina Deprem Yönetmeliği, TBDY-2018”, Ankara, Türkiye, 2018.

[4] A. Benavent-Climent and R. Zahran, “An energy-based procedure for the assessment of seismic capacity of existing frames: application to RC wide beam systems in Spain”, Soil Dynamics and Earthquake Engineering, vol.30, pp. 354-367, 2010.

[5] J.O. Malley, M. Celebi, M. Bruneau, M. Saaticioglu, M. Erdik, and P. Gulkan, "1992 Erzincan earthquake: Buildings", Earthquake Spectra, vol.9(S1), pp. 49-85, 1993.

[6] C. Dönmez, "Seismic Performance of Wide-Beam Infill-Joist Block RC Frames in Turkey", Journal of Performance of Constructed Facilities, vol.29(1): 04014026, 2015.

[7] M. Öztemel, "DBYBHY-2007 ve TS 500 Kurallarının Şantiyedeki Uygulama Hataları ve Asmolen Döşemeler Üzerine İnceleme: Hendek Örneği", M.Sc. Thesis, Sakarya University, Sakarya, Turkey, 2016.

[8] R. Nudo, G. Sara, S. Viti, "Influence of floor structures on seismic performance of RC frames", Proceedings of 13th World Conference on Earthquake Engineering, Vancouver, B.C., Canada, Aug. 1-6, 2004, pp. 424.

[9] D. Uzun, K. Guler, "Seismic behavior of a high-rise RC building with different types of slabs". 16th European conference on earthquake engineering, Thessaloniki, Greece, June 18-21, 2018, pp. 1-10.

[10] A. Coull, W.Y. Chee, "Design of floor slabs coupling shear walls", Journal of Structural

Engineering, Jan. 01, 1983, pp. 109-125.

[11] American Concrete Institute, “Building Code Requirements for Structural Concrete (ACI 318-11)”, Farmington Hills, MI, USA, 2018.

[12] S.A. Kulkarni, B. Li, "Seismic behavior of reinforced concrete Interior wide-beam column joints", Journal of Earthquake Engineering, vol. 13(1), pp. 80-99, 2008.

[13] F.L. Lopez-Almansa, D. Dominguez, A. Benavent-Climent, "Vulnerability analysis of RC buildings with wide beams located in moderate seismicity regions", Engineering Structures, vol. 46, pp. 687-702, 2013.

[14] M. De Stefano, B. Pintucchi, "A review of research on seismic behavior of irregular building structures since 2002". Bulletin of Earthquake Engineering, vol. 6, pp. 285-308, 2008.

[15] J.P. Moehle, "Seismic Response of Vertically Irregular Structures", Journal of Structural Engineering, vol. 110(9), pp. 2002-2014, 1984.

[16] C. Chintanapakdee, A.K. Chopra, "Seismic response of vertically irregular frames: response history and modal pushover analyses". Journal of Structural Engineering, vol. 130(8), pp. 1177-1185, 2004.

[17] O. İnce, “Asmolen döşeme sistemine sahip betonarme binalarda yumuşak kat düzensizliğinin incelenmesi”, M.Sc. thesis, Fırat University, Elazığ, Turkey, 2018.

[18] K. Turker, I. Gungor, "Seismic performance of low and medium-rise RC buildings with wide-beam and ribbed-slab", Earthquakes and Structures, vol. 15(4), pp. 383-393, 2018.

[19] A. Özdaş, “Asmolen döşemeli betonarme yapıların doğrusal olmayan statik itme analizi”, M.Sc. thesis, Karadeniz Technical University, Trabzon, Turkey, 2006.

[20] C. Özden, “Statik betonarme projeleri ulusal yapı analiz programları ile yapılan dolgulu dişli döşemeli binaların Etabs analiz program ile incelenmesi”, M.Sc. thesis, Akdeniz University, Antalya, Turkey, 2020.

[21] I. Anıs, “Comparative study of seismic performance of multistoried reinforced concrete

buildings with different slab systems", M.Sc. thesis, Gaziantep University, Gaziantep, Turkey, 2021.

[22] C. Dönmez, E. Karaaslan, M.A. Erberik, "Fragility analysis of wide-beam infill-joist block RC frames", Journal of Faculty of Engineering and Architecture of Gazi University, vol. 37:1, pp. 159-173, 2022.

[23] E. Karaaslan, "Seismic performance assessment of wide beam infill joist block frame structures in Turkey", M.Sc. thesis, Middle East Technical University, Ankara, Turkey, 2015.

[24] ETABS, "Building Analysis and Design Software", Computers & Structures Inc., California, USA, 2020.

[25] B. Bagheri, E. Firoozabad, "Comparative study of the static and dynamic analysis of multi-storey irregular building", International Journal of Civil, Environmental, Structural, Construction and Architectural Engineering, vol. 6, 2012.

[26] A.S. Patil, P.D. Kumbhar, "Time history analysis of multistoried RRC building for different seismic intensities", International Journal of Structural and Civil Engineering Research, vol. 02(03), Aug., 2013.

[27] Harshita, "Seismic Analysis of symmetric RC frame using RSM and THM", International Journal of Scientific Research and Education, vol. 02(03), March, 2014.

[28] M.D. Bhagwat, P.S. Patil, "Comparative study of Performance of multistoried building for Koyna and Bhuj earthquake by THM and RSM", International Journal of Advanced Technology in Engineering and Science, vol. 02(07), July, 2014.

[29] S.R. Padol, "Review paper on seismic response of multistoried RCC building with mass irregularity", International journal of research in engineering and technology, vol. 04(03), March, 2015.

[30] S.K. Dubey, S. Prakash, A. Ankit, "Dynamic analysis of structures subjected to earthquake load", International Journal of Advance Engineering and Research Development, vol. 02(09), Sep., 2015.

[31] Pacific Earthquake Engineering Research Center (PEER), “Ground motion database.” peer.berkeley.edu. https://peer.berkeley.edu/peer-strong-ground-motion-databases (accessed September 05, 2021)

[32] G. Dok, M. Aktaş, “Zaman Tanım Alanında Doğrusal Analiz ile Mod Birleştirme Yönteminin Kıyaslaması: 32 Katlı Betonarme Yapı Örneği”, International Science and Technology Conference, Dubai, Dec. 13-15, 2012.

[33] K.N. Ramanathan, “Next generation seismic fragility curves for California bridge incorporating the evolution in seismic design philosophy.” Ph.D. Dissertation, Georgia Institute of Technology, 2012.

[34] C.P. Contiguglia, A. Pelle, B. Briseghella, C. Nuti, “IMPA versus Cloud Analysis and IDA-Different Methods to Evaluate Structural Seismic Fragility”, Multidisciplinary Digital Publishing Institute, vol. 12(3687), March 25, 2022.

[35] American Society of Civil Engineers, “ASCE 41-13 Seismic Evaluation and Retrofit of Existing Buildings”, American Society of Civil Engineers, Reston, Virginia, USA, 2014.

[36] F. McKenna, G. L. Fenves, “Open System for Earthquake Engineering Simulation, Version 2.4.0.” Pacific Earthquake Engineering Research Center, Berkeley, CA, 2012.

[37] J.W. Baker, “Efficient analytical fragility function fitting using dynamic structural analysis”. Earthquake Spectra, vol. 31(1), pp. 579-599, 2015.